Scanning and motion capturing of vertebral kinematics

by

Lorita Christelis

Thesis presented in partial fulfillment of the requirements of the degree of Masters of Science of Industrial Engineering

at

Stellenbosch University

Department of Industrial engineering

Faculty of Engineering

Supervisor: Dr. AF van der Merwe

Date: December 2008

Declaration

By submitting this thesis electronically, I declare that the entirety of the work contained therein is my own, original work, that I am the owner of the copyright thereof (unless to the extent explicitly otherwise stated) and that I have not previously in its entirety or in part submitted it for obtaining any qualification.

Date: . . . . . 24 November 2008 . . . . . .

Abstract

In the context of intervertebral disc replacement and customized implants, human simulation studies are of great importance. Simulation models need input data. This study investigated different in vivo motion capturing methods to capture spinal kinematics that will serve as input for simulation models. Available scanning and motion capturing techniques for capturing cervical kinematics range from simple clinical methods, to expensive specialized equipment and software. With a variety of technologies comes a variety of applications. In this study the focus is on capturing the kinematics of the cervical spine.

An important distinction was made between two types of motion capturing technologies: external motion capturing and internal imaging technologies. The available external motion capturing technologies pose many advantages in terms of cost, safety, simplicity, portability and producing accurate three dimensional position and orientation. However, the ability for external motion capturing technologies to give accurate information on the movements at each vertebral level is doubted by critics reasoning that the true vertebral motion is concealed by the skin and soft tissue. Although it would be ideal to use external motion capturing systems, one needs to be confident that these surface markers or sensors truly reflect the vertebral motion at each vertebral level.

An empirical study was conducted to evaluate the relationship between motion captured on the skin surface and motion of the vertebrae. Twenty-one subjects received low dosage X-rays, while radio opaque markers were attached to the skin at each respective vertebral level. The motion of external markers and that of the vertebrae could be seen simultaneously on one medium. In the empirical study, two outputs were achieved. Firstly, intervertebral kinematic data, for use in further simulation studies was obtained. Secondly, the relationship between surface markers and vertebrae in different motion instances was investigated. Distance and angle parameters were constructed for vertebral prediction from skin surface markers. The causes of variation in these parameters were identified by investigating the correlations of these parameters with anthropometrical variables. Strong correlations of the parameters were observed in flexion, but in extension, especially full extension, the correlations were poor to insignificant. It was concluded that in neutral, half flexion and full flexion it is possible to predict the vertebral position from surface markers by using the parameters and anthropometrical variables. In half extension this prediction would be less accurate and in full extension alternative methods should be investigated for external motion capturing.

Opsomming

In die konteks van die volledige vervanging van rugwerwel kussinkies en die moontlikhid om die implante per individue te ontwerp en te vervaardig, speel menlike bewegingsimulasies 'n belangrike rol. Hierdie studie fokus op die in vivo tegnologië wat beskikbaar is om beweging vas te vang en die nodige inset data vir simulasie modelle te voorsien. Daar is 'n verskeidenheid tenologië beskikbaar wat strek vanaf eenvoudige metodes tot ingewikkelde stelsels met hoogsgespesialiseede toerusting. Elke tegnologie hou sy eie voordele en nadele in en daarom is dit gepas vir 'n spesifieke toepassing. Die toepassing van die studies is om die beweging van die nek vas te vang.

'n Belangrike onderskeid word getref tussen twee tipe tegnologië: stelsels wat vanaf die buite kant van die liggaam beweging vasvang en tegnologië wat na die binnekant van die liggaam kyk. Die eksterne tegnologie hou al die praktiese voordele van koste, veiligheid, eenvoud en gerieflikheid in. Die belangrike vraag is egter of daar werklik vanaf velmerkers akkurate kommentaar oor die werklike beweging van die nekwerwels gelewer kan word? Baie kenners op die gebied twyfel in die vermoë van die stelsels om werklik op interwerwel vlak akkurate inligting oor die beweging van die werwels weer te gee. Volgens die kenners word die werklike beweging verskuil agter die beweging van die vel en sagte weefsel.

Daarom is 'n empiriese studie gedoen om na die verhouding tussen beweging van merkers op die vel en die werwels te kyk. 21 deelnemers het lae dosis X-strale ontvang in vyf verskillende posisies, terwyl metaalmerkers op die veloppervalk geplaas was by elke werwelvlak. Op die manier kon die beweging van die velmerker en die werwel gelyktydig en op dieselfde medium waargeneem word. Twee uitsette is met die empiriese studie bereik. Eerstens is daar bewegingsdata wat gebruik gaan word in verdere simulasie studies beskikbaar gestel. Tweedens is die verhouding tussen beweging van merkers op die vel en beweging van die vertebrae ondersoek. Hoek- en afstandsparameters om werwelposisie van die velmerker te voorspel is ondersoek. Die oorsaak vir variasie in die parameters is geïidentifiseer nadat sterk korrelasies tussen die parameters en antropomtriese veranderlikes gevind is, veral in fleksie. In ekstensie, was die korrelasies swakker. Die gevolgtrekking is gemaak dat in die neutral en fleksie posisies die vertebrae vanaf die velmerkers voorspel kan word met behulp van die parameters en antropometriese veranderlikes. In half ekstensie sal die voorspelling minder akkuraat wees en in volle ekstensie sal alternatiewe metodes moet ondersoek word om van velmerkers gebruik te maak.

Acknowledgements

I would like to express my sincere gratitude to the following people who have contributed to make this work possible:

- The LODOX group at UCT for the use of the equipment and especially for Stef Steiner and Virginia Sanders for investing their time and expertise into this study.
- Hope Gangata, the physiotherapist who assisted in this study.
- All the participants for their time and willingness to take part in the study.
- Dr AF van der Merwe, for the study guidance and always having an open door and a ready ear.
- Neal de Beer, research colleague for time and interest invested in this project.
- Other staff at the Department of Industrial Engineering who were always willing to answer questions and assist.
- Dr. Theo Nell from the Department of Physiology, for advice on the anthropometrical measurements.
- Prof. Daan Nel for advice on the statistical aspects of the study.
- My husband, Christian, for his love, support and interest in the study.

After studying a part of the human body, I stand in greater awe to God who created it. Therefore this work is dedicated to Him, the ultimate Engineer.

Table of Contents

List of Figures

List of Tables

Glossary

Accelerometer	Instrument used to measure the direction and amount of velocity change
Arthroplasty	A surgical procedure in which an artificial joint replaces a damaged joint.
Collagen	A natural protein found in humans that forms connective tissue and provide strength, resilience and support to the skin.
Coupled Movements	Movement in all directions, especially in rotation and lateral flexion, will cause movement on other planes. Such movements are known as coupled movements.
Extension	A backward movement in the median plane.
Flexion	A forward movement in the median plane
Goniometer	A goniometer is an instrument that either measures angle or allows an object to be rotated to a precise angular position. The term goniometry is derived from two Greek words, gonia, meaning angle and metron, meaning measure.
Gyroscope	A device for measuring or maintaining orientation, based on the principle of conservation of angular momentum.
In vitro	Translated as "in glass"; meaning studies conducted in a laboratory dish or test tube; an artificial or controlled environment.
In vivo	Translated as "in life" meaning studies conducted within a living organism (eg, animal or human studies).
Inclinometer	A device that measures the change of angle relative to the direction of gravitational pull.
Inter / Intra	The prefix inter means among or between, while intra means within. For example: intra- and inter-examiner reliability is the reliability between the same examiner and different examiners respectively.
Kinematic	A term that describes the movement of a body without reference to force or mass.
Kinetics	The study of forces associated with the motion of a body.
Kyphotic	(Greek - kyphos, a hump). Normal backward bending curvature of the thoracic spine.
Lateral Flexion	Movements to the left and right in the coronal plane.
Left/Right Rotation	Movements in the transverse plane
Lordotic	Normal forward bending curvature of the cervical and lumbar spine.
Palpation	The act of examining the spine with your fingers

List of Abbreviations

ALL	Anterior Longitudinal Ligament
AVA	Anterior Vertebral Angles
COR	Centre of Rotation
CT	Computed Tomography
DDD	Degenerative Disc Disease
DOF	Degrees of Freedom
DVF	Digital Video Fluoroscopy
MRI	Magnetic Resonance Imaging
PLL	Posterior Longitudinal Ligament
ROM	Range of Motion
TDR	Total Disc Replacement
N	Neutral
HF	Half Flexion
FF	Full Flexion
HE	Half Extension
FE	Full Extension

1 Introduction

This thesis forms part of a research area of Industrial Engineering applied in the medical field, specifically research on the development and manufacturing of customized intervertebral disc implants. The background of this field and the motivation for the problem statement is discussed in this section. The reader is firstly provided with fundamental medical terminology and knowledge of the human spine along with a roadmap to the rest of the document.

1.1 Background and Context

In the medical field, standard terminology is used to describe spatial orientation of a particular feature or a feature relative to another. The three main reference planes, as seen in Figure 1-1, are the median, coronal and transverse planes.

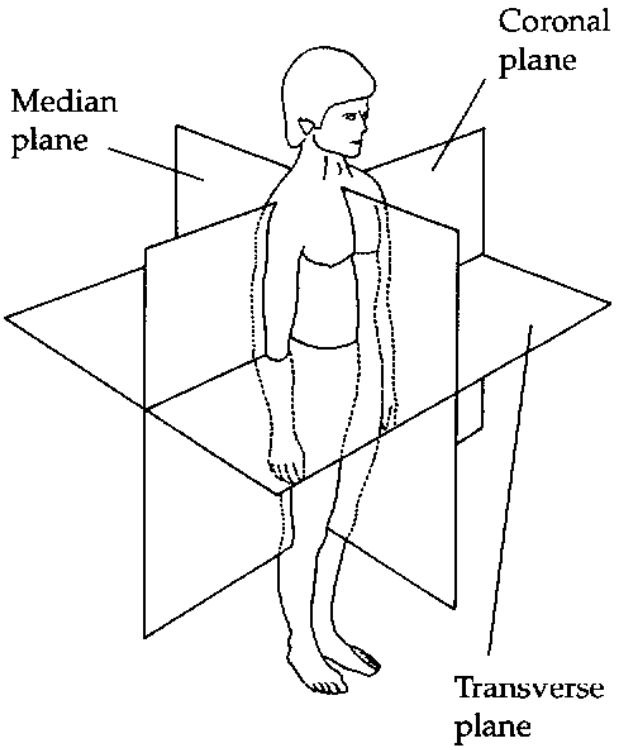

Figure 1-1 – Reference Planes [1]

Coronal (or frontal): The terms **anterior** (to the front) and **posterior** (to the back) describe position relative to the coronal plane. The words ventral and dorsal are interchangeably used in literature for anterior and posterior respectively.

M**edian** (or midsagittal): A **sagittal plane** is any plane parallel to the median plane. The terms **lateral** and **medial** are used to describe a position relative to the median plane. Lateral means further away from the median plane and medial means closer to the median plane.

Transverse (or horizontal): Any plane perpendicular to the median and coronal plane. The terms **superior** (upward or above) and **inferior** (downward or below) are used to describe position with respect to the transverse plane.

§

The complex human spine (or vertebral column) has many individual parts working together in harmony, serving each other to accomplish the tasks that it, as a whole, has been designed to do. If the spine is not injured or impaired it easily and sufficiently performs its functions of protecting, supporting and providing flexibility and mobility.

Protect

The spinal elements are aligned to create a canal that provides protection and support for the spinal cord. This is a very important function, since the spinal cord connects the brain with the rest of the body, allowing controlled movements and functioning of organs.

Support

Without the spine it would be impossible to be in an upright position. The spine forms a strong pillar for the support of the head and trunk. The spine is also crucial for balance and weight distribution. Upper body weight is distributed through the spine to the pelvis. The natural curves in the spine distribute body weight and stress during movement. The spine, by means of the intervertebral discs, also acts as shock absorber in response to impact loads.

Provide flexibility and mobility

The spine constitutes flexion, extension, lateral bending, rotation and combinations of these movements, made possible by the joints. The joints and ligaments also restrict motion that can cause injuries.

Other

The spine forms a base of attachment for ligaments and tendons. The spine also has physiological functions such as the production of red blood cells and mineral storage in the vertebrae.

The spine extends from the base of the skull to the pelvis. The individual bones of the spine, the vertebrae (p 11 - 16), are the building blocks of the spine and constitute three quarters of the length of the spine. The 33 vertebrae are arranged in 5 regions, called the cervical (C), thoracic (T), lumbar (L), sacral (S) and coccyx (Co) as shown in Figure 1-2. Each vertebra is named according to its region and its position from the neck downwards, for example, the third vertebra from the top is C3. In adults the five sacral vertebrae are fused to form the sacrum and the four coccygeal vertebrae are fused to form the coccyx. Therefor only 24 of the 33 vertebrae are moveable. Variations may occur in the number of thoracic, lumbar and sacral vertebrae, but the number of cervical vertebrae is constant.

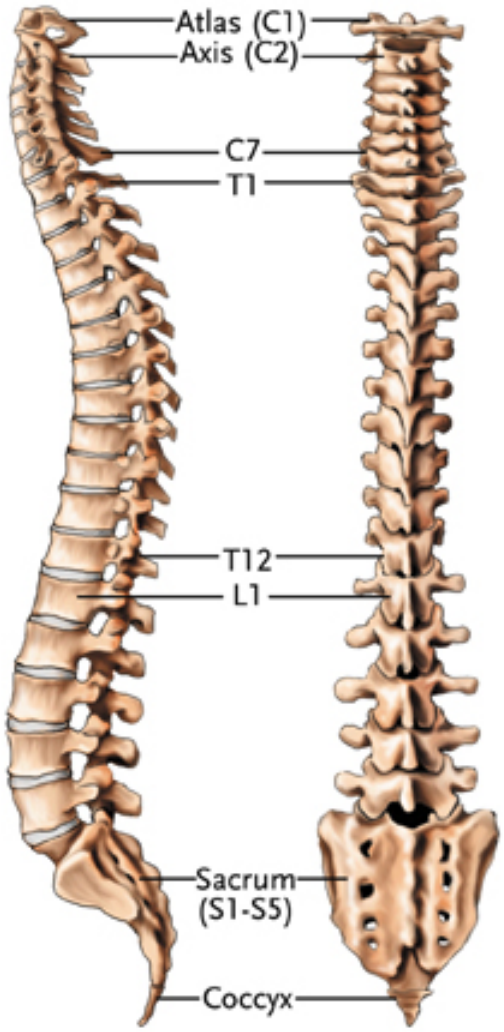

Figure 1-2 – Lateral and posterior view of the spine [2]

The movable vertebrae are connected by resilient intervertebral joints, the intervertebral discs (p 18) and zygapophyseal joints (p 21), which facilitate movements between the vertebrae. Vertebrae are held together by groups of ligaments (p 22). Figure 1-2 also shows the natural lordotic ("C" shape) or

kyphotic (backward "C" shape) curvature of the spine. When the trunk is in an upright position the normal spine has four curves in the median plane, but is straight in the coronal plane. This "S" curve helps the spine withstand all kinds of stress and provides rotational stability by distributing body mass away from the straight line between the skull and pelvis.

The characteristics of the cervical region are discussed in detail in the literature study. The distinguishing features of the other regions are discussed in short.

Thoracic

The thoracic spine has a kyphotic curve and 12 vertebrae, T1–T12. These vertebrae could be distinguished by the presence of facets[a] (zygapophyseals) on bodies that connect to the ribs and long spinous processes that overlap each other. The thin and narrow intervertebral discs provide limited movement.

Lumbar

The lumbar region has a lordotic curve and 5 vertebrae, L1–L5, with a sixth vertebra not uncommon or dangerous. These vertebrae are the largest in the entire spine. The main distinguishing feature of the lumbar vertebrae is the orientation of the facets on the superior and inferior articular processes which limits rotation of the lumbar vertebrae in a transverse plane. The thick intervertebral discs ensure a much greater range of movement in other directions. Most weight bearing and body movement takes place in the lumbar region, resulting in lower back pain being a common complaint.

Sacrum and Coccyx

The sacrum is sandwiched between the left and right hip bones and thus provides a firm base for the rest of the spine. The sacrum provides strength and stability to the pelvis and transmits the weight of the body to the pelvic girdle. The vertebrae become progressively smaller from S1–S5 and hence the triangular shape. The Coccyx (tailbone) does not participate in the support of the body weight, but provides attachment for ligaments and coccygeus muscles.

Back pain

Back pain is one of the most common physical complaints. "Seventy to eighty percent of the population of the Western world experiences low-back pain at one time or another" [3]. This high percentage implies that there is a great need for further treatment research and also that there is great

a A small articular surface, usually relatively flat

economic potential in this market. Back pain is estimated to cost the UK economy up to £ 5 billion a year [4]. In the Netherlands it is 1.7% of the gross national product. The direct medical costs were $368 million; the indirect costs were $4.6 billion [5]. In the US the cost is estimated to be $50 Billion yearly, which still excludes costs associated with lost personal income and lost employer productivity [6].

In most cases of back pain an individual would improve quickly, but in some unfortunate cases this acute pain (days to weeks) would develop into chronic pain (more than three months) and become a cause of great misery. Even with fewer people experiencing chronic pain, the need for treatment of chronic back pain is still significant. "In 2005, the Total Disc Replacement market in the five largest European Union countries (France, Germany, Italy, Spain and the United Kingdom) was estimated at approximately $58 million. This market is expected to grow at a compound annual rate of approximately 18%, reaching an estimated $132.3 million in 2010" [7]. This number is extremely high considering that Total Disc Replacement is just one of many procedures and only few people are potential candidates for the procedure.

Disc degeneration

There are many causes of back pain, but intervertebral disc degeneration, known as Degenerative Disc Disease (DDD) is a condition that most people experience to some extent. Discs dehydrate and wear away as the body ages and due to minimal blood supply, discs lack the ability to heal or repair themselves. This degeneration is a normal part of aging and is generally not a problem itself. Many people do not experience symptoms, but for others DDD leads to disorders such as lumbar spinal stenosis (narrowing of the spinal canal, resulting in compression of the nerve roots or the spinal cord), spondylolisthesis and retrolisthesis (forward and backward slippage of the disc and vertebrae) and a condition where the inside of the disc pushes through the tears in the outside of the disc and press on the nerves beside it (herniated / bulging / compressed / prolapsed / ruptured / slipped disc). These conditions can cause great pain and greatly affect one's quality of life.

Total Disc Replacement

DDD and diseases caused by this condition are in most cases successfully treated with the correct combination of rest and exercise, physical therapy, anti-inflammatory medications, and spinal injections. Surgery may be an option when conservative treatments do not provide relief. Deciding on the best surgical option depends on many factors. Traditional surgical treatments such as spinal fusion[a],

[a] A procedure that joins two or more vertebrae with a bone graft in order to eliminate motion and relieve pain.

disectomy[a], laminectomy[b] and laminotomy[c] make use of one of two basic principals to remove pain. Firstly, to create space by permanently removing a part of the spine or secondly, to restrict the movement that causes the pain by fusing anatomical parts together. The fact that Total Disc Replacement (TDR), or disc athroplasty, completely replaces the damaged disc by an artificial disc and therefore has the potential to restore normal disc height, movement and flexibility, makes it a promising option and can become and an alternative to the 450 000 lumbar and cervical fusions performed annually in the US [8]. Cunningham [9], summarizes the current growth in arthroplasty for spinal surgery as follows:

> "Total disc arthroplasty serves as the next frontier in the surgical management of intervertebral disc pathology. The concept of total disc arthroplasty represents a new paradigm in the surgical management of discogenic pathology. As we move from an era of interbody spinal arthrodesis to one in which segmental motion is preserved, this promising new technology offers a variety of clinical and research challenges".

It is however important to note that TDR is only considered after all other treatments have been exhausted and an individual has undergone various investigations to prove that the pain is caused by a damaged disc. The age and overall health of the individual would play a role. There should be no sign of infection, osteoporosis or arthritis. No operation can guarantee total pain relief or no long lasting negative effects; therefore surgery should always be weighed carefully against its risks. The individual should have long-standing intolerable pain and experience loss of normal bodily functions to justify taking the risk. There should also be degeneration in only one disc.

Design Improvements

Since the first published study on disc replacement in 1955 by David Cleveland, there has been a range of prosthesis designs and numerous attempts to successfully replace a damaged disc. Today some devices have been successfully implanted, especially the Charité III and Prodisc-L that have been approved by the US Food and Drug Administration (FDA). Still, according to some critics, design improvements are necessary to eliminate material wear debris, insertion related complications and to improve the support, constraint and mobility that the artificial disc provides [10].

Customization

Another aspect that should be considered when striving to imitate the functioning of the natural disc is that each individual's body is different. The ideal is a complete customized disc, but in the field of customized discs and the customization process there are many unanswered questions. For example,

[a] The surgical removal of part or the entire intervertebral disc.
[b] A surgical procedure that removes the lamina to relieve pressure on the spinal cord or nerve roots.
[c] An opening made in a lamina, to relieve pressure on the spinal cord or nerve roots.

one study pointed out how the extent of an individuals' activities of daily living may need to be a variable in choosing the device design, "Device manufacturers may determine that 'one-style or one-size' should not fit all individuals, and the estimated life of the spinal arthosis may need to be based on personal activity level" [11]. The full effects of different designs and styles are still to be investigated.

Creating simulations of generic natural movement and of a specific individual's movement would play an integral role in developing a customized disc. For the generic simulation model, normative data and information from literature could be applied. In vitro studies could also prove to be useful in the first stages of the model. In vitro models permit accurate measurements of intersegmental motions and a more controlled environment for studying the physical properties of the spine in flexion, extension axial rotation and lateral bending and the coupled rotations associated with each of these movements. The downside to in vitro studies is that the skeletal movement without muscles and other soft tissue does not accurately reflect the movement of a living individual. Still it provides sufficient data for first iterations and establishes the type of motion to be expected, thus preparing for and enhancing the subsequent in vivo study [12].

A point in the customization process will however be reached where kinematic data of the particular individual is needed. Obviously at this point in the process only in vivo methods are considered and the question is posed: what technologies or techniques are available for capturing accurate and reliable in vivo intervertebral motion? This question within the context of back pain, TDR and customized discs sets the stage for the problem statement of the thesis.

1.2 Problem statement

The problem statement of the thesis is to evaluate the scanning and motion capturing techniques to capture vertebral kinematics. The many ways that spinal kinematics have been and are being measured are investigated in terms of a literature review. The available technologies range from simple clinical methods, such as palpation or goniometry, to expensive technologies like optical systems consisting of ten specialized cameras. There are also invasive methods, like stereoradiography or other radiographic methods that exposes a patient to radiation. Some methods are easy and simple to use and others are limited to laboratories or have extensive calibration procedures. A study is conducted of some potential in vivo motion capturing technologies that could form an important part of the customization process. This is further discussed in the literature study (In Vivo Motion Analysis) and conclusions are made to what type of technologies would be suited for the customization process chain.

An important observation of this research of in vivo motion capturing systems is that a distinction can be made between two types of motion capturing technologies. First of all motion capturing with

external markers, sensors or transmitters placed on the skin (further referred to as external motion capturing) and secondly motion capturing with technologies that render images of the inside of the body (further referred to as internal imaging technologies).

The available external motion capturing technologies pose many advantages in terms of cost, safety, simplicity, portability and producing accurate three-dimensional position and orientation. It would be ideal to use such systems in the customization process chain. The ability of these external motion capturing systems to provide accurate information on the movements at each vertebral level is questioned. This information of movements at vertebral level is essential to produce realistic simulation models.

> "Quantitative assessment of the spinal kinematics at the individual vertebral level can yield useful insights leading to improved veracity of biomechanical models of human spine or torso movements" [13].

One wants to take all the advantages of external motion capturing systems and combine it with the abilities of internal imaging technologies to provide information of motion at each intervertebral level. This way of thinking led to the first critical questions concerning the problem of the empirical study. What is the relationship between data from external motion capturing systems and internal imaging technologies? Can skin surface makers accurately represent vertebral motion? Can data captured on the outside be transformed into usable information of internal segmental motions? What factors contribute to conceal true vertebral motion?

To investigate the relationship between motion on the skin surface and motion of the vertebrae it is necessary to consider both simultaneously. The problem for the empirical study is therefore to evaluate the relationship between external marker-defined and internal segmental vertebral kinematics.

Objectives of this research include:

- Conclusions regarding the use of in vivo motion capturing systems.
- Two dimensional internal segmental kinematic data, for use in further simulation studies.
- Observations from the empirical study (discussed in more detail on p 54).
- Conclusions to what extent external motion capturing could be used to represent vertebral motion.

Scope

An important question for determining the scope of the research was whether to focus on a specific part of the spine and on which part of the spine to focus. Concerning spinal treatment the cervical and lumbar regions are of importance. Most of the movement of the spine takes place in these two regions. The cervical region is easily injured, but the most complaints of back pain occur in the lumbar region, due to its sustaining the most forces and stresses during everyday activities. The natural inclination was towards the lumbar region. In the lumbar region the anatomical surface landmarks are generally more prominent than in the cervical region. Although C7 is very prominent in most people, the other cervical spinous processes are actually difficult to palpate. In the lumbar region one would be able to place the surface markers more accurately, but the fact that the surface markers in the cervical region are subject to more motion of soft tissue makes it an attractive choice to investigate. Several studies asking similar questions as this study have been done in the lumbar region and to a much lesser extend in the cervical region (see Previous Studies p 54). This fact greatly contributed towards deciding to focus on the cervical region. The following reasons also contributed to this decision:

- The focus of the study is only indirectly related to medical conditions. The primary focus is in vivo motion capturing technologies. Where the most pain occurs is irrelevant to this research.
- The largest range of motion is in the cervical region, which gives more scope for capturing motion in different positions.
- Investigating the neck as opposed to the lower back also had added benefits in terms of participant practicality. There was no need for participants to remove any clothing and participants could easily be positioned to get scans in different positions.
- For simulation purposes it would be easier to simulate and interpret the motion of the neck together with the movement of the head, as opposed to the motion of the lumbar region with the rest of the trunk.

For the purposes of this study only cervical kinematics is investigated. Kinetics is not within the scope of the project. Kinetics will be crucial in the latter stage, when the actual design of the disc takes places. The anatomy was studied with the purposes of recognizing features and understanding articulations in order to know what constitute spinal motion and what to expect in the empirical study. Muscles play a role in producing motion, but are not included in the scope of the study, since the focus of the study lies more in describing the kinematic behaviour of the vertebral bodies, as opposed to describing the influences causing motion. A brief study was however done on the spinal ligaments since they are

attached to the vertebrae and play a vital role in allowing or constraining the amount and type of motion.

1.3 Roadmap of the document

Section 2.1 is concerned with the fundamental knowledge of the structure and function of the cervical region, or more generally referred to as the neck. With an understanding of the anatomical structure and the articulations of the cervical spine the kinematics of the cervical spine and the kinematic measuring parameters is discussed in Section 2.2. In section 2.3, ways to capture the motion that is now understood, is investigated. The external motion capturing systems and internal image technologies were investigated to compare the types of systems available and the advantages and disadvantages that each poses. This section concludes the literature review.

From the literature review a need for an empirical study arose. Section 3 deals with the rationale behind this empirical study, discussions on similar studies previously conducted and the particulars regarding the study. The aspects concerning the Committee of Human Research are mentioned in section 3.2.1. Section 3.3 - 3.5 explains how the data was acquired, processed and analysed.

The results from the empirical study are discussed in section 4, and the conclusions of the study as a whole in section 5.

2 Cervical spine anatomy, kinematics and motion capturing

This chapter discusses the anatomy and the kinematics of the cervical spine as well as the available methods and techniques for capturing motion.

2.1 The Anatomy of the cervical spine

The first seven vertebrae, the cervical spine, is the body's most complicated articular structure. It is situated between the skull and thoracic spine. The orientation of the zygapophyseal joints, the short transverse processes, the relatively thick intervertebral discs, and the relatively short spinous processes of C3 - C6 all combine to give a large range of motion in the cervical region. The cervical spine is very flexible, but also very much at risk for injury from strong, sudden movements. The cervical spine's natural lordotic curve develops when an infant first lifts its head to move around. The curve enables the absorption of more energy during a collision. For example, without this curve, or when the neck is flexed about 30°, the forces applied to the top of the head are directed to a straight-segmented column and less energy is needed for the neck to fail under axial load.

For all kinematic and anatomic purposes the cervical spine can be divided into two sections: the upper cervical spine (C1 and C2) and the lower cervical spine (C3 to C7). The vertebrae of these two regions are different in structure and function.

2.1.1 Lower cervical vertebrae

As shown in Figure 2-1, a typical vertebra consists of two essential parts: an anterior segment, the body, and a posterior part, the vertebral or neural arch which encloses a foramen[a]. The vertebral arch consists of a pair of pedicles, a pair of laminae and supports seven processes: four articular, two transverse, and one spinous.

[a] An opening, a hole or passageway in a bone for blood vessels or nerves

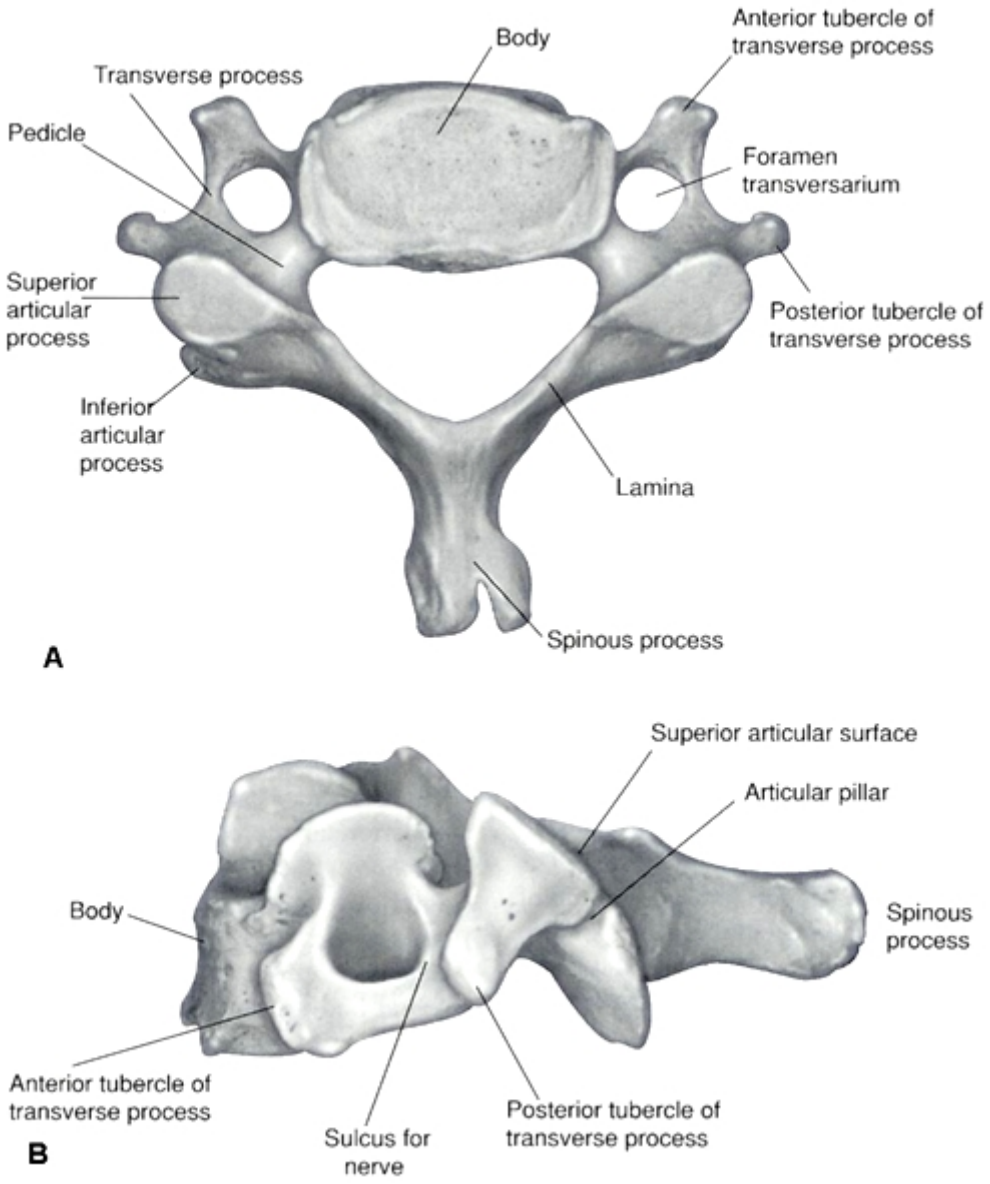

Figure 2-1 – Superior and lateral view of a cervical vertebral body [14]

Body

The small body of the cervical vertebrae consists of a hard and strong outer shell, called cortical bone, and a soft and spongy inside, called cancellous bone. The anterior and posterior surfaces are flat and equal in depth. The anterior surface is slightly inferior to the posterior surface, so that the most inferior border protrudes downward and overlaps the most superior border of the vertebra below.

Uncinate processes

The upper surface of the body is transversely concave, and presents a projecting lip on either side. This feature is unique to the cervical region and known as the uncinate processes. The lower surface is concave from front to back, convex from side to side, and presents laterally shallow concavities which receive the corresponding uncinate processes of the vertebra below. These processes form the uncovertebral joints.

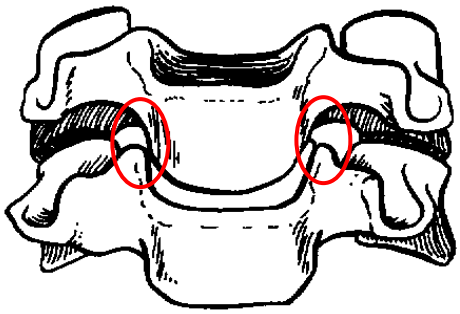

Figure 2-2- The uncovertebral joints [15]

Vertebral foramen

The vertebral or neural foramen is the opening posterior to the vertebral body, and is the smallest in the cervical region. When the vertebrae are articulated, a hollow tube is formed (spinal canal) which contains the spinal cord, its protective membranes, nerve roots and blood vessels. Without the foramen, nerve signals could not travel between the brain and the rest of the body.

Pedicle

The pedicles are two short, thick processes consisting of cortical bone, which project posteriorly, one on either side, from the upper part of the body, at the junction of its posterior and lateral surfaces. The concavities above and below the pedicles are called the **vertebral notches** and when the vertebrae are articulated, the notches of each adjacent pair of bones form the **intervertebral foramina**. Nerve roots that branch off to specific body parts passes through the intervertebral foramina on both sides. In the cervical region they branch off to the upper chest and arms

Lamina

The laminae are broad flat plates of bone extending medially and posterior from the pedicles to form the posterior wall of the vertebral foramen. The laminae are narrower and thinner above than below.

Their upper borders and the lower parts of their anterior surfaces are rough for the ligament attachment. From the lamina several outgrowths extend, known as the **vertebral processes**.

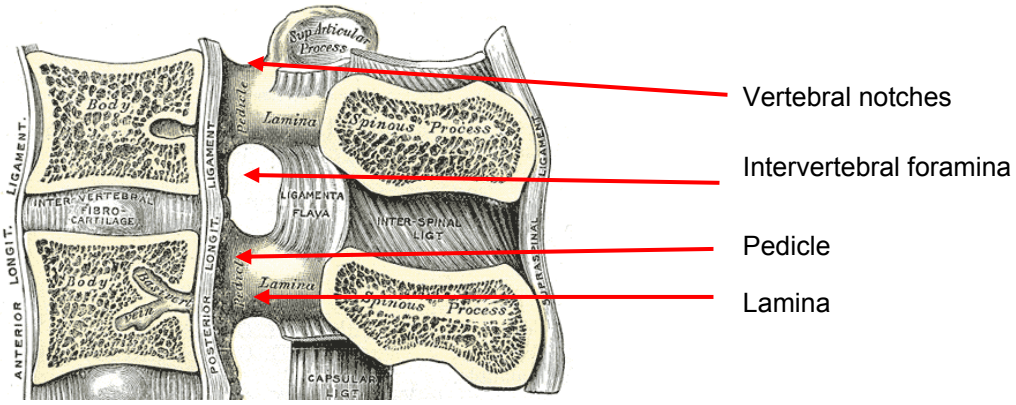

Figure 2-3 - The laminae, pedicles, intervertebral foramina and vertebral notches [16]

Transverse processes

The two transverse processes project on both sides from the point where the lamina joins the pedicle. These processes act as levers and provide attachment for the deep back muscles, helping them to increase their leverage on the spine. Unlike the rest of the spine, there are special openings for the arteries, called transverse foramen (Figure 2-1 A), in each transverse process. The anterior and posterior parts of the transverse processes are joined outside the foramen, by a bone which exhibits a sulcus[a] on its upper surface for the passage of the corresponding spinal nerve. It arises from the side of the body and is directed laterally in front of the foramen and ends in a tubercle[b], the anterior tubercle. The posterior part springs from the vertebral arch and is directed anterior and laterally, ending in a flattened vertical tubercle, the posterior tubercle. The tubercles and sulcus can clearly be seen in Figure 2-1 B.

Spinous processes

The spinous processes protrude backward and downward from the junction of the laminae. The spinous processes are all bifid[c] and short, but gradually increase in length. The two divisions are often of unequal size. The spinous processes overlap with the vertebra below. Muscles and ligaments that move and stabilizes the vertebrae, attach to the spinous processes. The spinous processes is felt when one's hand is run down a person's back.

---

a A groove
b A small, rounded or knoblike elevated process on a bone
c Cleft in two

Articular processes

The two superior and two inferior articular[a] processes are of great importance, because they form the zygapophyseal joints that lock the vertebrae together. The facet surface on each process are flat and of an oval form and articulate in oblique planes. The surfaces of the inferior articular facets face downwards and forwards at an angle of approximately 45 degrees, while the superior surfaces of the vertebra below face upward and backward

Vertebra prominens

The name vertebrae prominens is given to C7 because of its distinct and long spinous process that is easily felt on the skin. The spinous process is thick, nearly horizontal in direction and not bifid, but ends in a tubercle. The transverse processes of C7 are of considerable size. The posterior tubercles are extremely prominent, while the anterior are small and almost absent (Figure 2-4). The transverse foramen may be as large as those in other cervical vertebrae, but it is generally smaller and sometimes double or absent.

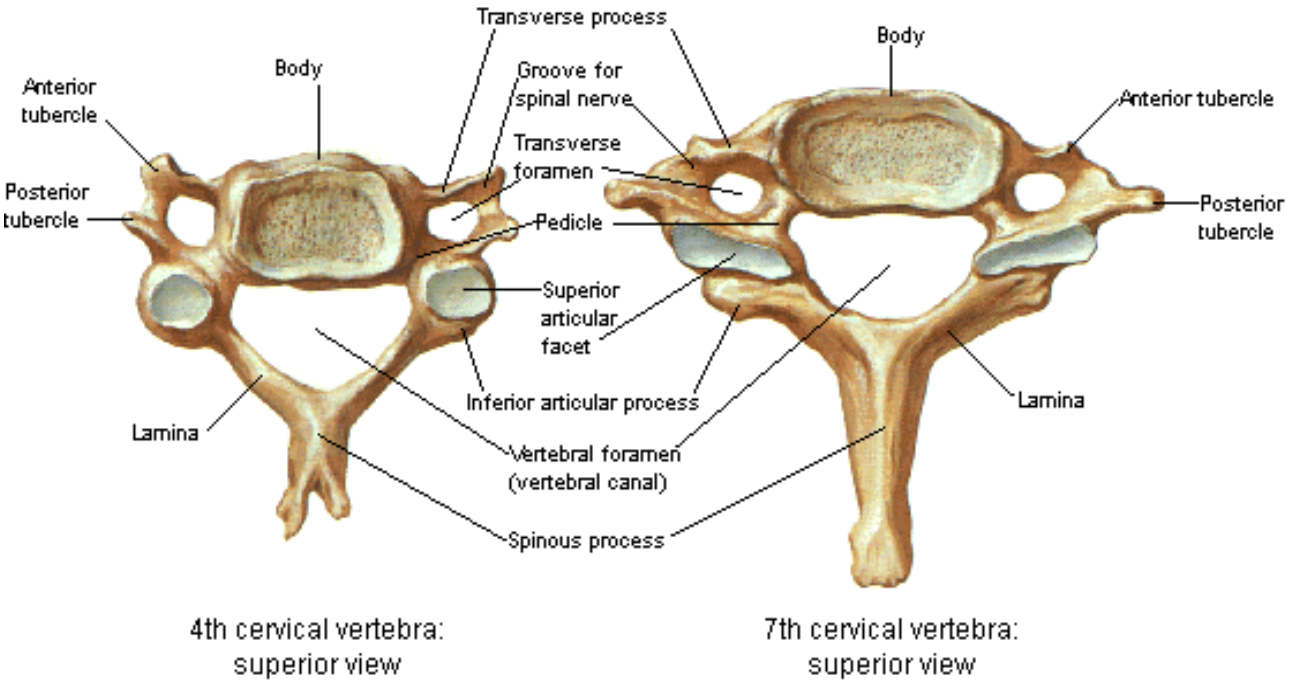

Figure 2-4 – Superior View of C4 and C7 [17]

[a] From the Latin word articularis, meaning 'of the joint'

2.1.2 The upper cervical vertebrae

The first two vertebrae in the cervical spine, the **atlas (C1)** and the **axis (C2)** connect the skull to the spine and allow great range of movement. These two vertebrae are atypical.

Atlas

The atlas supports the skull and hence received its name from the mythical character that supports the globe on his shoulders. The atlas is a ring shaped bone with no body or spinous process, but a thick anterior arch, a thin posterior arch and two prominent lateral masses. The anterior surface of the anterior arch is convex and has a tubercle in the center for muscle and ligament attachment. The posterior surface of the anterior arch is concave with a smooth circular facet for articulation with the dens of the axis. The posterior arch ends behind in the posterior tubercle, which gives origin to the ligamentum nuchae[a]. The absence of a spinous process allows greater flexion and extension movement between the atlas and the axis. The lateral masses are the most solid parts of the atlas in order to support the weight of the head. Each carries a superior and inferior articular facet that articulates with the condyles[b] of the occipital bone[c] and the superior articular facets of the axis. The superior articular facets are oval and concave and the inferior articular facets are circular and slightly convex. The large transverse processes project laterally and downward from the lateral masses. They are long and their posterior and anterior tubercles are one mass. The transverse foramen is directed from below, upward and backward.

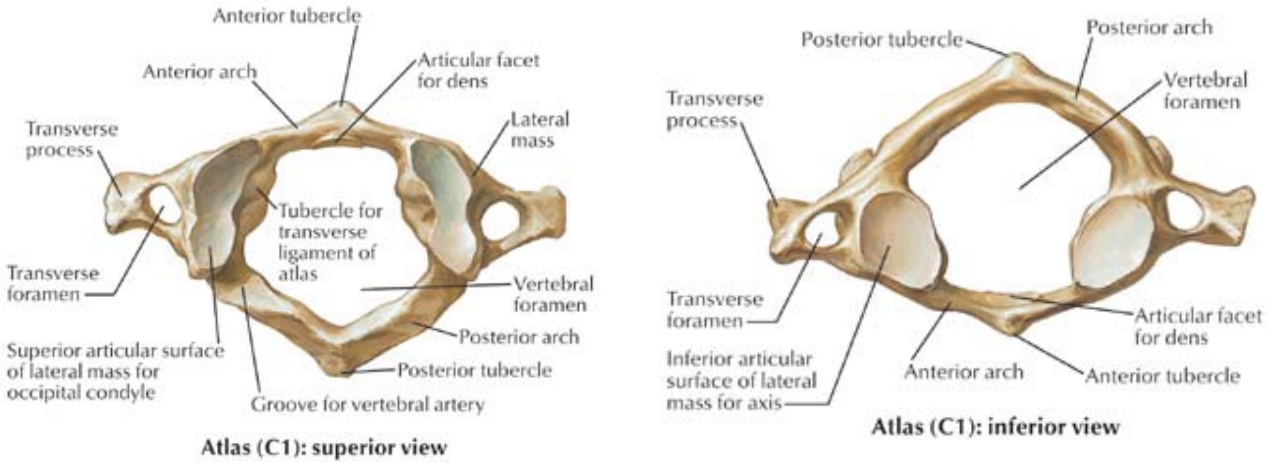

Figure 2-5 – Superior and inferior views of the Atlas [17]

a A fibrous membrane in the posterior part of the neck - see p 23
b A rounded projection of bone that provides the base for a rounded articular surface
c A saucer shaped membrane situated at the back and lower part of the cranium

Axis

The axis forms the pivot on which the atlas rotates. The distinguishing feature of the axis is called the dens[a] or odontoid process. It looks like a dull tooth that extends from the body of C2 and joins with the inside of the ring of the atlas. The body is prolonged downward anteriorly and overlaps the superior and anterior part of C3. The pedicles and laminae are thick and strong. The vertebral foramen is large, but smaller than that of the atlas. The transverse processes are very small and each ends in a single tubercle. The transverse foramens are directed obliquely upward and laterally. The round and slightly convex superior articular processes extend from the body, pedicles and transverse processes and are directed upward and laterally. The atlas rotates on the large, flat surfaces of the superior articular processes. The inferior articular processes are similar to the other cervical vertebrae. The spinous process is large, strong, deeply channelled inferiorly and presents a bifid, tuberculated extremity.

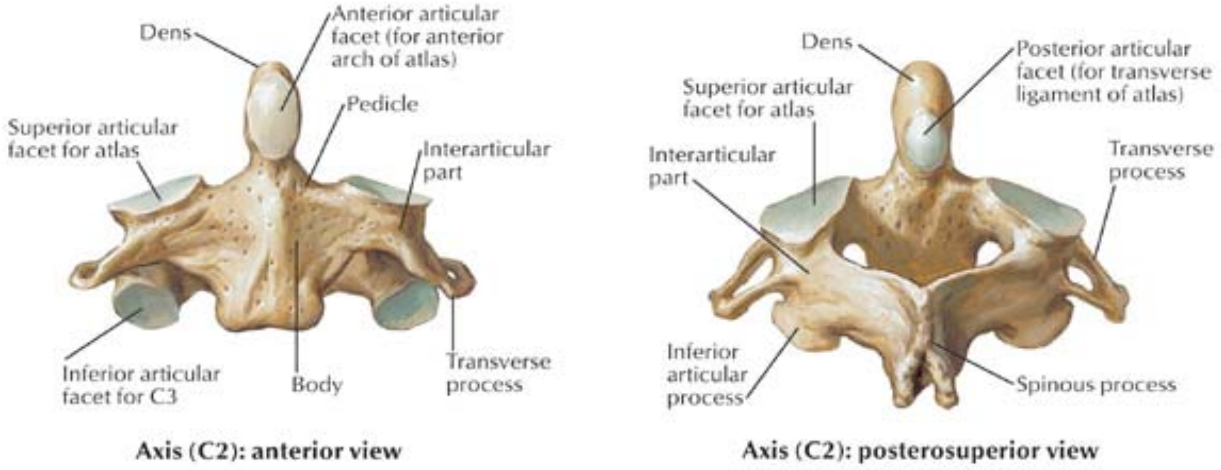

Figure 2-6 – Anterior and posterior view of the Axis [17]

2.1.3 The lower cervical motion segments

The motion segments from C2/C3 to C7/T1, consists of two adjacent vertebrae that constitute movement due to associated joints and ligaments. A joint, also referred to as an articulation or an anthrosis, is defined as a region where two or more bones are connected. Joints facilitate relative motion between bones and transmission of force from one bone to another. The intervertebral joints consist of the intervertebral disc that separates the two adjacent vertebrae, two zygapophyseal joints and related ligaments. The five lower cervical vertebrae also have two uncovertebral, or Luschka's, joints formed by the uncinate processes that project superiorly from the vertebral body below.

[a] Latin for tooth

2.1.3.1 The intervertebral disc

The intervertebral disc is a specialized symphysis joint. A symphysis joint is a type of cartilaginous joint in which the opposed surfaces are united by cartilage[a]. The discs are identified by specifying the particular vertebrae they separate, for example, the disc between the fifth and sixth cervical vertebrae is named C5/6. Although the cervical vertebrae are the smallest movable vertebrae, resulting in proportionally small discs, the intervertebral disc has the highest proportional thickness, resulting in a larger range of motion.

The biomechanical requirements of an intervertebral disc are threefold: the disc must (1) have height to separate the adjacent vertebrae (2) be able to sustain weight and transfer loads from one vertebra to the next, without being injured and (3) be pliable to accommodate rocking movements without compromising its strength.

A closer look is taken at the components that constitute the intervertebral disc to see how these biomechanical requirements are met. The intervertebral disc consists of an outer annulus fibrosus, which encloses the inner nucleus pulposus (Figure 2-7). Although the nucleus pulposus is quite distinct in the centre of the disc and the annulus distinct in its periphery, the boundary between them is unclear. Each articular surface of the vertebral bodies is covered by a vertebral end-plate.

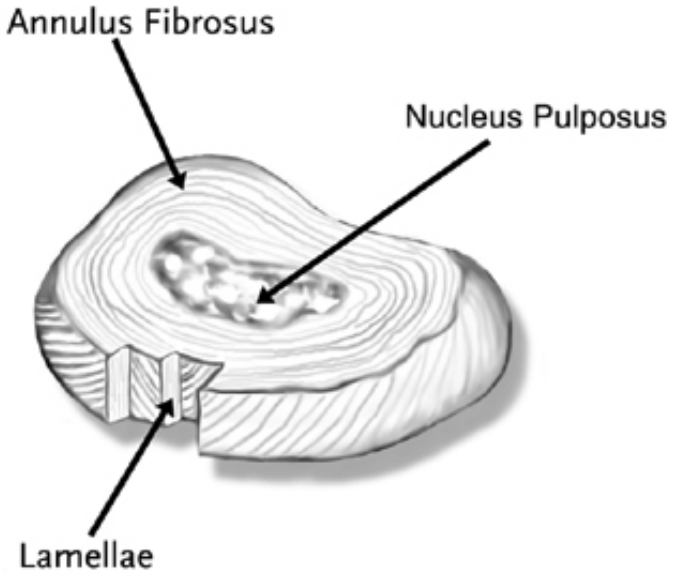

Figure 2-7 – Basic structure of the intervertebral disc [2]

[a] Cartilage is a dense, tough and elastic connective tissue. Unlike bone, cartilage does not contain blood vessels and lacks the ability to regenerate.

Annulus fibrosus

The annulus fibrosus is actually a ligament in structure and function and one of the toughest materials in the body. It consists of 10-20 sheets of collagen[a] fibres, called lamellae, tightly packed together in a circumferential fashion around the periphery of the disc. In a lamella, the orientation of all the fibres is the same—about 35° from the horizontal [18]. This angle remains the same between lamellae, but the direction alternates with each lamella (Figure 2-7). With this layer arrangement the tightly packed lamellae can withstand considerable loads, thus supporting the weight of the spine and preventing excessive motion while keeping the gelatinous centre intact. The outer lamellae, which have a high proportion of thick collagen fibres, can resist excessive bending and twisting. In the cervical region the posterior portion of the annulus is less developed due to the lamellae being finer and more tightly packed than in the anterior and lateral parts. This results in a wedge shaped disc, which follows the normal spinal curvature.

Due to the annulus fibrosus being collagenous, it is still sufficiently pliable and deformable to enable bending movements between vertebral bodies. However, its pliability is also its liability. If it buckles it loses its stiffness and is less able to sustain compression. To prevent this, the annulus fibrosus requires the second component of the intervertebral disc—the nucleus pulposus.

Nucleus pulposus

The nucleus pulposus is the hydrated gel in the centre of the disc. The nucleus can be deformed, but cannot be compressed. When subjected to pressure, the nucleus will attempt to deform and will thereby transmit the applied pressure by expanding in a radial fashion. As mentioned the annulus fibrosus functions to resist this expansion, but the nucleus pulposus returns the favour. This expansion braces the annulus fibrosus from the inside, preventing inward buckling that would cause the annulus to lose its stiffness and its capacity to transmit weight. Together these two components meet the design features of maintaining stiffness to sustain considerable loads and being pliable enough to allow some degree of movement between vertebral bodies. The nucleus also exerts pressure on the vertebral end-plates. This pressure serves to transmit part of the applied load from one vertebra to the next, thereby lessening the load on the annulus fibrosus.

The nucleus receives water from the vertebral bodies via the vertebral end-plates. Due to the nucleus being enclosed, its capacity for expansion is limited. Therefore when more water is absorbed, the pressure within the nucleus will simultaneously increase and consequently also the thickness of the disc.

[a] The main structural protein in connective tissues. It provides strength, resilience, and support the skin, ligaments, tendons, bones, and other parts of the body.

This process ceases when the pressure exerted on the nucleus pulposus via the casing is equal to the osmotic swelling pressure—the force exerted by the nucleus pulposus that allows water to be absorbed.

When the spine does not have to support the weight of the upper body, the amount of water that the nucleus pulposus can absorb is only limited by the extensibility of the corresponding annulus fibrosus. Consequently, during rest, sleep or any other condition where the compression load on the spine is reduced, the nucleus absorbs the maximum possible amount of water and the discs achieve maximum thickness. For this reason most people are at their tallest just after getting out of bed in the morning.

The disc responds elastically to impact loads, but viscoelastically to continuous loads [1]. During normal daily activities, when continuous loading is experienced, the amount of water that can be absorbed is limited by the size and duration of the compression loads, which mostly exceed the osmotic swelling pressure. Consequently, water is gradually forced back into the vertebral bodies such that the discs become thinner. Normally the loss of water is gradual due to the low permeability of the hyaline cartilage[a,] but at the end of a normal day the cumulative reduction of height in the spine may be as much as 2 cm [1]. This process of water absorption and water loss helps with the nourishment of the disc.

Vertebral end-plates

The superior and inferior aspects of the disc are covered by cartiligous plates that bind the disc to their respective vertebrae. Each endplate covers almost the entire surface of the adjacent vertebral body; only a narrow ring of bone, called the ring apophysis, around the perimeter of the vertebral body is left uncovered by the cartilage. Each vertebral endplate is about 0.6 – 1 mm thick. The end-plates consist of hyaline cartilage and fibro cartilage[b]. Hyaline cartilage appears towards the vertebral body and fibro cartilage towards the nucleus pulposus. As discs ages, the end-plates consist more and more of only fibro cartilage.

The end-plates help to equalize the loading of the vertebral body. It also functions as a chemical and biological filter between the nucleus and the blood vessels of the vertebral body. Discs are avascular and therefore depend on the end-plates to diffuse needed nutrients. When this process is inhibited through repetitive movement, injury or poor posture, the discs become thinner and more prone to injury. By preventing rapid fluid loss from the nucleus into the vertebral body during sustained loading, the end-plates maintain the water content and internal pressurisation of the disc.

a Hyaline cartilage is a mesh of collagen fibers and ground substance, with considerable elasticity and a translucent appearance.
b Fibro cartilage is a type of cartilage that closely resembles dense, regular connective tissue. It appears as a transition between tendons, ligaments or bones.

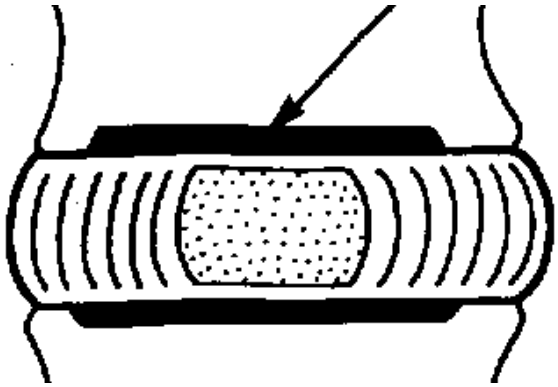

Figure 2-8 – A representation of the vertebral end-plates [19]

2.1.3.2 The zygapophyseal joints

Zygapophyseal[a] or facet joints are found between the inferior articular processes of the upper vertebrae and the superior articular process of the lower vertebrae on each side of the vertebral body. Zygapophyseal joints are synovial[b] which means that the opposed surfaces of the bones are not attached to each other, but held together by a joint capsule and ligaments, enabling greater movement than cartilaginous joints.

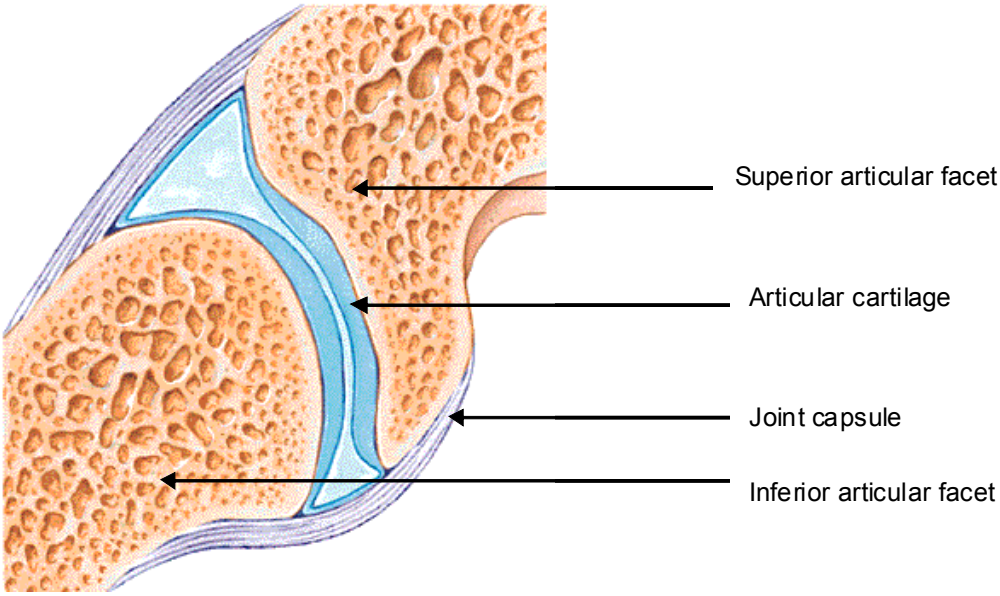

Figure 2-9 – Capsule of Zygapophyseal Joint [20]

a Greek: apophysis (outgrowth) and zygos (yoke/bridge). The term therefore means a 'bridging outgrowth'
b syn = with; vial = cavity

The surfaces of the joints are covered with hyaline cartilage that helps these parts of the vertebral bodies glide smoothly on each other. The joint capsule encloses a small joint cavity. The inner wall of the capsule and the nonarticular bony surfaces inside the joint are covered with synovial membrane. The cavity is filled with synovial fluid that nourishes the cartilage cells and lubricates the articular surfaces to prevent excessive wear. The capsules are longer and looser in the cervical region, facilitating greater flexion.

The zygapophyseal joints have an important mechanical function. They lock the vertebrae together to form the spinal column and allow or restrict motion. They allow vertebrae to move relative to one another, by pivoting; sliding towards, or away from each other. The orientation of the articular surfaces changes throughout the spine and determines the function of the zygapophyseal joints. In the cervical region the orientation allows them to play a weight bearing role and to provide resistance to anterior translation.

2.1.3.3 Ligaments

Ligaments are fibrous bands of connective tissue that attach to bone and connect bones or joints together. They are made up of densely packed collagen fibers. The system of ligaments in the spine, combined with the tendons and muscles provides a brace to help protect the spine from injury. Ligaments keep a joint stable during rest and movement and help to prevent injury from hyperextension and -flexion movements.

The **Anterior** and **Posterior Longitudinal Ligaments** (ALL and PLL) are primary spine stabilizers. These strong and broad ligaments run the entire length of the spine. The ALL covers and connects the anterior aspects of the vertebral bodies and annuli fibrosi. The ALL is thinner and weaker in the cervical region. The ALL maintains the stability of the intervertebral joints and helps prevent hyperextension of the spine. The PLL is situated in the vertebral canal and runs along the posterior aspect of the vertebral bodies and annuli fibrosi. It is widest in the cervical region. It has short, deep fibres that span consecutive vertebrae, and longer, more superficial, fibres that span three, four or five vertebrae. PLL helps to prevent hyperflexion of the spine and posterior protrusion of the nuclei pulposi.

The **Ligamentum flavum**[a] runs from the axis to the sacrum and connects consecutive laminae. It is the strongest of the spinal ligaments and consists of 80% elastin[b]. Therefore it stretches with flexion, but upon resumption of the neutral posture the fibres recoil and shorten, without buckling. This

[a] The ligament received its name from its yellow elastic tissue (L. Flavus, Yellow)
[b] A protein similar to collagen that is the principal structural component of resilient fibers

ensures that the neural elements are always presented with a smooth flat surface and also relieves the load on the back extensor muscles. At segmental level, the ligamentum flavum is a symmetrically paired structure. The superior attachment of the ligament is connected to the lower half of the anterior surfaces of a pair of laminae. Inferiorly the ligament divides into a medial and lateral portion. The medial portion attaches upper posterior surfaces of the succeeding pair of laminae. The lateral portion extends to the articular capsules of the zygopophyseal joints and contributes to the posterior boundaries of the intervertebral foramina.

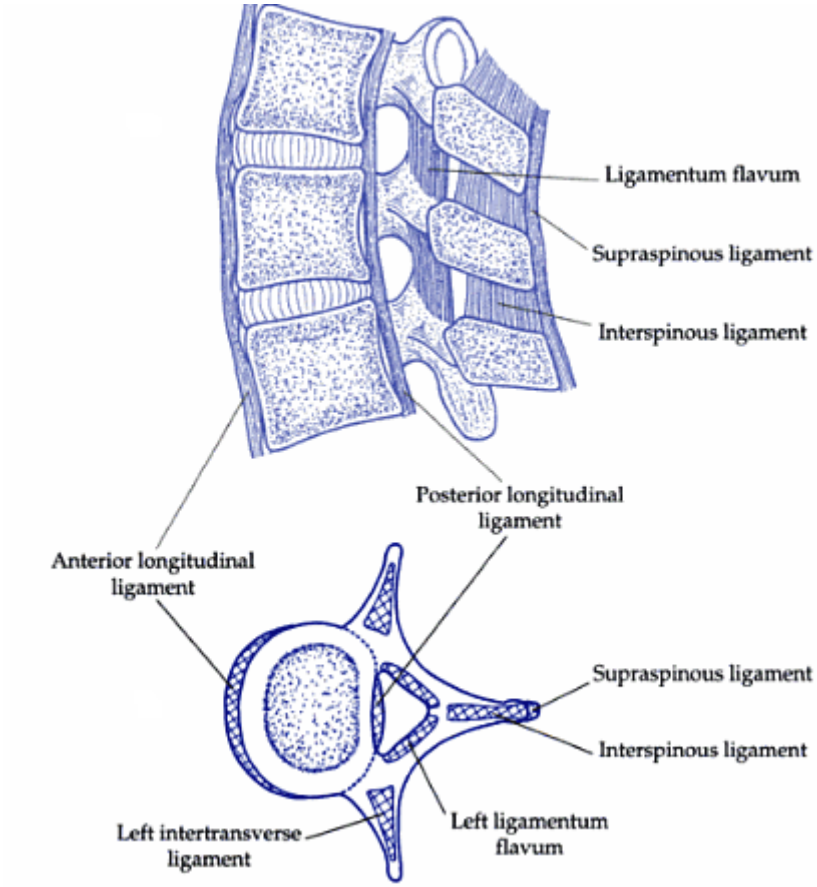

Figure 2-10 – The main ligaments of the spine [1]

In the neck the supraspinous and interspinous ligaments are represented by a fibrous membrane, the Ligamentum Nuchae. It extends from the external occipital protuberance and median nuchal line to the spinous process of C7. The ligamentum nuchae consists largely of regular elastic tissue. The elasticity of these ligaments helps to restore the head to neutral position after flexion and also relieves the load on the extensor muscles of the neck.

The transverse processes of adjacent vertebrae are connected by thin sheets of collagen fibres, called the **intertransverse ligaments.** These structures are too insubstansive to function as ligaments. They

constitute membranes that separate the anterior muscle compartment of the spine from its posterior muscle compartment.

The **capsular ligaments** (capsules of the zygapophyseal joints) are oriented approximately orthogonal to the articular facets. Although they are thick and dense they are lax to allow a great range of motion.

2.1.4 The upper cervical motion segments

The joints between the skull and the atlas, atlanto-occipital joint (Oc/C1) and between the atlas and the axis, atlanto-axial joint (C1/C2) differ from the other motion segments in the sense that they have no intervertbral discs or zygapophyseal joints.

Atlanto-occipital joints

The atlanto-occipital joint, one on each side is between the superior articular facets of C1 and the condyles of the occipital bone. These joints are synovial joints of the condyloid type[a] and have thin loose articular capsules each lined with synovial membrane. The skull and atlas are also connected by **anterior** and **posterior atlanto-occipital membranes.** These membranes extend from the anterior and posterior arches of C1 to the anterior and posterior margins of the foramen magnum[b], preventing excessive movements of these joints. The **tectorial membrane** is the superior continuation of the PLL. It runs from the body of C1 to the internal surface of the occipital bone. It covers the dens and associated ligaments.

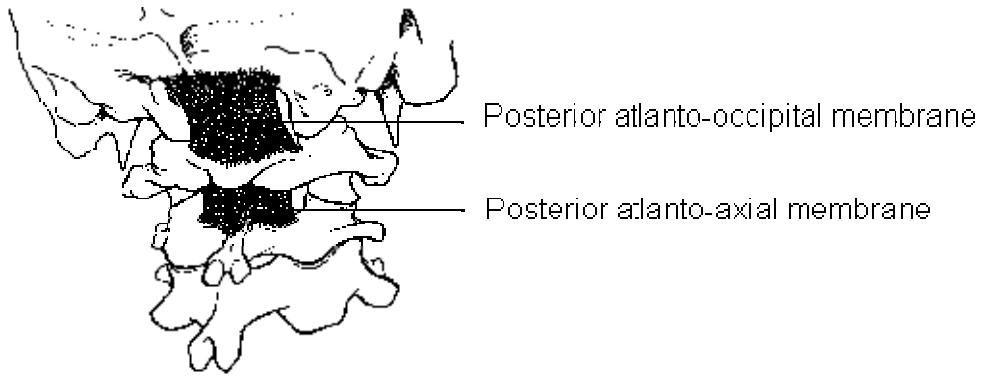

Figure 2-11 – Ligaments of the upper cervical motion segments [19]

[a] A condyloid joint is a biaxial joint which allow movement in two directions. They have two axes at right angles to each other.

[b] The large opening in the back of a skull through which the spinal cord passes.

Atlanto-axial Joints

Above the lamina of C2 the Ligamentum Flavum becomes the **posterior atlanto-axial membrane** for the portion spanning C1 and the **atlanto-occipital membrane** for the portion spanning C1 to the occiput.

During rotation the skull and C1 rotate as a unit on C2. The joints that permit this rotation are the pivot joint[a] between the dens and C1 and two gliding joints between the articular processes of C1 and C2, called the **lateral atlanto-axial joints.** The pivot joint is formed by the strong **transverse ligaments** of the atlas that extends from the tubercles of the lateral masses of C1 and holds the dens of C2 against the anterior arch of C1, preventing horizontal displacement of the atlas and allowing the head to turn from side to side. The transverse ligaments form part of the **cruciate ligament complex**, which is an important stabilizer of C1 and C2. It received its name from its cross like shape. An ascending band and descending band extends from the transverse ligaments and attaches to the occipital bone superiorly and the body of C1 inferiorly

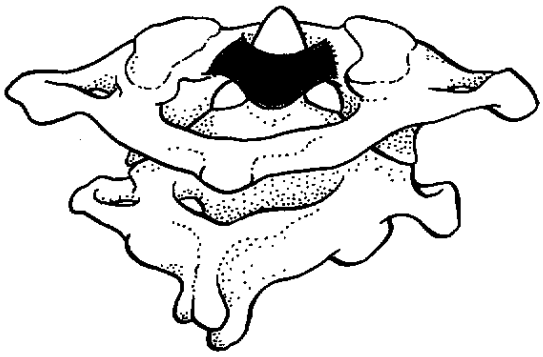

Figure 2-12 – Transverse ligament of the cruciate ligament complex [19]

The **alar** and **apical ligaments** are located immediately anterior to the cruciate ligament complex. The short and strong alar ligaments extend from the sides of the dens, while the apical ligament extend from the tip of the dens and both attach to foramen magnum, thus preventing excessive rotation of the pivot joint and enabling the occiput, atlas and axis to move as a unit.

a A uniaxial joint that allows rotation.

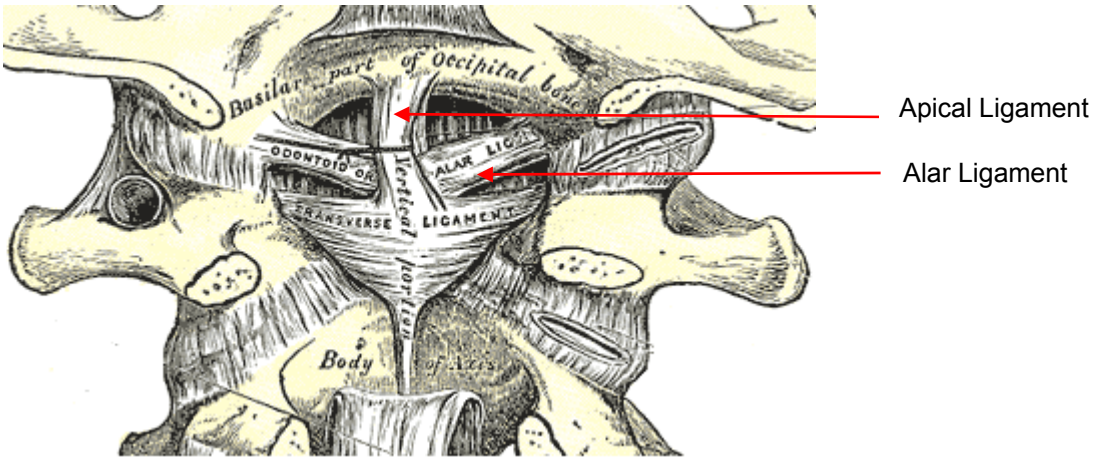

Figure 2-13 – Alar and Apical Ligaments [16]

2.2 Cervical kinematics

With a fundamental knowledge of the anatomy and articulations of the cervical spine, kinematics is investigated.

2.2.1 Lower cervical kinematics

In the lower cervical region flexion, extension, lateral flexion and rotation occur. Flexion and extension is the prominent motion, due to the alignment of the zygapophyseal joints and the uncinate processes.

2.2.1.1 Flexion and extension

The vertebrae undergo anterior sagittal rotation and translation during flexion and posterior rotation and translation during extension. Generally there is greater anterior than posterior translation. The orientation of the facets is one of the primary restraints to the anterior shear that occurs with flexion. The uncinate processes function as a guide rail for this sagittal plane motion, resulting in minimum lateral motion between adjacent vertebrae.

As illustrated in Figure 2-14, during flexion the:

- vertebra above tilts and slides forward
- anterior aspect of the disc compresses resulting in tensile force on the posterior aspect
- inferior facet of the superior vertebra slides superiorly and anteriorly over the superior facet of the inferior vertebra
- the spinous processes become separated

This motion pattern is reversed for extension. The complete spine has more stiffness in extension than in flexion, which is especially noticeable in the cervical and lumbar regions. The posterior joint complex plays a significant role in limiting extension.

Apart from atlanto-occipital joint, C4 to C6 display the largest ranges of cervical flexion and extension [19].

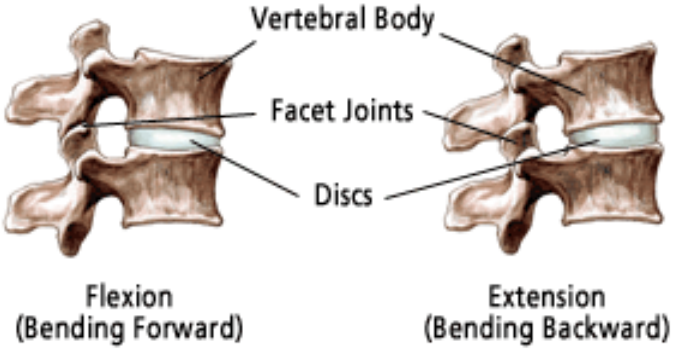

Figure 2-14 - Joints in motion [22]

2.2.1.2 Axial rotation and lateral flexion

Rotation is always accompanied by lateral flexion as lateral flexion is accompanied by rotation. This is due to the orientation of the zygapophyseal joints. The amount of coupling is not uniform throughout the cervical region, but is determined by the obliquity of the articular surfaces in the frontal plane. The more vertical the joint surface, the more side bending is coupled; the more horizontal the joint surface, the more rotation is coupled.

During lateral flexion the spinous processes move towards the opposite direction than the lateral bending direction, due to the obligatory vertical rotation. With rotation to the right, the left inferior articular facet of the upper vertebra glides superiorly, anteriorly and laterally on the superior articular facet of the vertebra below; the right inferior articular facet of the upper vertebrae glides inferiorly, posteriorly and medially on the superior articular facet of the vertebra below. The anterior, posterior, medial and lateral movements constitute rotation and the inferior and superior movements constitute lateral flexion [15]. Apart from C1/2, the midcervical region displays the largest rotation.

2.2.2 Upper cervical kinematics

Motion between these joints is very complex due to the uniqueness of the joints. Due to the absence of intervertebral discs and vertebral bodies, the role of the ligaments and muscles are very important.

2.2.2.1 Flexion and extension

Flexion and extension occurs at Oc/1 and C1/2, but to a greater extent at Oc/C1, which is the pivot for the flexion and extension motion of the head. Flexion is achieved in Oc/C1 by the occipital condyles rolling on the lateral masses of C1 and translating forward and the atlas translating backwards and tilting upwards. The reverse motions occur for extension.

In Oc/1 flexion is restricted by the anterior rim of the foramen magnum, the superior surface of the dens and the alar ligaments. Alar ligaments are stretched the most when the head is rotated and flexed together, and they are relaxed during extension. Extension is limited by the connective tissue of the tectorial and anterior atlanto-occipital membranes. The inherent stability of this region is evident by the fact that the amount of sagittal plane translation seldom increases beyond 1mm [19].

The dens is closely held between the anterior arch of the atlas and the thick transverse ligaments. This prevents excessive flexion and extension. During flexion of the atlas on the axis, the dens is pushed towards this ligament and flexion of the atlas and anterior displacement is controlled.

2.2.2.2 Axial rotation and lateral flexion

C1/C2 is designed for axial rotation of the head and atlas as one unit on the remainder of the cervical spine. Rotation is in the order of 40° (the largest range) in each direction and is limited by the alar ligaments. The flattened surfaces of the articular processes assist the rotary motion. The majority of total rotation of the cervical spine occurs at this joint.

At this level rotation is coupled with vertical translation. During rotation to the left, the right inferior facet of C1 moves forwards and slightly upwards on the superior facet of C2 and the left inferior facet of C1 moves backwards and slightly downwards.

A small or negligible amount of axial rotation [23] occurs between the occiput and the atlas. The shape of the bony articulations and the alar ligaments restrict rotation at this joint.

2.3 Studying and observing kinematics

The important parameters that vertebral kinematics are measured in is Range of Motion (ROM) and Centre of Rotation (COR). The Sequence of Motion (SOM) also plays a vital role in measuring and modeling the kinematics.

2.3.1 Range of motion

A popular measuring tool to understand motion is range of motion (ROM), measured in degrees. "Knowledge of normative values for cervical range of motion is essential for design and execution of rehabilitation programs" [24].

ROM often appears in literature measured as a total range of motion (for example form C3 – C6), rather than motion at segmental level (C1/2; C2/3; C3/4 etc). Grant [12] criticizes this type of study, since the maximum ROM of a specific cervical segment is not necessarily reflected by the ROM of motion from full flexion to full extension of the neck as a whole. A specific segment can reach its maximum range of flexion or extension before the neck reaches its final position. While the neck continues towards full flexion, a vertebra may actually start to reverse its motion and extend. This behavior is particularly prominent in the upper cervical vertebrae. Thus the "total range of motion of the neck is not an arithmetic sum of its segmental ranges of motion" [12].

Although ROM forms an integral part of most kinematic studies; it is actually a volatile parameter. ROM can be influenced by the sequence of motion i.e. whether motion is executed from flexion to extension or from extension to flexion. This could result in great differences (5-15 degrees per segment), especially at the Oc-C1 and C6-7 levels [12]. ROM also varies considerably on different instances [25]. The same technique could be used at a different time and would yield different values, especially at Oc-C1, C5-C6 and C6-C7 [12]. These variations are not due to any abnormality. The normal ROM of an individual is not a discrete number, but rather a range of variation. This must be kept in mind when interpreting ROM data. In general, motion is least for the C2-C3 and C6-C7 levels, and greatest for the C4-C5 and C5-C6 levels [12]. Other variables also influence ROM and are considered for the empirical study and discussed in Section 3.2.2.

The many articulations between the cervical vertebrae make the extensive ROM in the cervical region possible. Normal ROM is limited by the thickness and compressibility of the intervertebral discs, the resistance of the muscles and ligaments of the back and the tension of the articular capsules of the zygapophyseal joints.

Figure 2-15 and Figure 2-16 provide a general overview of cervical ROM in comparison to the other spinal segments.

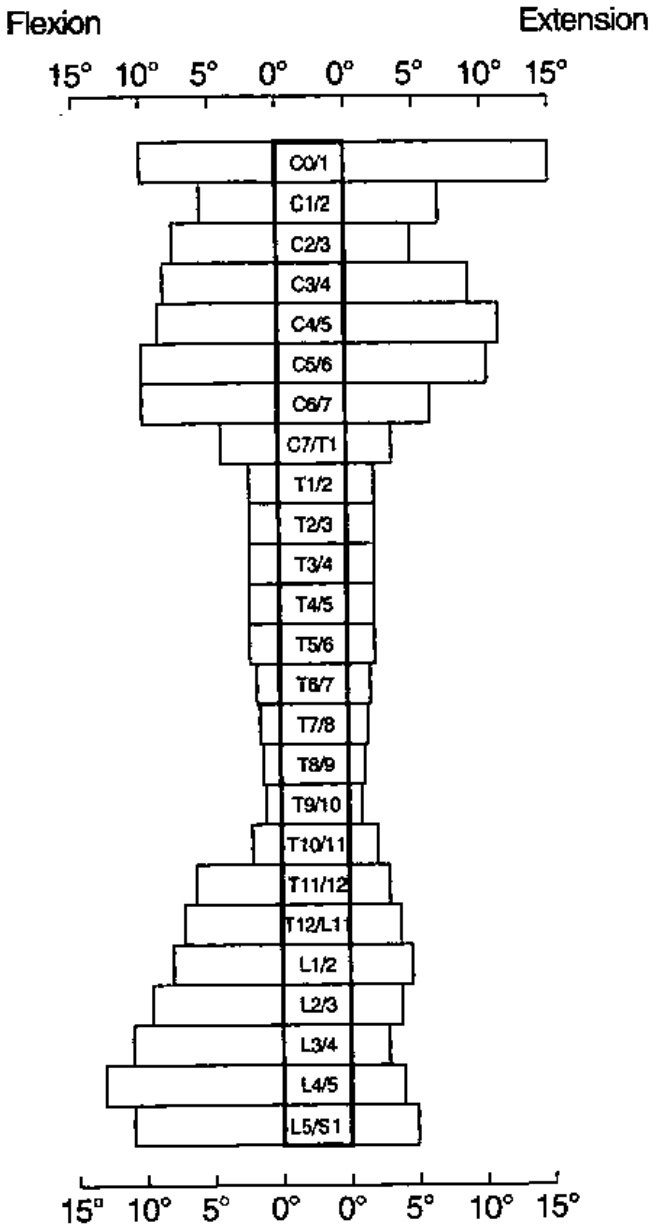

Figure 2-15 – Degrees of flexion and extension at each vertebral level [15]

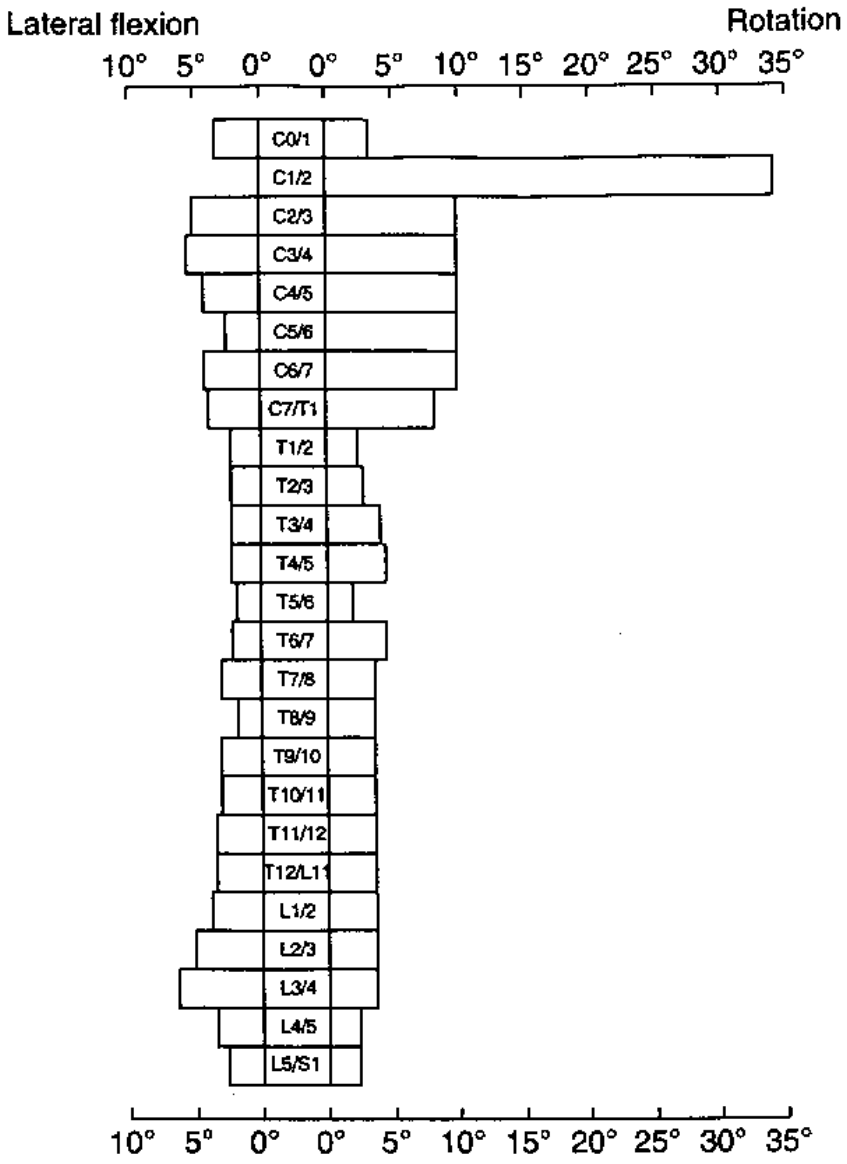

Figure 2-16 – Degrees of lateral flexion and rotations at each vertebral level [15]

2.3.2 Centre of rotation

The Centre of Rotation (COR), also referred to as the instantaneous axis of rotation (IAR) or Finite COR (FCR), is a common measurement used for clinical diagnosis of joint function, including the spine. When a cervical vertebrae moves from full flexion to full extension, the path a vertebra follows lie along an arc whose centre lie somewhere below the moving vertebrae (Figure 2-17). The centre of the arc is the COR. It is the point that is unchanged by a rigid transformation involving a translation and a rotation [26] or the point with relatively zero angular velocity over a specific time [13]. Discrepancies exist whether this point should be considered as an average COR as opposed to an instantaneous COR [13].

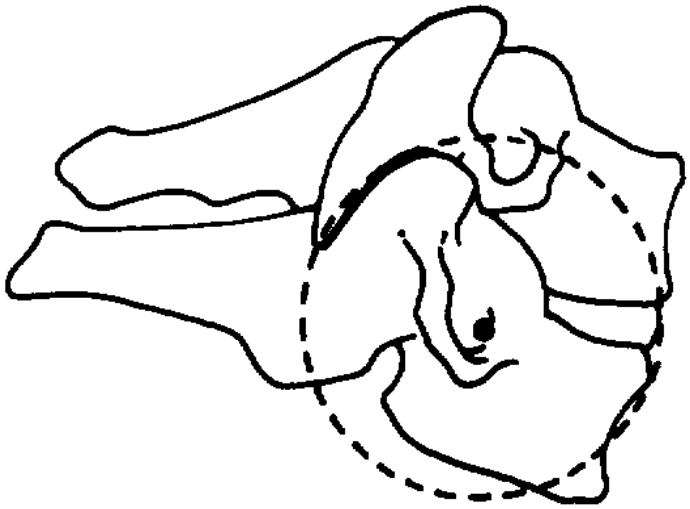

Figure 2-17 – Location of the COR for the lower cervical spine [19]

The COR is obtained with simple geometry, using two radiographs of flexion and extension in the sagittal plane. The COR is independent to the sequence or type of motion and is also stable over time, making it a "reliable, stable parameter of the quality of vertebral motion through which abnormalities of motion could be explored" [12].

The COR for flexion and extension in the lower cervical spine is different than in other areas. The COR is within the subadjacent vertebra. When the COR is located, the upward and anterior glide of the inferior facet on the superior facet can be better appreciated, since the motion follows the arc of the COR. The radii of curvature differ as the facet plane gradually increases in moving downwards in the cervical spine. The COR for flexion and extension between C1 and C2 falls in the region of the dens.

2.3.3 Sequence of motion

Many kinematical studies mention ROM and COR, but only few studies have shed light on the sequence of movement (SOM) in the lumbar region [27] and the cervical region [12]. One intuitively thinks that the cervical spine would separate in a smooth fan like progression during flexion, which is not the case. Although there is a definite pattern, it is much more complex and variation occurs at certain phases of motion. The motion pattern can roughly be divided into 3 phases for both flexion and extension.

Flexion

Phase 1: Flexion is always initiated in the lower cervical region (C4-C7). During this phase C6-C7 usually makes its maximum contribution which is then followed by C5-C6 and then C4-C5.

Phase 2: The middle phase starts with motion at Oc-C2 followed by C2-C3 and C3-C4. The order of C2-C3 and C3-C4 may vary in this phase. During this phase slight extension occurs at C6-C7 and in some individuals in C5-C6.

Phase 3: The last phase of flexion again involves the C4-C7 in the order C4-C5, C5-C6, and C6-C7. Flexion is thus initiated and terminated by C6-C7. During this phase the Oc-C2 exhibits some extension. Oc-C4 thus mainly contributes in the middle phase in variable order.

Extension

Phase 1: Extension is initiated from C4-C7, in a variable order.

Phase 2: This is followed by motion in Oc-C2 and C2-C4. Between C2 and C4 the order varies.

Phase 3: The final phase starts with another contribution by C4-C7 in the regular order from C4-C5, C5-C6 and C6-C7. During this phase the contribution of Oc-C2 also reaches its maximum.

The lumbar study has also reported that different spines exhibit different motion sequences [27]. Another interesting phenomena that Grant [12] pointed out and that has been confirmed in later studies [28] is that some joints can exhibit movement in the opposite direction than the spine or spinal region as a whole is moving in.

2.4 In vivo motion analysis

The science of human motion analysis is interdisciplinary, with a wide range of applications. Applications in the medical field include analysis of abnormalities and pathologies with gait analysis, physical medicine and rehabilitation, orthotics and prosthetics, neuroscience, medical robotics and medical training. Yet the medical field is not the only drive behind research and development of motion analysis. The competitive sport world and the fast growing animation industry are also stakeholders in the advancement of technologies in this field. In the animation industry motion analysis is used with the making of video games, movies and television programs and also virtual reality situations and simulations. In sport, motion analysis is used to enhance performance, prevent injuries, rehabilitate, develop training and treatment methods and see effects of orthopaedic and athletic devices. Other applications include industrial product design and industrial measurement and control.

The earliest spinal in vivo investigations superimposed flexion and extension radiographs and measured the angles between reference points to determine the complete ranges of motion. Advances in the technology of measurement systems have allowed investigators to gather more detailed and accurate data on normal spinal movement patterns, including axial rotation and lateral bending.

It must be kept in mind that although in vivo studies give a better reflection of true human motion than in vitro studies, one may expect considerable variation in results. This variation may be due to the natural variation with time and also the fact the in vivo loads that are applied to the spine by the subject are unknown and can thus vary since it is not controlled as with in vitro studies.

With a wide range of applications for motion analysis data collection protocols, measurement precision, and data reduction, systems are developed to meet the requirements for a specific application. The application that is focused on in this research is the motion analysis of the spine, especially the cervical region. External motion capturing and internal imaging technologies were investigated to see how motion capturing technologies have been applied to capture spinal motion. This literature review aimed to find the strengths and weaknesses of these systems when applied to capture spinal motion.

2.4.1 External motion capturing technologies

A wide range of external techniques are used and have been used to measure spinal motion. In clinical practice functional assessment is the main tool used to evaluate spinal joint movement and restriction. Functional assessment includes mobility measurements (Fingertip to floor distance, distance between tip of middle finger and floor, Schober index, Tragus to wall distance etc.), skin palpation and questioning of the patient. Although there have been efforts to develop a standardized motion palpation technique, great variability and poor inter- and intra-examiner reliability is achieved [29]. Simple and inexpensive goniometers or inclinometers have also been used to measure spinal motion [30].

More complex devices making use of potentiometers [31][32][33][34], inclinometers [25][35], gyroscopes and accelerometers [36][37][38][39][40][41], as well as optical [13][42][43][44], electromagnetic [25][34][45][46][47] and ultrasonic [24][30][31][35][48][49][50][51] technology have been developed and used. Fueled also by the advancement in other fields of application, these sophisticated technologies are prevalently used in studies and increasingly in clinical setups. This section focuses on the capabilities, advantages and disadvantages of these sophisticated motion capturing systems by investigating previous studies conducted using these technologies. These technologies have been divided into four main groups: optical and imaged based systems, electromagnetic systems, electromechanical systems and ultrasonic systems.

2.4.1.1 Optical and image based systems

Optical tracking or motion capturing is a sophisticated technique where a set of static and global coordinate systems is used from which the positions of markers are measured. Optical systems have been the most prevalently used to capture complex and dynamic human motion [37] and is seen as an established and reliable method. Therefore in studies investigating alternative methods, optical systems were typically used as comparative system to validate the findings of the new method. The Vicon system (Vicon Peaks, USA) [37] and a six camera motion analysis system (MAS, Eva HiRes, Motion Analysis Corporation, USA) [52] are among the systems used to evaluate the accuracy of inertial sensors.

Optical systems triangulate the 3D position of a marker between one or more cameras calibrated to provide overlapping projections. Tracking a large number of markers or multiple performers or expanding the capture area is accomplished by the addition of more cameras. These systems produce data with 3 degrees of freedom for each marker, and rotational information must be inferred from the

relative orientation of three or more markers. For instance, the markers of the shoulder, elbow and wrist will provide information about the angle of the elbow.

The most common marker system used is the passive marker system; using reflective markers (see Figure 2-18). Cameras send out infra red light signals and detect the reflection from the markers. Other type of optical marker systems include active marker system, where the markers themselves are powered to emit their own light, and also semi-passive imperceptible markers systems where photosensitive marker tags are used instead of reflective or active light emitting diode (LED) markers. In these cases the markers can compute not only their own locations, but also their orientation, incident illumination, and reflectance.

Figure 2-18 – The reflective balls of the Vicon optical system while compared to the Moven inertial system [53]

Studies making use of optical systems are mostly concerned with gait analysis or other gross movement analysis such as the evaluation of neck and upper limbs during daily activities [42], or postural and functional analysis of patients affected by spinal deformities [43], as opposed to motion at each vertebral level. However, some studies [13][44][54] that estimated vertebral motion from skin markers have made use of optical systems. A study by Gracovetsky et al. in 1995 [54] was the first study to succeed in using an opto-electronic system to measure the motions of a series of light-emitting-diode (LED) markers placed on the surfaces of individual spinous processes during trunk flexion.

A study [55] quantifying the accuracy of kinematics measured by an optical and electromagnetic tracking device has found that both systems underestimated the range of motion. This was concluded after a mechanical articulator that mimicked three-dimensional joint motion through known ranges was measured with the two systems. With the application of post hoc smoothing and correction algorithms, noise was eliminated and the results of these systems were improved.

The down side to using optical systems is the cost and volume of the equipment, which restrict this method to a laboratory environment. Occlusion, resulting in lost position data, is another problem experienced with optical systems. This problem is overcome by adding more cameras, which once again adds to the cost of such a system.

Systems with standard video camera/s are an attractive prospect due to lower costs. Research in computer vision is leading to a markerless approach to optical motion capture, especially in the field of animation and virtual reality. Markerless systems do no require subjects to wear special equipment. Computer algorithms identify the human forms and break them down into small segments that are then tracked. These systems work well with large motions, but tend to have difficulties with fingers, faces, wrist rotations and small motions. This approximation is crude and far from the true motion. In medical application such systems would provide very gross kinematic analysis, but could however be supplementary to a study to investigate topics such as amount of bends of an individual during a normal day [11], that does not require the tracking of small movements.

2.4.1.2 Electromagnetic systems

Another established method for motion capturing is electromagnetic motion tracking systems. Magnetic systems calculate position (X, Y, and Z Cartesian coordinates) and orientation (yaw, pitch and roll) by the relative magnetic flux of three orthogonal coils on both the transmitter and each receiver. The 3SPACE Fastrak motion tracking systems (Polhemus Inc., USA) is frequently used in neck research, and was therefore considered as the criterion for investigating the capabilities of new wireless orientation sensors for neck assessment [40].

The Fastrak generates a low-frequency magnetic field which is detected by sensors. Studies using systems from Polhemus have been conducted measuring lumbar ROM [45], cervical rotation [46] and the relationship between the lumbar spine and hip movement [59][60][61][62]. The lumbar ROM study [45] measured 100 subjects across age and gender. The results compared well to X-ray studies and proved the system to be a good tool to use routinely in a clinical environment.

An interesting study using an electromagnetic device, Flock of Birds (Ascension Technology, USA) developed a technique to measure spinal motion of a rower with the potential for real time feedback for training purposes. The findings were validated with MRI [47].

Although the electromagnetic sensors are relatively small (0.9 mm x 0.9 mm x 0.9 mm [28]), studies are rarely measuring the intervertebral range of motion with sensors at each or at every second spinous process. However, a successful and recent study predicting intervertebral lumbar movement using four electromagnetic sensors has been conducted [28]. The data from the sensors, shown in Figure 2-19, have been used as input for a probabilistic graphic model that achieved great correlation with radiographic images.

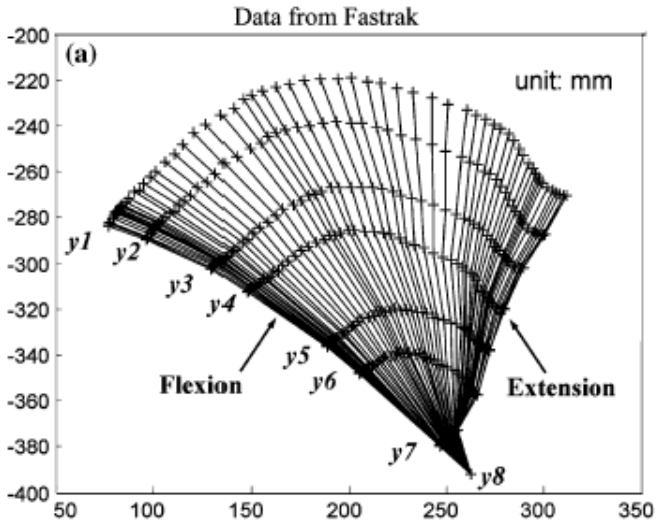

Figure 2-19 - Data from Fastrak used in study by Lee et al. [28]

The advantages of electromagnetic devices are that they are accurate and relatively inexpensive. The Fastrak system achieves angular accuracy of ± 0.2° [56] and a XYZ coordinate accuracy of 0.03" [57]. The costs of the Fastrak systems start at $2500 and can go up to $35,000 [58]. Since the sensor output is 6 DOF, useful results can be obtained with two-thirds the number of markers required in optical systems. Most electromagnetic systems are portable and easy to use. Some sophisticated devices such as the Flock of Birds, shows high precision and a good intraobserver and interobserver reliability, but is not easy to use in a clinical setting, because it is not portable and has an extensive calibration procedure [25]. The markers are not occluded by non-metallic objects but are susceptible to magnetic and electrical interference from metal objects in the environment, such as steel reinforcing bars in concrete or wiring, which affect the magnetic field, and electrical sources such as monitors, lights, cables and computers. This limits the use of secondary instruments that could enhance a study such as electromyagraphy (EMG). The capture volumes for magnetic systems are smaller than they are for

optical systems, due to tracking reliability being a function of distance from the electromagnetic source [40]. Still magnetic tracking is seen as "a promising technique for clinical evaluation of joints" [36].

2.4.1.3 Ultrasonic systems

According to Cagnie et al. [24] sophisticated systems like the Ultrasound based measuring system Zebris (Zebris Medical GmbH, Germany) has been a significant breakthrough in measuring spinal motion and "appears to be one of the best devices available at the moment to measure spinal ROM". The results of studies using Zebris is in agreement with this statement. Ultrasonic systems are relatively new technology and since 2000 several studies have shown the Zebris to be an accurate and reliable tool [24][35][50] for longitudinal tracking [32] of spinal motions, "delivering precise and reproducible data of spinal motion in the three main planes" [30]. As discussed in the previous section the system exhibited good agreement with goniometric systems [32][35][50].

The Zebris measurements are based on determining spatial coordinates of miniature ultrasound transmitters positioned relative to a fixed system of three microphones. By means of triangulation, the measurement is derived from the time delay between the ultrasound pulses. The unit is connected to the parallel port of a personal computer, allowing the data transmission. The spatial position is calculated by the system's software and graphically displayed in time. An extensive report is also available that presents the data as total and local mobility capacity (flexion, extension, rotation, lateral flexion and coupled movements) as well as mobility coordination (quality of performance, ability to reproduce movements or movement restrictions as seen in the coefficient of variability). During the measurement the patient makes fluent movements to his maximum mobility.

In terms of spinal motion there are two types of systems: a single marker system (Figure 2-20 A) and a triple marker system (Figure 2-20 B and C). With the single marker system small flat ultrasound transmitters are attached to the skin along the back, allowing motion capture at vertebral level. A non-random motion pattern of the body surface markers with 1° of accuracy is achieved. The triple marker system uses a harness approach and hence only motion capture of a spinal region is possible. However, by means of the special mounts, an optimum transmission of the ultrasound pulses to the measuring sensor is ensured during all movements, achieving 0.5° accuracy.

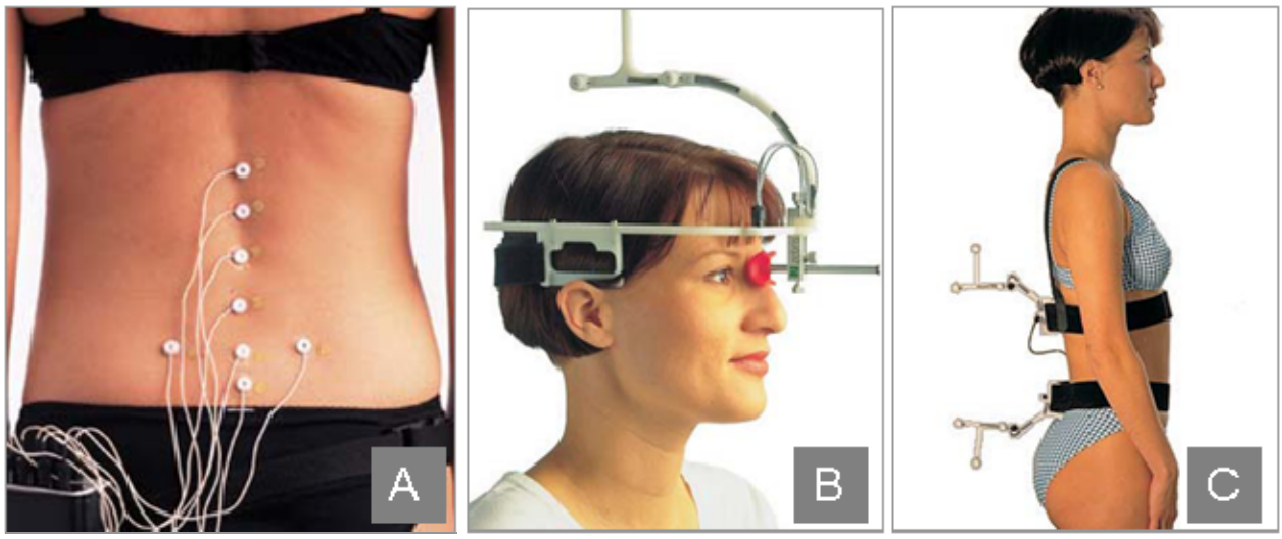

Figure 2-20 – Ultrasound based system, Zebris [63]

Research in the cervical region has been conducted with the Zebris with large subject groups considering age and gender [30][48] and pain [24][49]. Although the Zebris has the capacity to measure intervertebral motion all these studies have been done with the triple marker system, measuring gross cervical motion.

Ultrasonic systems prove to be a reliable tool. It is also non-invasive, patient mountable, portable, and the markers are small (d = 10 mm) and light (3 g each), which does not hinder natural movement. Yet, like any other system there are limitations. The subject has less freedom to move with ultrasonic systems, since he must remain within a prescribed distance of the microphones (1m) to ensure accurately conveyed ultrasonic signals [32].

2.4.1.4 Electromechanical systems

Systems making use of electromechanical components or a combination of components can be divided into two groups operating on different principles. The first includes systems that measure orientation with regard to a change in inertia, hence inertial systems. The second is systems that measure body joint angles, referred to as goniometric systems.

Inertial systems

Inertial systems have the capacity to determine absolute orientation and track movements in three dimensions. Inertial motion capturing systems is not as established as optical or electromagnetic systems, but is a promising option and attracts research attention. "Orientation sensors are becoming more prevalent for biomechanical and motion analysis, both for research and in the clinical environment" [64].

Other fields of application, such as aerospace, virtual reality systems and robotics also make use of inertial systems to obtain orientation information of solid objects in 3D [37]. For motion capturing there is a variety of inertial systems, and the components that are typically used include gyroscopes and accelerometers. A gyroscope is a device for measuring or maintaining orientation, based on the principle of conservation of angular momentum. It measures the angular rate of rotation. An accelerometer is an instrument that measures the amount and direction of change in velocity. Gyroscopes have been shown to be highly correlated with video based motion capture [65][66][67].

The technological advancements in micro-electro-mechanical systems (MEMS) and the use of magnometers or advanced filters to compensate for accumulating drift error [36][38][39], has inspired the development of more sophisticated inertial systems. Sophisticated software to make data available in real time, user friendly and intuitive has also added to the attraction of such systems [36].

When looking at the progress of these systems a study that stands out is a study done by Lee et al. in 2003. Lee commented that there was a need to develop a "new method of measuring lumbar spine motion that can be used routinely in clinical assessment" [36]. The purpose of the study was to examine the reliability of a new method of measuring lumbar spine motion using a three-dimensional gyroscopic system. The system consisted of two inertial sensors, each comprised of three orthogonally aligned gyroscopes. The sensor also contained solid-state gravitometers and magnetometers which sensed the gravitational and magnetic fields of the earth. Such information was used to eliminate drift of the gyroscopes using a Kalman filter. "The results of this study indicate that the inertial tracking system is a reliable device for measuring movements of the lumbar spine" [36].

Another study [40] that more recently validated the use of inertial systems verified the performance and suitability of new generation 3D wireless orientation sensors to measure cervical range of movement against a criterion standard instrument (Fastrak). The wireless orientation sensor (InertiaCube 3) consists of 9 motion-sensing elements: 3 accelerometers, 3 angular velocity rate transducers and 3 magnetometers. Measurements of cervical range of motion in each primary plane were directly compared and high cross-correlations of 0.97 to 0.99 were obseved.

Good results were not only delivered from studies concerning spinal kinetics, but also kinematics of trunk and upper limb movement [39][41].

Inertial systems overcome many of the problems experienced with other methods [36].

- Its portability provides freedom from studios or laboratories
- Large capture areas

- No occlusion problems
- No latency
- Inexpensive
- Patient mountable
- Non invasive
- Use other devices (such as EMG) simultaneously

Drawbacks of inertial systems include:

- Accumulating drift errors - which can mostly be resolved with advanced filters or additional components
- Inaccurate measurements of linear translations, Inertial sensors are not true 6 DOF systems as electromagnetic systems [40]
- The size of typical sensors are too big to be used in measuring spinal motion at intervertebral level (see Figure 2-23)

Goniometric systems

Goniometric systems are typically rigid structures of jointed, straight metal or plastic rods linked together with potentiometers that articulate at the joints of the body [31] and are often referred to as exo-skeleton motion capture systems, due to the way the sensors are attached to the body. The skeletal-like structure is attached to the body and the mechanical part move as the body does, measuring the relative motion. In the cervical region it is typically attached to the body by a thoracic strap and a helmet. An example of a typical exo-skeletal goniometric system is seen in Figure 2-21.

Figure 2-21 – Goniometric system – Gypsy6 [68]

Another goniometric system that is continually used for spinal ROM studies [31][33][34] is the CA6000 Spine motion analyzer (OSI, USA). This device consists of six potentiometers and seven links. The changes in relative angles of the link system results in changes in voltage that provides information that can express 3D motion components in Euler angles within an accuracy of 0.1°.

The accuracy of rotational motion was questioned in studies using earlier versions of CA6000 [33], but in more recent studies motion in all planes was successfully captured. This system has been confirmed as a reliable, accurate and reproducible tool to study cervical kinematics [31] and normative ROM databases have been developed using this system for the cervical region with 250 subjects [31] and 405 subjects in the lumbar region [33]. This is however gross motion of the cervical spine and intervertebral motion is not measured with this system [31].

The CA6000 was compared to the Fastrak system. Although both systems were confirmed to be reliable in single measurements and in longitudinal studies, the results did not always compare well between the systems. These results may be due to the systems not being used simultaneously [34].

The CA6000 Spine Motion Analyzer has also been compared the newer Ultrasonic device, Zebris. Both devices were found to be highly reliable and suited for longitudinal studies. In this study the devices yielded reliable and comparable measurements in the primary planes of motion. Axial rotation in flexion or extension showed poor correlation and significant differences [32].

Other systems measuring joint angles include inclinometers. Inclinometers measure change of angle relative to the direction of gravitational pull. They are simple and inexpensive. The Cybex Electronic Digital Inclinometer (EDI-320) has been compared to the Flock of Birds electromagnetic system and a

substantial and significant difference was found between the two systems and also over time [25]. In a study by Malstrom et al. [35], the Myrin goniometer (RR Parir, Sweden) was compared to the Zebris. The Myrin consists of an inclinometer and a compass. Inclinometers cannot measure motion in the transverse plane, hence the use of a compass that measured horizontal rotation. Both the Myrin and Zebris were found to be reliable and showed good agreement with each other [35].

Goniometric or mechanical motion capture systems are real-time, relatively low-cost, free- of-occlusion systems. With the CA6000, the whole device is patient mountable and the only limitation in terms of capture area is the length of the cable interfacing the device to the computer. Due to the bulkiness or exo-skeletal structure of the systems some consider the accuracy of electrogoniometric systems to be low [42].

2.4.1.5 Summary of external motion capturing systems

In the application to spinal motion capturing the different systems investigated showed both strengths and weaknesses, as summarized in Figure 2-22.

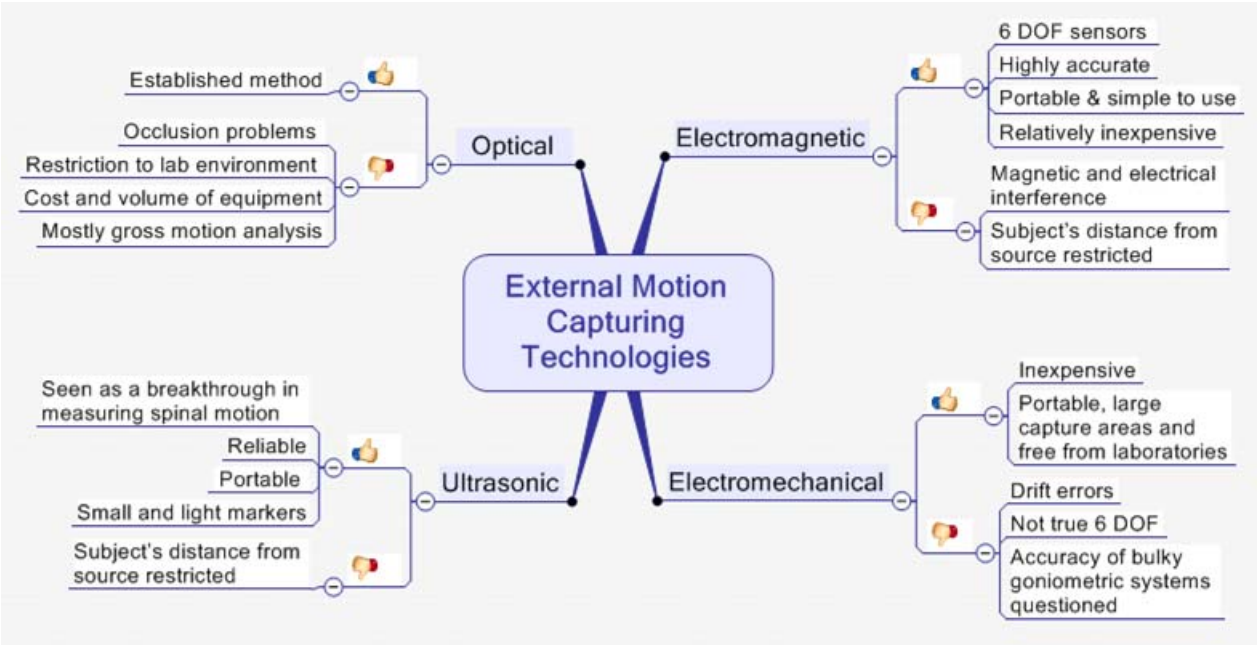

Figure 2-22 – Strength and weaknesses of external motion capturing systems

The advantages of external motion capturing systems in terms of safety, costs, ease of use, portability and diversity are abundant. Although each type of technology has drawbacks, in most cases it could be overcome by another type of technology. Therefore external marker systems as a whole can meet most motion capturing needs and applications.

A common drawback of external motion capturing systems is that these systems often lacked the ability to accurately capture motion at the intervertebral level. "Quantitative assessment of the spinal kinematics at individual vertebral level can yield important and necessary information" [13] and is crucial for the purposes of obtaining kinematical data for simulation studies and research on the intervertebral disc. Although many external marker systems provide valuable information about gross motion or posture, they failed to produce information about motion at each vertebral level and correlated poorly with measurements taken for each vertebral level [74][79][80].

As discussed in section 2.3.1 and 2.3.3, the motion of a whole spinal region does not necessarily relate to the motion of each motion segment of that region. Therefore it is important to look at motion at each intervertebral level. The main reason for systems not being able to capture intervertebral motion appears to be the sizes of the sensors or markers.

The space between adjacent spinous processes is very small and especially with extension in the cervical region the space for external markers is greatly limited. Studies relying on surface marker measurement have mostly focused on gross kinematical information, putting markers at for example, T1 and S1 [38] for trunk motion, L1 and S1 [36] for lumbar motion and C7 and the head [40] for cervical motion. The weight and size of markers could also hinder the natural movement of the spine, for example when markers lie close together and interfere or stick together [69].

Inertial sensor units (Figure 2-23) used were typically too large for measuring motion at each intervertebral level (26.9 mm x 34.0 mm x 30.5 mm [36]). Typical electromagnetic and ultrasonic sensors, seem more suitable (Fastrak: 0.9 mm x 0.9 mm x 0.9 mm [28], single marker system from Zebris: d = 10 mm, h = 4 mm [63]) and could be considered for obtaining data of motion segments. Altough these sizes are smaller, they might still be impractical for capturing intervertebral motion. As sensors continue to become smaller, this problem could be overcome.

Figure 2-23 – Size of typical Inertial sensor, Xsens

There is one fundamental problem that featured in all external spinal motion capturing systems: the external markers, transmitters or sensors are subject to movement of the skin and tissue between the vertebrae and the markers and therefore its credibility to reflect the true vertebral motion at each level is questioned. Several studies mentioned this problem and warn of the errors in measurement due to skin effects [13][28][36][42][55][70].

> "Any measurement of movements of sensors or markers attached to the overlying skin will suffer from the movement of soft tissues disguising the true vertebral movements [71].
>
> "The great disadvantage of using surface markers is that skin artefacts and muscle deformations can change the anatomical meaning of each of the markers and reduce the accuracy of the kinematical estimation" [44].

Skin elasticity and folding as well as the varying soft tissue thickness remains the biggest issue and the most difficult to overcome. Several studies have made effort to minimize this effect. Lee's studies with inertial sensors [36][59][60][61][62] has made use of a velcro band threaded through the plastic plate containing the sensors, which is tightly wrapped around the subject's body to minimise movement between the sensor and the skin. Another study [13] lessened the effect by filtering the non-circular motion component and high-frequency noise.

In conclusion, external motion capturing systems have great value and pose many advantages, but the great disadvantage of having reduced accuracy due to skin and soft tissue will not easily be overcome. Therefore one needs to include a look at motion capturing technologies that are more than skin deep.

2.4.2 Internal imaging technologies

The problem with external surface markers is overcome by using technologies that can evaluate the movement of the spine at intervertebral level. "Only radiographic techniques are able to determine movement of the vertebrae with acceptable accuracy in vivo." [72] Technologies such as X-rays, MRI and Fluoroscopy have often been chosen to be used in motion capturing studies for this particular reason. Other benefits of using internal imaging technologies is that it does not only provide information on motion, but also on possible causes of pain, such as tumors, infections and fractures. Therefore internal imaging technologies are standard procedure when investigating back and neck pain in a patient.

The downside to X-ray imaging (Radiographs, Fluoroscopy, and CT) is the exposure to ionizing radiation. In 1895 Roentgen discovered the X-ray and it was soon used in various applications. X-rays were put to diagnostic use very early before the dangers of ionizing radiation had been discovered. After the development of the image intensifier in 1955, the radiation dosage was decreased. Today X-ray technology is widely used, but one is still cautious not to expose an individual to a high radiation dosage. Therefore when capturing motion with X-ray technologies, only a limited number of static images are typically obtained. These images are usually in the neutral position and the extreme positions of mobility.

The SI unit for radiation is sievert (Sv). This is the unit for effective dose. Radiation affects different body parts in different manners. Effective dose is used to compare radiation doses on different body parts on an equivalent basis. Therefore it is a weighted average that takes a particular body part and the associated radiosensitivity into consideration.

Other units include rad, rem, and roentgen and for human tissue they can be considered as equal in value. Exposure is a measure of the strength of a radiation field at some point in air and is most commonly measured in roentgen (R). Rem is an acronym for "roentgen equivalent in man." One rem is equivalent to 0.01 Sv.

CT and procedures using contrast material[a] expose an individual to much higher radiation than other procedures. Table 2-1 shows different procedures compared to background radiation exposure that the average American is typically exposed to. This background radiation is from natural occurring radioactive materials and cosmic radiation from outer space and varies throughout physical location.

[a] A fluid injected into the body which is opaque to x-rays and allows a radiologist to examine the organ or tissue it fills

Table 2-1 - Dose of procedures compared to background radiation [73]

Procedure	Effective radiation dose	Comparative natural background radiation
CT- Abdomen	10 mSv	3 years
CT - Body	10 mSv	3 years
Radiography - Lower GI Tract	4 mSv	16 months
Radiography - Upper GI Tract	2 mSv	8 months
CT - Head	2 mSv	8 months
CT- Spine	10 mSv	3 years
Myelography	4 mSv	16 months
CT-Chest	8 mSv	3 years
Radiography - Chest	0.1 mSv	10 days

As with the external systems there are different types of technologies available, with different advantages, disadvantages and applications. Procedures typically used in literature for capturing motion include radiographs and fluoroscopy (2D) and MRI and CT (3D).

2.4.2.1 2D Imaging with radiographs and fluoroscopy

Radiographs, or X-rays, are the application of radiation to produce a film or image on a screen of a part of the body to show the structure of the bones and outline of the joints. Sagittal plane radiographs evaluating flexion and extension motion at segmental level are most commonly used to assess spinal mobility and instability. Radiographs show angular movement and translation of one vertebra on the one below [29]. Several studies have developed and assessed techniques for both manual and computerized measurement techniques to capture motion from radiographs [23][29][74][75].

When considering motion, radiographs are usually taken at neutral, flexion and extension. If abnormal motion occurs in the middle ranges of spinal motion, then radiographs may not accurately identify the abnormality [79]. There fluoroscopy, or Digital Video Fluoroscopy (DVF), can aid in better understanding the complete motion. Fluoroscopy is basically an X-ray movie, showing the motion of internal body structures. "The vertebral landmarks throughout fluoroscopic imaging provided an objective and precise quantification of intervertebral movement" [76].

The subject is positioned between the X-ray source and image intensifier and sequential, two-dimensional X-ray images are taken. The X-ray beam can be positioned freely, which makes positioning easier, especially for patients with reduced mobility. A trade off between image quality and radiation dosage exists, hence the fluoroscopy image is of poorer quality than an X-ray. The quality also varies across the image because of the point-like X-ray source. Fortunately, being in digital format, image-processing techniques can be used to enhance features.

A series of DVF images (66 images) was taken of the flexion-extension motion of the neck. It was done to see what the capabilities of the technology are. A few of these images are presented in Figure 2-24.

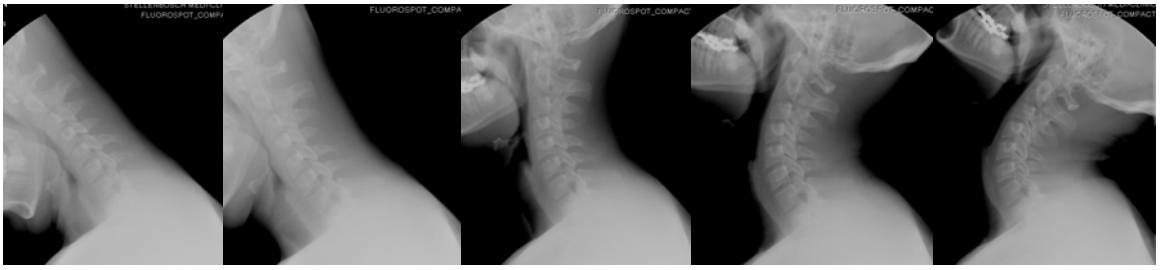

Figure 2-24 – Extracts from a series of DVF images

For a flexion and extension study on cervical intervertebral motion [77] and intervertebral angulation and translation [78], DVF was chosen because it was digital, provided images comparable to radiograph without requiring more radiation and at a rate of 30 frames per second it produced more than enough images to capture the continuous motion of each intervertebral level. The average radiation exposure on each subject was 0.45 R (roughly 4.5 mSv) [77].

In three studies [79][80][81] dynamic 3D spinal models driven by an individual's kinematic data have been constructed. The spine was constructed by using data from computed tomography (CT) and the motion was modelled from 2D kinematic data. In these studies DVF was chosen as the motion capturing tool. Several motion capturing methods were explored [79][80], but a radiographic approach was followed to get accurate information of kinematics at segmental level and from there fluoroscopy was chosen. According to Cooper et. al. [80], DVF is the only method currently available to perform a reliable segmental analysis with minimal invasion. "DVF has all the benefits and capabilities of radiographs it just have the added benefit of obtaining real-time motion, without subjecting the patient to more radiation" [79].

It must be kept in mind that an individual image using DVF may expose a patient to less radiation, but that it adds up and lengthy procedures could once again result in high exposure levels.

The largest drawback to radiographs and DVF is the fact that it can only capture motion in two dimensions, giving no information on for example coupled movements. Biplanar radiography was the first tool to measure in vivo coupled motions. It constructs 3D data from two radiographs taken at angles of 90° apart. This method has a large potential for intra- and interobserver variability in identifying the same reference points on separate views precisely. These reference points could however be enhanced by implanting metal pins into a subject. This technique is known as stereoradiography or radio stereophotogrammetry and can provide precise motion measurements.

However, the invasiveness as well as the extensive laborious measurement process makes it less attractive for routine clinical scenarios. Therefore other three dimensional dynamic imaging techniques are pursued.

2.4.2.2 3D imaging with MRI and CT

Magnetic Resonance Imaging (MRI), formerly referred to as Magnetic Resonance Tomography (MRT), or Nucleur Magnetic Resonance Imaging (NMRI), is a non-invasive method that renders three-dimensional images of internal body structures using a powerful magnetic field, radio waves and computer technology. MRI does not use ionizing radiation. In MRI a magnet is rotated around body, exciting its hydrogen atoms. A scanner is then utilized to detect the energy emitted by the excited atoms. Since the human body is composed primarily of water (which is two parts hydrogen), MRIs provide exceptional detail of the body and in particular the spine's anatomy. It is used in medical imaging to demonstrate pathological or other physiological alterations of soft tissues, for example intervertebral disc disorders in the spine. "MRI was first introduced into clinical practice in 1980, and has since become the modality of choice in the evaluation of persistent back pain." [82] MRI has also been used to determine kinematic data in asymptomatic individuals.

A series of studies done by Ishii et al. [70][83][84] has showed the worth of MRI in kinematical studies. These studies were concerned with in vivo 3D motion of the upper cervical, the cervical and lumbar spine and produced the first in vivo coupled motion for the cervical spine during head rotation [83] and lateral bending [84]. They have also investigated relative motions of individual lumbar vertebrae during trunk rotation [70].

In these studies 3D MRIs were obtained in several different positions of asymptomatic volunteers. A novel system that evaluated 3D motion, using voxel[a] image registration with coefficient correlations was used. The method of voxel-based registration determines relative positions between volume images represented at different coordinates, using a corresponding method based on correlation between voxel values. The correlation coefficient is used as a measure of similarity. A segmented 3D MRI of the vertebra in the neutral position was superimposed over images for each position. Relative motion of the spine was then calculated by starting from initial transformation parameters and finally finding the parameters allowing maximal correlation of the two images. Relative motions were measured and described with 6 degrees of freedom by rigid body Euler angles and translations.

[a] A voxel is a 3D version of a pixel. Voxels are generated by imaging systems, such as CT and MRI.

Although MRI can render valuable information on intervertebral kinematics its use could be limited by the fact that it is a very expensive technology with high maintenance costs.

Computed Tomography[a] (CT), originally known as computed axial tomography (CAT) or body section roentgenography, provides very high quality three-dimensional images of the internals of an object from a large series of two-dimensional X-ray images taken around an axis of rotation. The patient is required to keep stationary during image acquisition and hence CT cannot yield motion information. To obtain CT's in several incremental positions, as often done with radiographs and MRI, could yield information on motion, but would result in a very high radiation dose. Therefore CT is not suited for capturing motion. In literature CT is used to construct 3D visualization models, while the kinematic data is obtained in 2D with other technologies [79][81].

2.4.2.3 Summary of internal imaging technologies

The strength and weaknesses of internal imaging technologies is summarized in Figure 2-25.

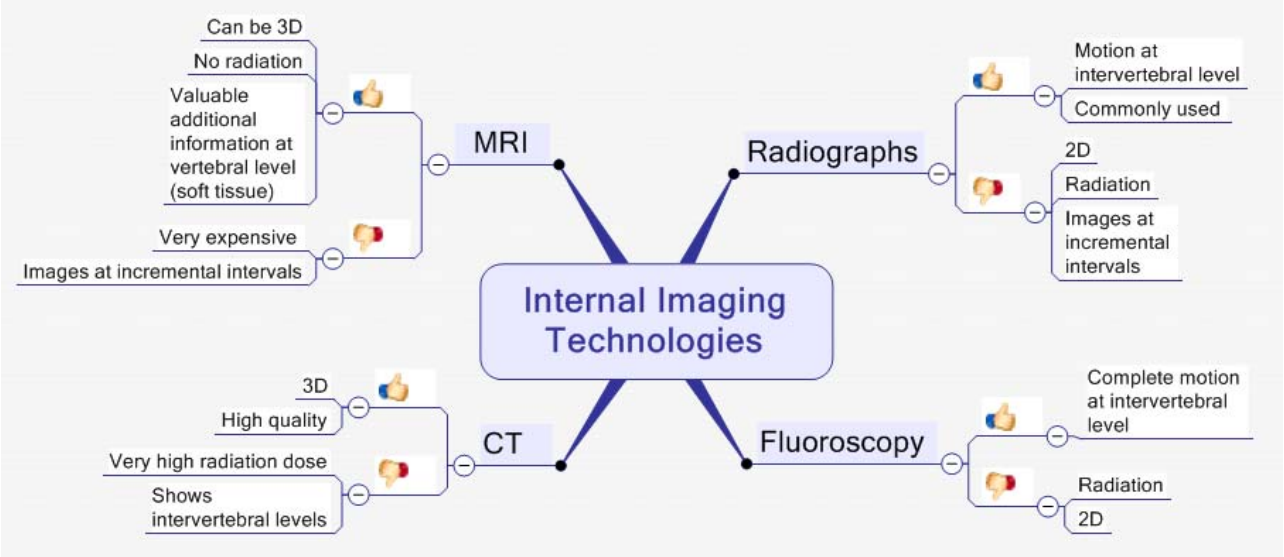

Figure 2-25 – Strength and weaknesses of internal imaging technologies

Internal imaging technologies all have the potential to provide valuable information of motion at intervertebral level, although in practice CT would not be used for motion capturing due to high radiation dose. In terms of the advantages that external systems poses towards low cost, safety, simplicity, portability and producing accurate three dimensional position and orientation, these internal technologies did not compare well. Although MRI showed excellent potential in being used for 3D kinematics, it also has the downside of being expensive and high in maintenance. It would be ideal to

[a] Greek: tomos (slice) and graphein (to write)

have all the practical advantages of external motion capturing systems along with the capabilities of internal imaging technologies.

2.4.3 Need for empirical study

The ideal is therefore to use the external motion capture systems with the confidence that it reflects the true motion of vertebra at each level. The essence of the questions posed in the problem statement is firstly whether any surface makers can in principal accurately represent vertebral motion. Thereafter more information could be deducted concerning the relationship and the factors that influence this relationship.

To attempt answering this fundamental question one needs to be able to see the vertebrae and the surface marker and the same medium and instance, without any discrepancy of accuracy of different systems or variability from motion at different instances. To accomplish this one would need to approach this problem with a radiographic method, while radio opaque markers, representing the reflective markers, sensors or transmitters, is placed on the individual's neck. Both the motion of the radio opaque objects and the vertebrae have to be visible simultaneously. With radiographic images at different motion instances, the correlation between the motion of the skin markers and the vertebrae of the cervical region can be investigated.

3 Empirical study

Reviewing available motion capturing technologies initiated the need to observe the relationship between surface marker motion and vertebral motion in the cervical spine.

3.1 Previous studies

Some of the earliest studies posing the question of intervertebral motion from skin markers was conducted in 1989 by Bryant et al. [85] where the vertebral body positions were determined from skin markers. In 1995 a key study was conducted by Lee et al. [86] In this study flexion, neutral and extension radiographs were taken of the motion of the lumbar spine, while lower limb motion was constrained by a frame. Radio opaque markers were attached to the skin at the spinous processes of L1-S1. A non-linear regression model, taking into consideration skin folds and skin distraction values, was developed and validated. The result of this study was that this model could yield intersegmental sagittal motion from skin markers within an error range of 0.05-0.56 degrees. In 1996 they applied this model by using data from a radiographic and optical motion capturing system and compared the sets of mobility angles [87]. In 2003, a study [13] was published with a different approach to this problem. A mathematical model was developed that interpreted motion in terms of CORs, located for each motion segment from skin markers. The model did not take any anthropometric data into consideration, as with other studies [86][88], but the effect of skin motion artifacts was lessoned by filtering out noise and non-circular motion components. This study also only considered rotation (average CORs) and translational motion was not taken into account. In 2004 Cerveri et al. [44], started to address three dimensional intervertebral motion obtained from skin markers. A kinematical model was constructed that used video recording and three skin surface markers at each motion segment to estimate vertebral rotations. In some studies [88][89], MRI has also proven to be a useful tool when developing methods and models to reflect the relationship between internal segmental and external marker defined motion.

The most recent study on this topic is by Lee et al. [28]. A Bayesian network dynamic model was developed to estimate the kinematics of the intervertebral joints of the lumbar spine. Radiographic images in flexion and extension were used as extreme value inputs and the intermediate motion was obtained from skin surface markers of an electromagnetic motion capturing system. The model was validated by comparing the predicted position of the vertebrae in the neutral position with those obtained from the radiographic image in the neutral posture. A correlation of 0.99 and a mean error of less than 1.5° were achieved.

Although there are a great variety of studies done with different tools and models, the focus is mostly on the lumbar spine. Studies have been done on different positions and postures of the lumbar spine

[90] and also on other parts of the body, such as hands [91]. Only few studies were found where the relationship between skin marker motion and vertebral motion in the cervical spine was investigated. A study by SK Wu et al. [76] has examined the reliability of measuring cervical motion with surface markers with the aid of video fluoroscopy. The average intraclass correlation coefficient of the paired vertebral angles throughout different ROMs between surface markers and bony landmarks ranged from 0.844 to 0.975. The mean absolute difference between the vertebral angles determined by surface markers and bony landmarks averaged 2.96°, indicating a high consistency between surface markers and bony landmarks.

3.2 Study particulars

This relationship between surface marker motion and vertebral motion was investigated by observing the motion with a radiographic method and radio opaque markers to see the vertebrae and the surface markers simultaneously on one medium.

The objectives of this empirical study are to:

- Deliver information on intersegmental mobility for the use in simulation models in further research in this field. This is done in the form of rotation and ROM.
- Report on the relationship between surface markers and vertebrae during motion, as well as what variables contributed to variation in this relationship.

3.2.1 Ethical aspects and technology used

When making use of a radiographic method there is inherent risk involved for the subjects. Therefore the study was first approved by the Committee for Human Research.[a]

This approval implies the following:

- The method was reviewed and approved.
- Everyone involved in the study agreed upon full confidentiality of participants' information.
- All participants were informed of what the study entail, the risk of ionizing radiation and the dosages that they were exposed to. They have given written consent to take part in the study.
- Participants were treated according to the requirements of the Committee of Human Research.

[a] Project Number: N/08/04/102

This risk involved also determined the choice of the technology that was used in the study. DVF was the initial choice and was investigated. A series of DVF images of a fellow researcher was obtained to investigate the capabilities of the system (Figure 2-24). Although it is digital and therefore exposes a participant to less radiation than normal film radiographs, in the case of a research study, one would want to expose a participant to as little as possible radiation and minimise or completely eliminate the risk involved. Therefore the digital Statscan Critical Imaging System from Lodox[a], especially known for its much lower dosages than its equivalents, was chosen to be used in the study.

Figure 3-1 - The Lodox Statscan [92]

A Lodox lateral cervical scan has an effective dose of 2.1 µSv [93]. This low dosage is accomplished by the 4 mm thin laser like beam that moves horizontally to complete a full scan, rather than the conventional large primary beam covering area of other systems. The scatter is also negligible, making it much safer for medical personnel and allowing multiple benefits to using this in the emergency and trauma milieu. For example, critical patients remain completely accessible to emergency professionals during the examination. The throughput rate is also much higher, making it ideal for assessing emergency patients. A full body scan can be completed in less than 13 seconds. The Statscan is also capable of ultra-low-dose low resolution full body screening as well as high resolution detail studies.

A practical advantage to using the Lodox Statscan was that such a system was available at a research unit, the Lodox Programme at the University of Cape Town. The system and the expertise of the employees of the Lodox Programme were available for the study free of charge.

[a] Lodox (Low Dosage X-rays) – a South African Consortium. Lodox began form a unique image detector technology that was originally developed for security purposes by De Beers.

The inherent risk of ionizing radiation would further be reduced by only taking the necessary area and at the lowest resolution. It was also decided that five scans is the least amount of images that would still provide a good impression on the complete motion path that a vertebrae follows. Images were also taken in only the sagittal plane. This adds up to a total of 10.5 μSv effective dosage per participant. The Health Physics Society allows the general public 1 mSv effective dose per year. "At this dose, risks of radiation-induced health effects are either nonexistent or too small to be observed" [94]. This study was well within the allowable dosages and safe for the participants.

3.2.2 Sample Size and Characteristics

The range of cervical flexion and extension is influenced by variables such as age [24][30][31][33][48] disc degeneration [95], motivation, pain[24][96] , time of day (the amount of water in the nucleus pulposus) [33][95], posture [95][97],, weight [95][30], muscle activity [95] and athletic activity [30].

Discrepancy in the literature exists whether ROM is gender dependant. Some have found differences in ROM, some only in lateral bending [31] and others none [24][33][48]. This may be due to the observation that the effect of gender may also differ within age groups. There seems to be agreement that no gender difference has been observed in studies with subjects between the ages of 20-30 [30][32]. Considerable differences have been observed in the age group above 70 [30][98]. Still the anthropometric data differs with gender and it would be interesting to see whether the influence of soft tissue differs with gender. Therefore a subgroup of female and male exists within the samples size.

The exclusion criteria for volunteers were:

- experience of neck pain
- any history of cervical pain or trauma
- abnormal posture
- pregnancy

The participants were young adults, which also decreased the probability of having people in the sample with bone pathologies. The participants were student volunteers. 23 subjects (12 males and 11 females) participated in this study. One male and one female took part in the initial tests and their data were not used for calculations. Therefore, for all statistical purposes the sample size is 21. Volunteer ages ranged between 21 and 26 years (average 23.09) and volunteers of different weight and athletic activity was recruited.

3.2.3 Limitations of the Empirical Study

Some boundaries had to be identified concerning the scope of the project and the practicality of giving attention to all facets of this topic. The following limitations were identified and are discussed:

Motion in the sagittal plane

The two dimensional imaging technology is used and in a single scan one can therefore only focus on one plane at a time. Either a lateral or a anterior posterior (AP) scan. One would not be able to measure coupled motion in this way but at least capture the amount of flexion-extension and also rotation and lateral flexion separately. Since the amount of X-rays taken (leading to amount of radiation dose) remains a concern it was decided to only focus on the motion in the sagittal plane. This was the obvious choice for several reasons:

1. Flexion and extension is the most prominent movement in the cervical spine
2. When investigating motion in one plane the assumption is made that only motion in that plane occurs. This is closer to the truth when flexion and extension motion is investigated as opposed to rotation which is always coupled with lateral flexion.
3. The skin fold and distraction is a more prominent occurrence in flexion and extension motion and therefore it should firstly be investigated in the sagittal plane.

The results of this study will determine whether the motion in other planes should also be investigated in a succeeding study.

Motion through five incremental images

Since the Lodox technology was chosen over DVF for its obvious advantages in terms of radiation dosages, the ability to capture the full motion path in action was traded off. In stead of having 8 images per second, only static images at different positions would be possible. Since one wanted to keep the dose as low as possible, it was decided that five images would be the minimum amount that would still give a good idea of the motion path of the vertebrae. Three scans would only reveal neutral and the extreme positions of flexion and extension. Therefore two intermediate positions between neutral and flexion and neutral and extension was added. This is not an ideal representation of motion, but sufficient for the purposes of this study.

Motion in one age group and small sample size

Due to practical constraints only a limited sample size could be investigated. Therefore only subjects in the age group 20 – 30 years were included in the study and investigated. The results obtained in this study are therefore particularly for this age group. The sample size of 21 subjects was a practical constraint rather than a statistical decision.

3.3 Data Acquisition

The method followed for the data acquisition, processing and analysis is discussed in this section. The experiment was conducted on 6 different days. Each day's session started at about 9h00. There were three phases that each participant had to undergo (1) the identification of the spinous processes and placing of the surface markers, (2) obtaining the images and (3) taking the anthropometric measurements. Each of these phases is explained in detail in the following section.

3.3.1 Identifying the spinous processes and placing the surface markers

The spinous processes of the vertebrae needed to be identified, to place the metal markers (4mm ball bearings) in such a way that it accurately represents the correct vertebral level. It was clear that professional expertise was needed to accomplish this.

Several options for accurately identifying the spinous processes were considered. The first option was to obtain literature about the vertebral dimension and positioning in order to place the markers accurately from anthropometric percentile data. Information about vertebral dimensions and distances from superficial landmarks were insufficient and this option could not be pursued.

The second option was to take an initial X-ray and from there determine the positions on the skin where the markers should be placed. This option could prove to be a very accurate method but it had several drawbacks.

1. An extra X-ray would mean losing one of the actual X-rays and therefore have less data about the motion path.
2. This process would take much longer since one would first have to do aspect correction and then measure the distance from landmarks and spinous processes on the scan and then on the body.

It was concluded that it is best to follow the option of identifying the processes by means of palpation. A physiotherapist at the University of Cape Town took part in the study and identified the processes by means of palpation. In most individuals all the spinous processes could be felt. The most prominent

ones were C2 and the vertebrae prominens, C7 (see Figure 3-2). By taking time to palpate and count the levels between C2 and C7, the other levels (3-6) could also be identified. In some cases, especially in individuals with a higher BMI, the other processes could not be identified and had to be estimated.

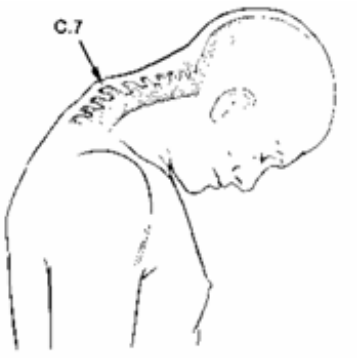

Figure 3-2 – Vertebrae prominence: Superficial landmark

A trail study scanning two individuals had been done. The physiotherapist estimated some of the markers and after each position had been scanned adjusted the markers to better represent the particular processes. Although each individual is different, this practice round and iterative process had given the physiotherapist a degree of confidence in estimating where to make the mark for the placement of the ball bearings.

C1 does not have a spinous process and cannot be felt from the skin surface. Therefore another marker was placed on the skull instead of on the first cervical vertebrae. A good landmark on the skull is the external occipital protuberance that can easily be felt at the back of the head.

While palpating the processes the head was in the position best suited to facilitate the palpation process, which was mostly a flexed position since the spinous process of C7 is then very prominent (Figure 3-2). The palpation was maintained while the subject raised the head and the identified places were only marked with a make-up pencil once the head was in a neutral position. This was done to avoid placement error due to the great displacement of the skin during flexion [90].

C7 played an integral role in identifying the spinous processes. An interesting phenomenon was encountered regarding C7. In 18% of the cases C7 was not the most prominent vertebrae. In these cases the data for one vertebral level of data was lost, since the levels were miscalculated as C7 was either mistaken for T1 or for C6.

In Figure 3-3 one can see the spinous processes of the different vertebral levels marked with make-up pencil.

Figure 3-3 – Identifying and marking the vertebral levels

After the correct placement had been identified, thin double sided tape was folded around a ball bearing and it was stuck onto the identified place. A piece of masking tape was stuck over each ball bearing to prevent them from sticking together during extension. The masking tape was cut into thin strips to prevent the tape from altering the skin motion. Masking tape was chosen over normal sellotape, since it was more flexible and did not obstruct the movement of the skin. As seen in Figure 3-3, participants wore swim caps. With a swimming cap, the ball bearings could easily be stuck onto C2 and the occipital protuberance, where hair would have prevented it. A R5 coin was stuck to the swim cap, which aided the aspect correction process. This then concluded the first phase that each participant went through. The participant then moved onto phase 2 and the next participant got seated for operation palpation.

Figure 3-4 shows in summary the markers that were put onto the skin and how they correlated with the vertebrae.

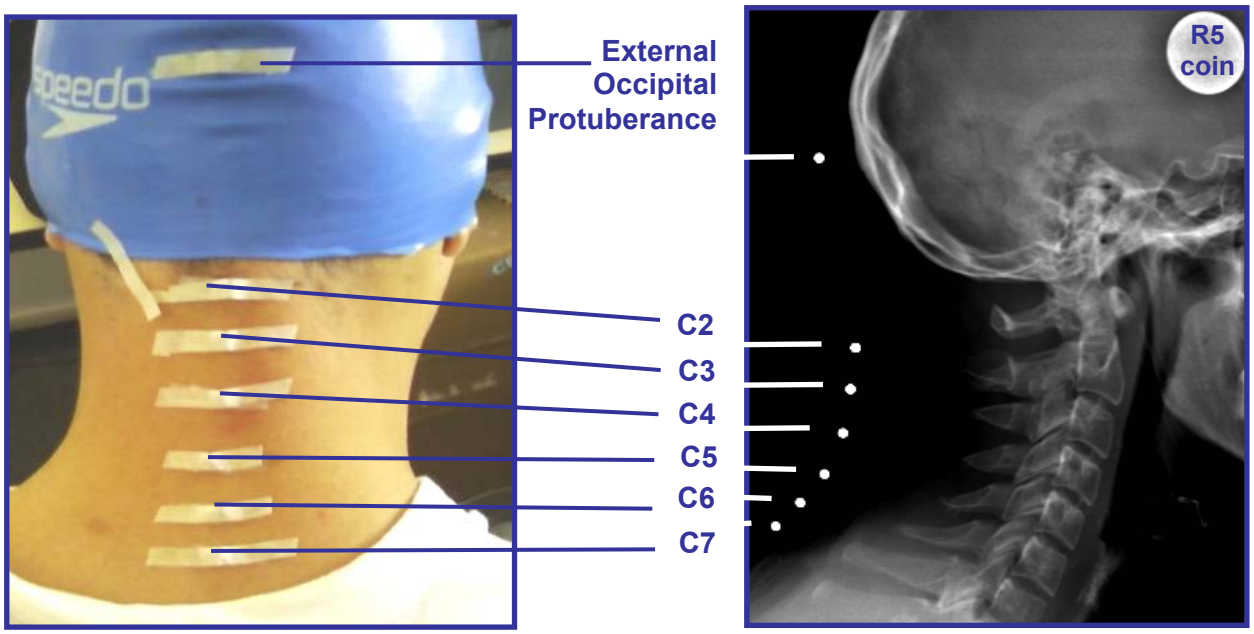

Figure 3-4 – Marker placement from the outside and inside, in a half-flexed position

3.3.2 Obtaining the images

For the image acquisition the beam of the Statscan was rotated 90° and the participant was seated underneath the arch of the Statscan, as seen in Figure 3-5. The chair (wheels removed) was adjusted for each individual. Five lateral X-rays were taken in neutral, mid flexion, full flexion, mid extension and full extension, in that specific order.

Figure 3-5 – Statscan position for taking lateral cervical X-rays

The Lodox radiographer positioned the participants for each scan to ensure that the participant is in an optimal position for a good lateral cervical scan. The radiographer firstly examined the ROM of each

participant and from there positioned the participants in a neutral (N), half flexed (HF), full flexed (FF), half extended (HE) and full extended (FE) positions for the five consecutive scans. The participant was required to be very still for about five seconds as each scan was taken.

3.3.3 Anthropometric measurements

In the last phase the participant's anthropometric measurements were taken.

In the study by Lee et al. [86] on the lumbar region stature, waist circumference, abdominal depth, L4 skin fold, and difference from L1 – S1 skin distraction were considered for the regression model, but only skin fold and skin distraction proved to be significant in predicting vertebral motion from skin surface motion.

The measurements taken in this study to see whether they influence the amount of correlation between marker motion and vertebral motion were the following: stature, weight, neck circumference, skin fold at C5 and difference between skin surface distance of C2 -C7 in a flexed and neutral position.

The measurements were all obtained in the late morning to account for diurnal variation in stature and weight. Measurements, except when indicated otherwise, were taken with the head in the Frankfort plane as illustrated in Figure 3-6. For most measurements three readings were obtained and the mean was calculated and used.

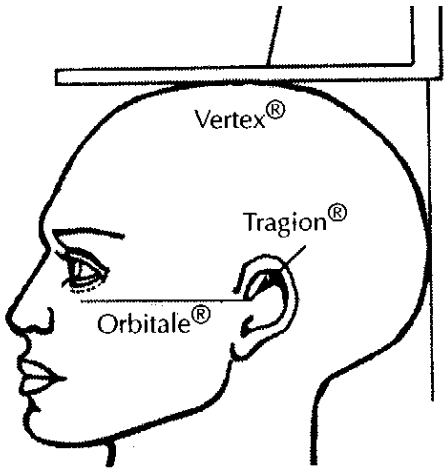

Figure 3-6 – The head in the Frankfort plane [99]

The Vertex is the most superior point on the skull when the head is positioned in the Frankfort plane. The Tragion is the notch superior to the tragus of the ear. The orbitale is the lower bony margin of the eye socket [99].

Stature (m)

The preferred technique for measuring length is the stretch stature technique. The participant stands with the heels against the wall (without shoes) and head in the Frankfort plane. The participant takes a deep breath when stature is measured. It was measured to the nearest millimeter.

Weight (kg)

Participants stood on the centre of the scale without support and with the weight distributed evenly on both feet. Shoes and jackets were removed. This is not a weight study and the accuracy achieved with basic clothing is sufficient.

Neck girth (cm)

Girth was measured with anthropometry tape. The subject assumed the relaxed seated or standing position with the head in the Frankfort plane. The circumference around the neck is measured immediately superior to the thyroid cartilage (Adam's apple). The tape is held perpendicular to the long axis of the neck.

Skin fold (cm)

No standard skin fold measurement in the cervical spine was found in the literature. A place for measurement was therefore chosen and standardized for all subjects.

The head was first moved in a slight extended position to make it easier to capture the skin fold. A skin fold caliper was used to measure the skin fold at the fifth cervical vertebrae. With the left hand a piece of skin in this region was grabbed and with the caliper in the right hand this was measured. The caliper was held horizontally. The reading after two seconds was taken down. In some subjects the reading varied considerably and therefore whenever the three different readings differed more than a millimeter, the measurement was stopped and redone a few minutes later.

Stretch: Difference in distance from C2–C7 (cm)

This measurement involved two sets of readings. Firstly with the head in the Frankfort position and secondly with the head fully flexed. The marks made by the physiotherapist were used and the skin surface distance form C2–C7 was measured with anthropometry tape. The percentage difference between the neutral and flexed distances serves as an indicator for skin distraction.

The anthropometric measurements is summarised in Table 3-1.

Table 3-1 – Anthropometric measurements

		Length cm	Mass kg	Girth cm	Stretch %	Skinfold cm
males	ave	180.71	81.34	38.32	43.98	1.36
	std	3.59	10.40	2.16	10.64	0.42
	max	187.00	103.00	42.23	58.99	2.27
	min	176.50	66.20	35.00	24.09	0.90
females	ave	170.57	64.40	32.18	29.20	1.17
	std	4.08	7.04	1.61	7.65	0.30
	max	175.10	77.00	36.10	45.43	1.88
	min	163.90	58.00	30.67	19.20	0.88
all	ave	175.88	73.27	35.40	36.94	1.27
	std	6.39	12.31	3.66	11.84	0.37
	max	187.00	103.00	42.23	58.99	2.27
	min	163.90	58.00	30.67	19.20	0.88

3.4 Data Processing

The Dicom files were read by the accompanying LODOX software, D.V.S version 2.8, and the data obtained from there was processed and plotted by making use of Python.

3.4.1 Obtaining the coordinates

The LODOX software is capable of calculating dimensions, angles and as well as the x-y pixel[a] coordinates. The coordinates of specific landmarks were identified and read from the software into a spreadsheet.

The landmarks that were identified were the following

- The centers of the ball bearings
- The corners of the vertebral bodies
- The most posterior parts of the spinous processes
- The most superior part of the dens of the axis
- The most anterior and posterior part of the atlas
- The external occipital protuberance

The raw data is presented in Appendix B.

[a] Pixel (PICture Element) - is the smallest element of a digital image. It is a small square of light that with the other squares make up an image.

3.4.2 Data Conversion

The data could however be more sensible and useable when transformed into metric distances. To accurately transform pixel coordinates into useable distances Pixel Aspect Correction (PAR) was performed. PAR refers to changing the dimensions of the pixel itself. The x value refers to the pixel width and the y to the pixel height as seen in Figure 3-7.

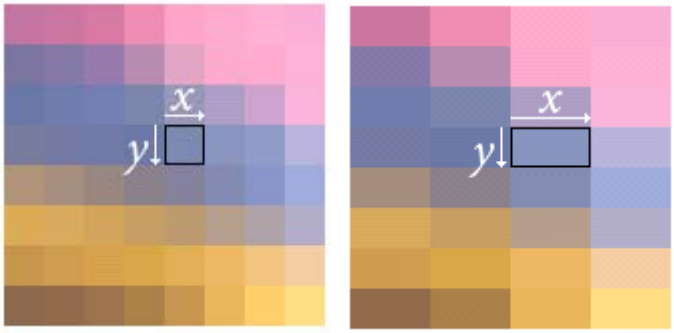

Figure 3-7 – Pixel Aspect Correction

Since the distance from the X-ray source was not constant the aspect correction for each individual would be different. If this is successfully done a millimeter as indicated with the Lodox software would be equal to a millimeter in reality. Each data entry was multiplied with a corresponding aspect correction factor. This factor was determined by measuring the ball bearings and R5 coins and adjusting the aspect ratio until it is the same size in across all scans. The R5 coin alone could not provide adequate aid for aspect correction and the ball bearings were also used. During motion the coin did not remain in the same plane and therefore its dimensions on the scan changed. The spherical balls remained a circle in all planes and were therefore a more reliable source to do aspect correction with.

3.4.3 Data capturing error

Obtaining the coordinates of the ball bearings was easy, unlike obtaining and being consistent with the corners of the vertebral bodies. The challenge with identifying the corner of the vertebral body was to remain consistent with the identified point throughout an individual in all different positions. When plotting the data the transcriptional errors could clearly be seen and corrected.

Translational errors were more difficult to correct. A measuring error was determined for each vertebral level in each position. The length of the anterior aspect of the vertebrae was compared in the different positions and the difference in each position compared to the neutral position was calculated. In some positions the error was up to 10mm. All outliers were identified and the data were reread from the scans. In the cases where the error did not decrease further investigations was done to ensure the

data accuracy. Due to the iterative process the average error decreased to 1.51 mm for females and 1.76 mm for males.

3.4.4 Motion reference point

Unlike fluoroscopy, the image capturing window did not remain stationary throughout the different scans. The result of this moving window is shown in Figure 3-8. A continuous motion path could not be established across the different positions. A marker that is not attached to the body could have been used in the scan to serve as common reference point. With such a reference point, the absolute movement of a point on the different scans could be determined. In the absence of an exterior reference marker, the body had to be used as a reference point. The anterior inferior corner of C7 was identified as reference point, since its absolute position varies the least across the scans. The anterior inferior corner of C7 (C7AI) was set to (0, 0) and all the other data points were then adjusted according to this value, which resulted in a clear motion path as seen in Figure 3-9.

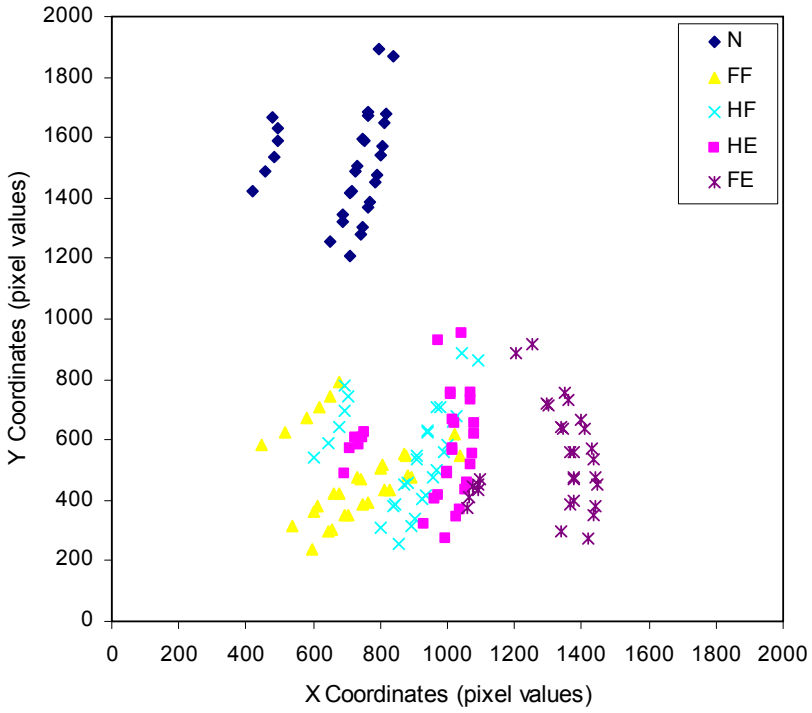

Figure 3-8 – Data from scans in different positions

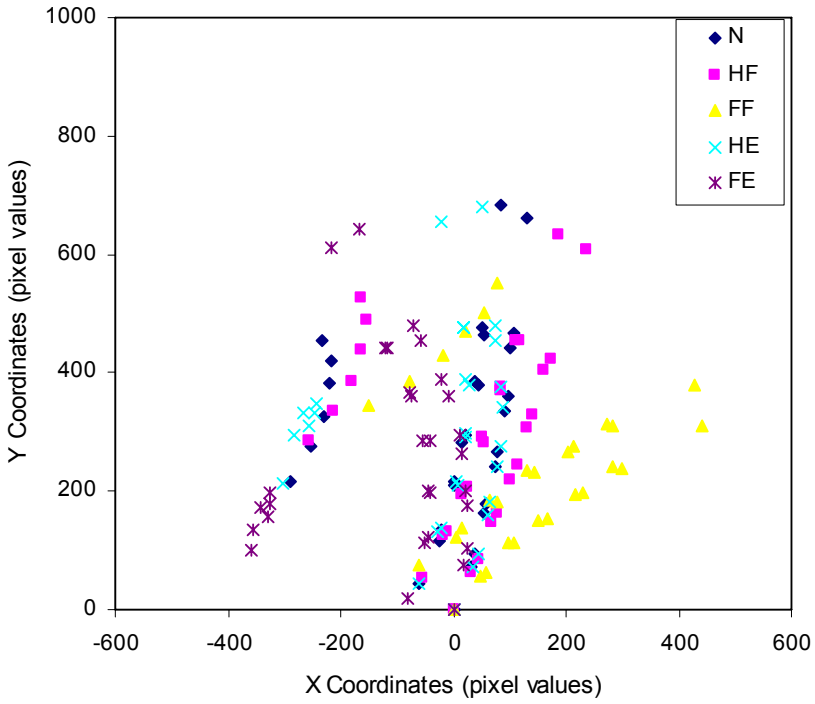

Figure 3-9 – Motion path for C2AI with C7AI as common reference point

This is a good visual representation, but unfortunately not the truth. There is an error due to using a landmark on the body as a reference point. This error is explained by several extracts from the DVF images taken (Figure 3-10). Unlike the scans that were taken, the image tool remained stationary and absolute translation and rotation could be observed. Looking at C7A1 (indicated by the red dot), the amount of translation during the forward and backward movements can be seen (Figure 3-10). As the scans are not in the same image frame, the amount that C7 translated throughout different positions is unknown. Therefore when setting all C7A1's to (0,0) and adjusting the other vertebrae accordingly, the relative motion that a vertebrae has towards the same vertebrae in a previous position is inaccurate.

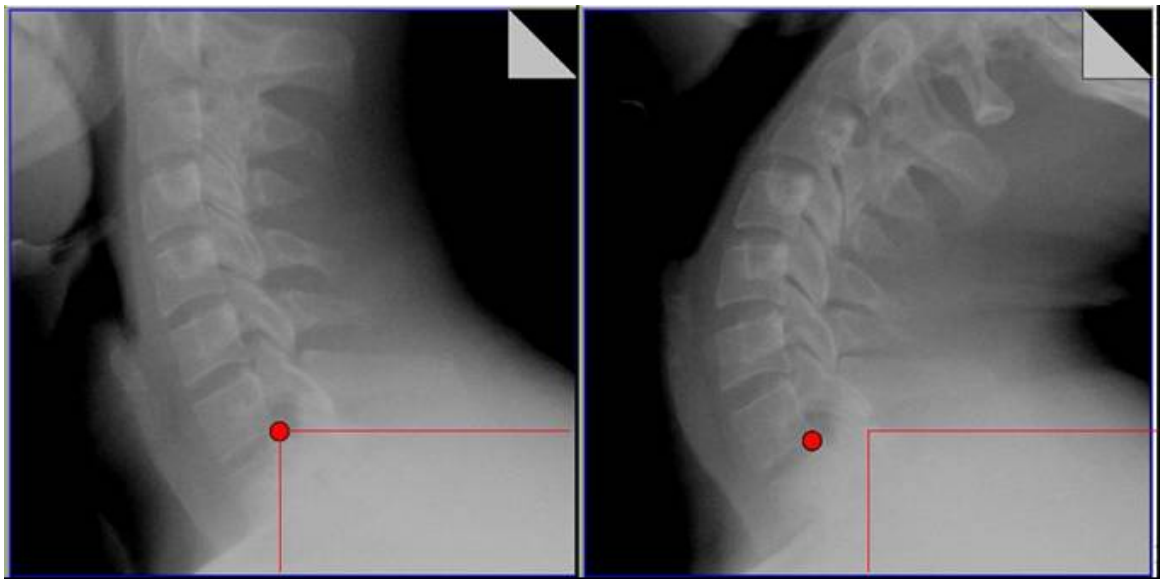

Figure 3-10 - Absolute translation of C7

It would therefore be better to use the head as reference point. With image processing the heads of different scans could be aligned. In the scope of this study the images were not processed, but only x-y coordinates were used. The absence of one common reference point implies that absolute translation throughout motion, could not be determined from these scans. The rotation calculations are not affected by the absence of a common reference point and are calculated with confidence. These calculations are reported on in section 3.5.1.

3.5 Data Analysis

In this section the methods for calculating absolute rotation, intervertebral rotation and intervertebral translation is discussed. The results obtained after applying these methods is presented in section 4. After investigating the motion patterns, the relationship between surface marker motion and vertebral motion is investigated. The method for investigating that relationship is discussed in 3.5.2.

3.5.1 Absolute and Intervertebral Rotation

Several techniques have been previously used to determine motion from flexion extension radiographs. These methods include Cobb angles [88][74], posterior and anterior vertebral angles [74], midplane angles [74][100], overlay angles [86] and coordinate parameters [23][29]. The Cobb angles and Anterior Verteral Angles (AVA) methods were investigated and applied.

Cobb Angles

"A line is drawn along the superior end plate of the superior vertebra and a second line drawn along the inferior end plate of the inferior vertebra. The angle between these two lines (or lines drawn perpendicular to them) is measured as the Cobb angle" [101]. Cobb Angles are commonly used in clinical practice to measure deformity and spinal ROM. Inter- and intra-observer reliability is high [102].

Anterior Vertebral Angles

The posterior or anterior vertebral angle is the angle between two straight lines through the anterior aspects or the posterior aspects of adjacent vertebrae. In a study comparing several different techniques [74], the method of AVA was proposed as the most reliable method for assessing segmental lumbar lordosis.

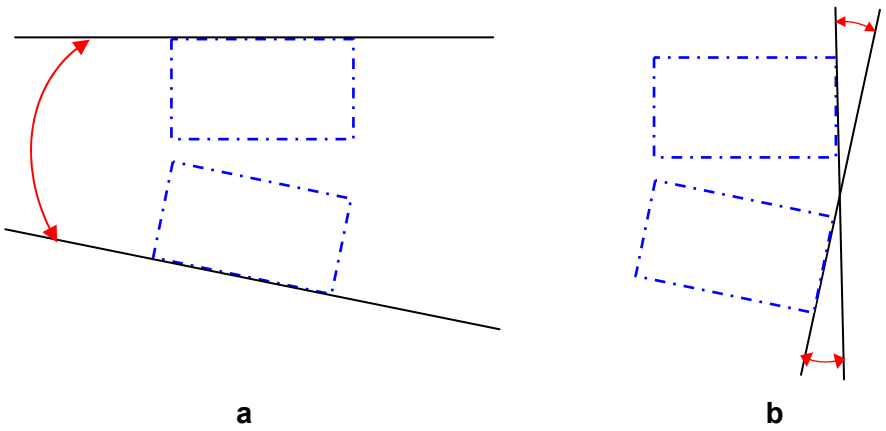

Figure 3-11 - An illustration of (a) Cobb Angles and (b) Anterior vertebral angles

The above mentioned methods as well as variations on the AVA method were computed to analyse vertebral and intervertebral rotation. Different techniques were considered, since possible errors from selecting the vertebral corners and other data points from the Lodox software could have occurred. Using the anterior aspects yielded the most reliable results. This is probably due to the fact that the anterior corners were more definite and one could be consistent with identifying the vertebral corners from the scans throughout the motion range. The AVA method was therefore used in this study.

Absolute rotation

The absolute rotation was determined for each vertebra in each position. The angle was obtained from the straight line through the anterior aspect of a vertebra. This method is also similar to the method

that Panjabi et al. [23] used, except that the anterior vertebral corners were used instead of the posterior corners. The angle θ was determined for each person for each vertebral level and in each position.

The standard angle configuration increases anti-clockwise from the positive X-axis. As seen in Figure 3-12, the angles do not correspond to this standard configuration. It was adjusted in order for the angle to increase clockwise from the negative Y-axis, representing the motion of the vertebrae from full extension to full flexion. In all cases, in the lower and upper cervical spine, full extension would therefore have the smallest angle and full flexion the largest.

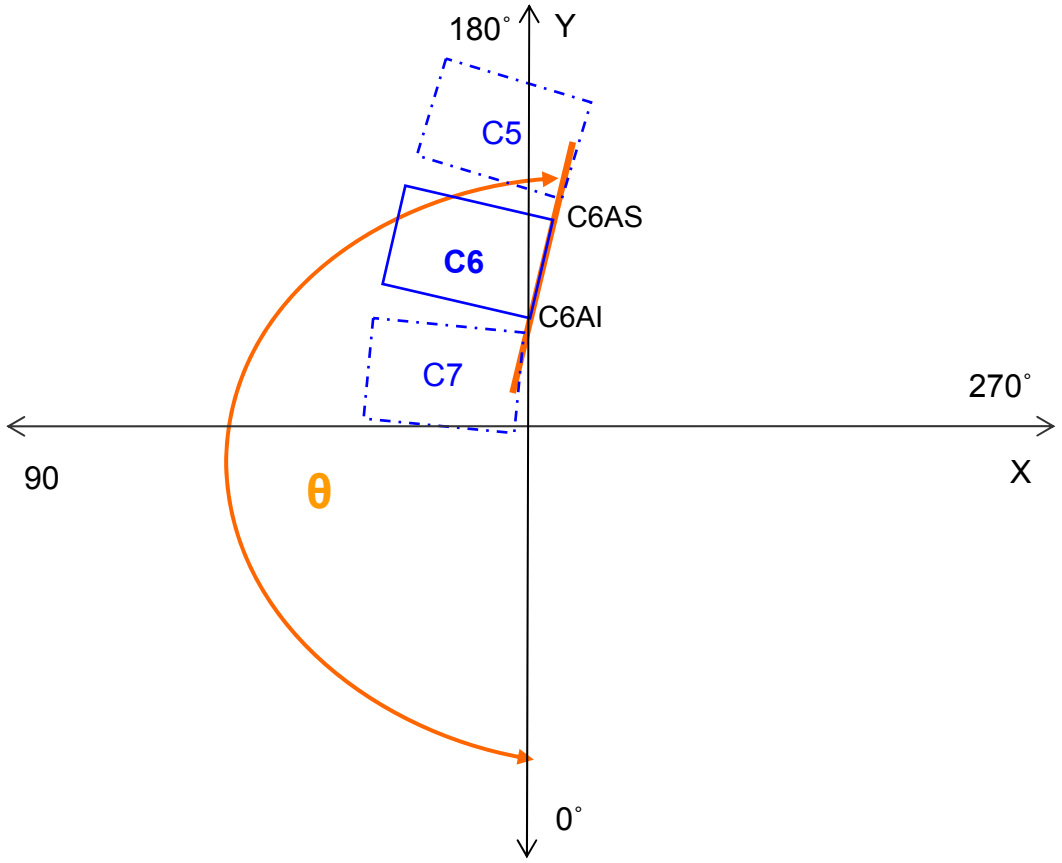

Figure 3-12 - Determining vertebral rotation

From the difference in x-values as well as in y-values of the landmarks ∂x, ∂y and θ was calculated:

$$\partial y = C1Py - C1AIy \quad \text{or} \quad \partial y = C2DSy - C2AIy \quad \text{or} \quad \partial y = C^{*}ASy - C^{*}AIy \text{ [a]} \qquad (1)$$

$$\partial x = C1Px - C1AIx \quad \text{or} \quad \partial x = C2DSx - C2AIx \quad \text{or} \quad \partial x = C^{*}ASx - C^{*}AIx \qquad (2)$$

[a] C^{*} represent C3, C4, C5, C6 or C7

$$\theta = \arctan(\partial y / \partial x) \quad (3)$$

The following conditions ensured the correct angle according to the configuration in Figure 3-12:

$$\text{if} \quad \partial y < 0 \text{ and } \partial x < 0 \quad \text{then} \quad \theta = 90 - \theta \quad (4)$$

$$\text{if} \quad \partial y > 0 \text{ and } \partial x < 0 \quad \text{then} \quad \theta = 90 + |\theta| \quad (5)$$

$$\text{if} \quad \partial y > 0 \text{ and } \partial x > 0 \quad \text{then} \quad \theta = 270 - \theta \quad (6)$$

$$\text{if} \quad \partial y < 0 \text{ and } \partial x < 0 \quad \text{then} \quad \theta = 270 + |\theta| \quad (7)$$

The upper cervical vertebrae do not have the same defined anterior aspect as the lower vertebrae and therefore other landmarks were chosen to determine the rotation of the upper vertebral bodies. The landmarks of the upper and lower cervical vertebrae can be seen in Figure 3-13 and is explained in Table 3-2.

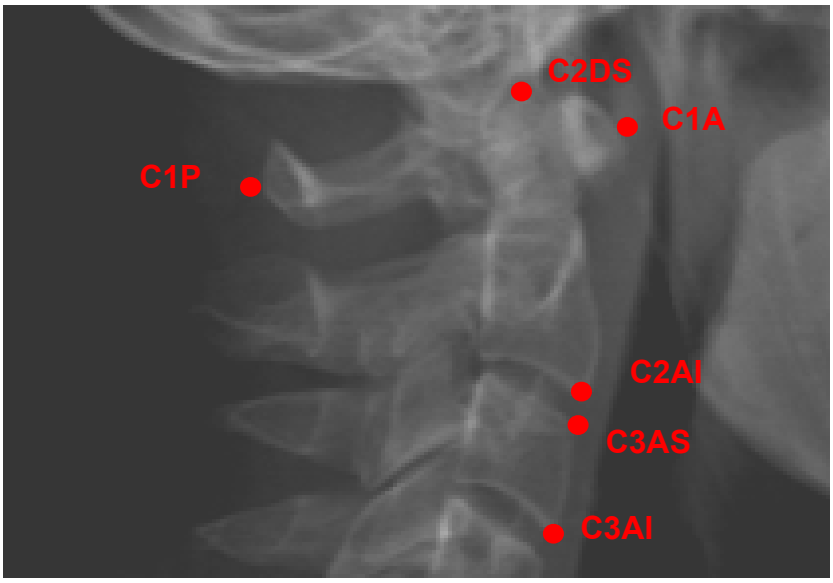

Figure 3-13 Landmarks used to determine vertebral rotation

Table 3-2 Landmarks used to determine vertebral rotation

Abbreviation	Description
C1P	Most posterior point of the atlas
C1A	Most anterior point of the atlas
C2DS	Most superior point of the dens
C2AI	Anterior inferior vertebral corner of C2
C3AS – C7AS	Anterior superior vertebral corner of C3-C7 (lower)
C3AI – C7AI	Anterior inferior vertebral corner of C3-C7 (lower)

Due to the landmarks of C1, the angle configuration was different to the other vertebral levels. It is illustrated in Figure 3-14.

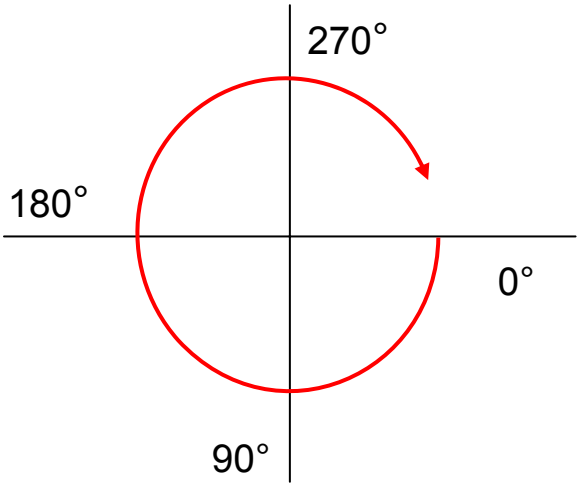

Figure 3-14 Angle configuration for calculating rotation of C1

The following conditions ensured the correct angle according to the configuration of Figure 3-14:

if $\partial y < 0$ and $\partial x < 0$ then $\theta = 180 - \theta$ (8)

if $\partial y > 0$ and $\partial x < 0$ then $\theta = 180 + |\theta|$ (9)

if $\partial y > 0$ and $\partial x > 0$ then $\theta = 360 - \theta$ (10)

if $\partial y < 0$ and $\partial x < 0$ then $\theta = |\theta|$ (11)

From the extreme values of the rotation, the ROM for each vertebral level was determined.

Intervertebral rotation

The AVAs were determined to see the rotation of a motion segment. The absolute rotation determined in the section before was used to determine the AVA. The angle of the inferior vertebrae of the given motion segment was subtracted from the angle of the superior vertebra. The AVAs for $\theta_{2/3}$ to $\theta_{6/7}$ were determined.

$$AVA = \theta_{\text{superior}} - \theta_{\text{inferior}} \quad (12)$$

The intervertebral rotation for the motion segment C2/C3 was combined with the upper cervical motion segments. The AVA was determined between the lines C1A-C2AI and C3AS-C3AI (see Figure

3-13). Throughout the motion the line C1A-C2AI forms an anterior aspect similar to that of the other vertebrae. The angle obtained from this line can then be compared to the angles obtained from the other anterior aspects. The landmarks C1A-C2AI were also easier to identify on the scans than the dens, and hence the probability of error was decreased.

From the extreme values of the intervertebral rotation the ROM for a motion segment was determined. The ROM was also determined for the whole cervical region. The cervical ROM was calculated from the extreme values of the vertebral angle between C1 and C7. $AVA_{1-2/7}$ was obtained by subtracting $\theta_{6/7}$ from the absolute rotational angle of the combined motion segment of C1 and C2.

$$AVA_{1-2/7} = \theta_{1\text{-}2/3} - \theta_{6/7} \tag{13}$$

3.5.2 Analysis of Surface Marker Motion

If a surface marker would have perfectly represented the vertebrae during motion, it would be as if the ball bearing was actually attached to the vertebrae itself, and thus following the same translation and rotation as the vertebrae. This ideal was used to determine parameter ε, that served as an indication of how well a specific surface marker represented the motion of the corresponding vertebra.

Figure 3-15 shows a schematic drawing of how ε was determined. The corners of each triangle represent two corners of the vertebrae and the corresponding ball bearing. These coordinates were transformed in order for each vertebra to start at the same point, (0,0) on the Cartesian plane.

In Figure 3-15, c* is the predicted position of the ball bearing if it rotated and translated exactly as the vertebral body did. The following coordinates was used to determine the c*:

a = Anterior inferior corner of vertebral body in neutral position

b = Anterior superior corner of vertebral body in neutral position

c = Ball bearing in neutral position

a' = Anterior inferior corner of vertebral body in flexed position

b' = Anterior superior corner of vertebral body in flexed position

c' = Ball bearing in flexed position

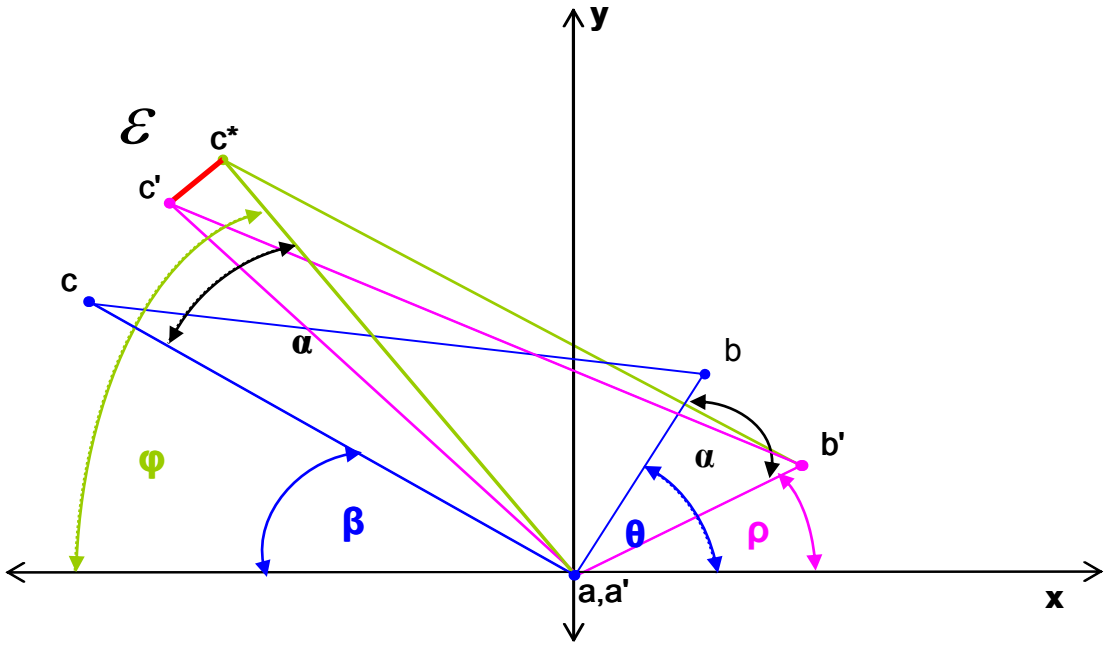

Figure 3-15 – Determining how well surface marker represented vertebrae

From these coordinates, θ and β were determined. The angle α, the rotation of the ideal solid body consisting of the vertebral corners and the ball bearing, could then be deducted as indicated in the following equation.

$$\alpha = \theta - \rho \tag{14}$$

Using angle **α**, one can easily obtain the angle **φ,** the rotation of the ball bearing if it followed the same motion of the vertebrae. To ensure that the coordinates of c* is in the correct quadrant angle **φ** is obtained by the following equations:

For flexed positions:

$$\varphi = 180^\circ - (-\beta + \alpha)$$

$$\varphi = 180^\circ + \beta - \alpha \tag{15}$$

Figure 3-15 only shows the scenario of a flexed position. In the extended position triangle a'b'c' would be below triangle abc. For extended positions α is $\rho - \theta$. Therefore α is a negative value and the equation follows:

$$\varphi = -\alpha - (-\beta)$$

$$\varphi = \beta - \alpha \tag{16}$$

The coordinates of c* can then be determined by the length a'c' and the angle φ.

$$x = a'c'\cos\varphi \tag{17}$$

$$y = a'c'\sin\varphi \tag{18}$$

In Figure 3-15, a representation of a typical neutral to flexion movement in one vertebra is presented. In reality the coordinates of these landmarks varied and often fell into different quadrants resulting in different angles. Therefore provision was made in the data processing to ensure that the coordinates of c* is correct. Once the coordinates of c*, the place where the ball bearing should have been if it perfectly represented vertebral motion, was known, ε, the resultant distance between c' and c*, was determined.

ε gives an indication of how well the surface marker represented the vertebral motion and was determined for each subject in half flexion, flexion, half extension and full extension as well as for all the vertebral levels from C2 – C7. The averages and standard deviations were determined over different combinations. In Figure 3-16 the average misrepresentation of the surface marker is determined for each vertebral level and positions.

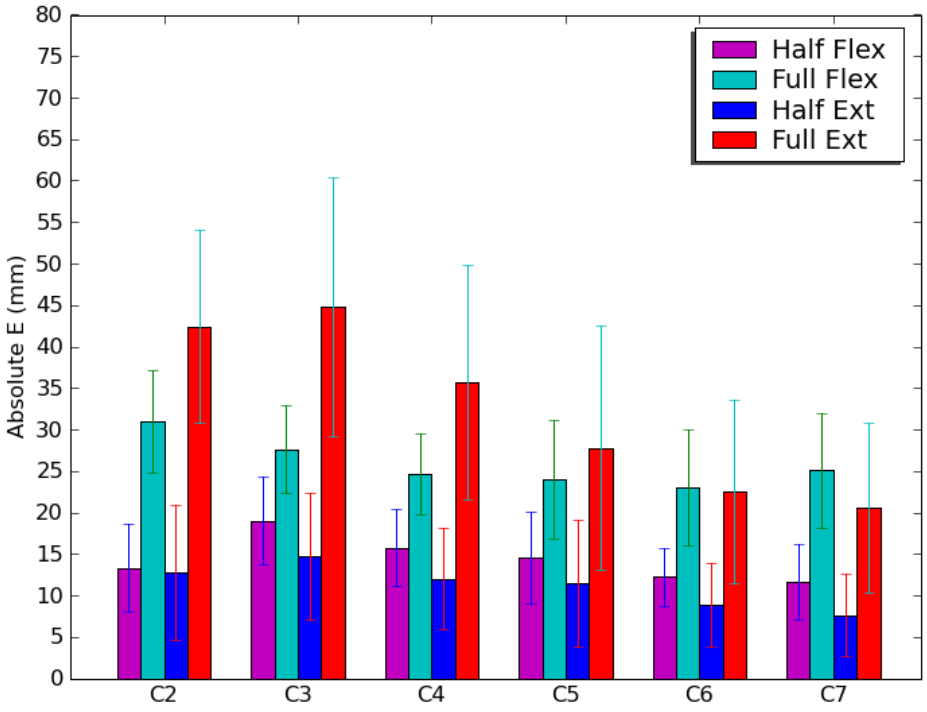

Figure 3-16 - Average ε over all subjects (n = 21)

Average ε ranged from 5mm to 45mm with large deviations. What is first observed is that the extreme positions have the largest ε. Full extension resulted in the largest ε followed, by full flexion, half flexion and lastly full extension.

One explanation for this order of magnitude of ε is the ROM. In the mid motion positions there has been less motion and the ball bearing still followed the vertebrae more closely than in the extreme positions. From the scan it could clearly be seen that there is more ROM in the flexion than in extension which would also explain why half flexion would result in a bigger R than half extension. This however contradicts the order of the extreme positions where full extension had a bigger R than full flexion.

With the neck moving more when moving forward than when moving backward one would expect that the R would be more in flexion than in extension, but in the case of full extension there were other factors that contributed more to the alteration of the vertebral movement than the motion itself. This factor is the size and position of skin fold in extension, which concealed true vertebral motion by making the ball bearing move differently than the vertebrae. The space that the ball bearings could have moved to was limited and the ball bearings were all bundled together.

So far the surface markers were only compared to an ideal surface marker position. Measuring this misrepresentation does not conclude anything about the relationship between surface markers and vertebrae, except that the surface markers did not represent the vertebral motion perfectly. The next step is therefore to investigate the relationship between the surface markers and vertebrae for any consistency and correlations with anthropometrical variables.

Two parameters are necessary to describe the relation between the surface marker and the vertebrae. The first parameter is the distance between the surface marker and the vertebrae (R) and the second parameter is the direction of that distance (β). These parameters are illustrated in Figure 3-17.

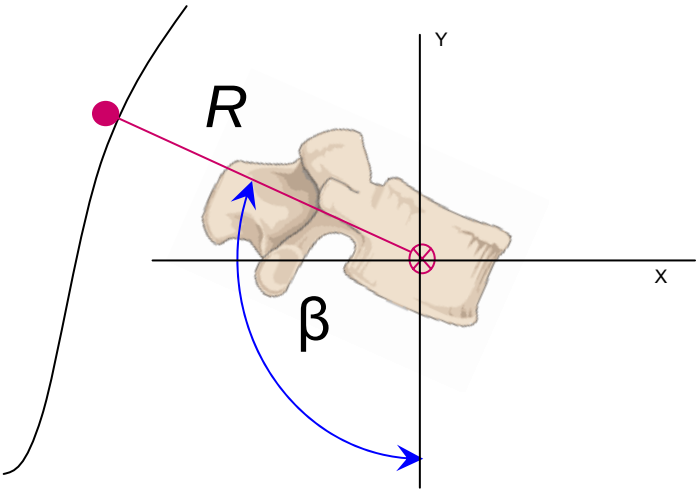

Figure 3-17 – Determining surface marker motion

By Pythagoras R was obtained from the difference in x and y coordinates of the centre of the surface marker and the centre of the vertebrae. The centre of the vertebra was calculated geometrically from the coordinates of the vertebral corners. β was determined as follows:

$$\partial y = BBy - CVy \tag{19}$$

$$\partial x = BBx - CVx \tag{20}$$

$$\beta = \arctan(\partial y / \partial x) \tag{21}$$

where BB is the ball bearing coordinates and CV, the coordinates of the centre of the vertebra. ∂x and ∂y were determined for each position. β was calculated according to the same angle configuration of Figure 3-12.

These parameters in different position and across different vertebral level will help to answer the following questions: What is the distance between the surface marker and the vertebrae, i.e. the amount of soft tissue? How did this distance change during motion? What influenced the change in distance? Was the distance consistent over all subjects? Did the surface marker follow the rotation of the vertebrae?

4 Results

The results yielded from the questions posed and methods discussed in section 3.5 is presented and discussed in this section. This includes the rotation data that can be used for simulation purposes as well as the investigation on the surface marker motion and how it compared to that of the vertebrae.

4.1 Absolute rotation

The absolute rotation, as explained in section 3.5.1, was determined for C2 to C7. As Figure 3-12 shows, the angles were determined in order for full extension to have the smallest angle and full flexion the largest. Therefore when looking at the results summarized in Figure 4-1, one can imagine the head moving all the way from the back to the front. Although all the averages are between 180° and 270°; some of the individual values were below 90° in the lower left quadrant (see Figure 3-12).

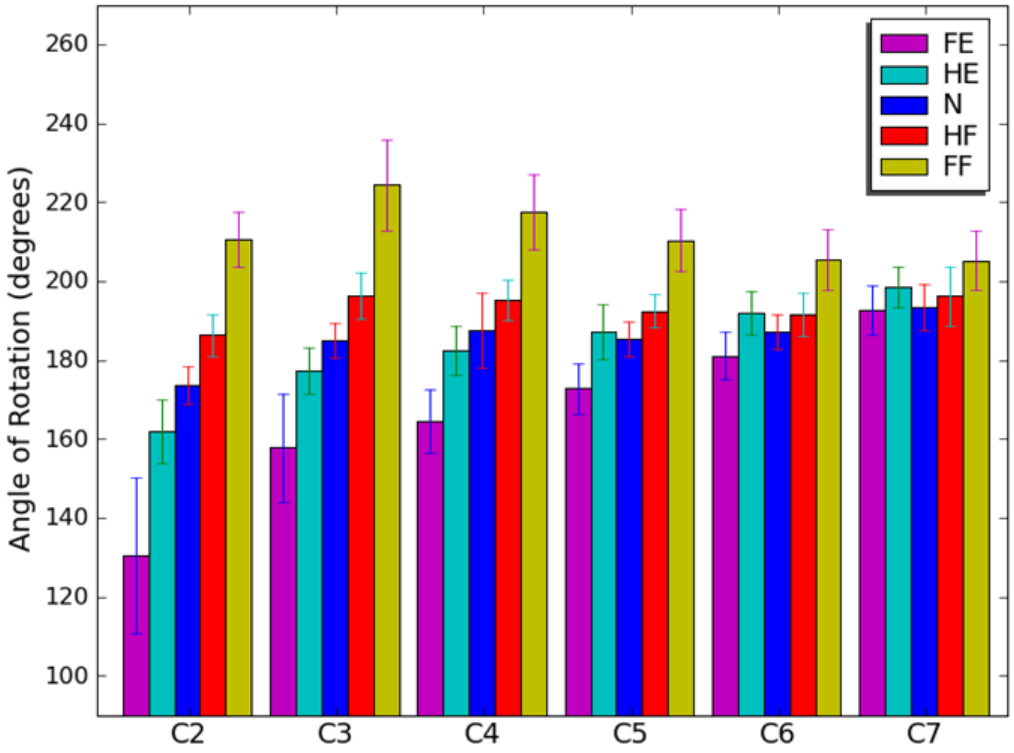

Figure 4-1 - Average absolute rotation of all subjects (n = 21)

With the given angle configuration one would expect the rotation to increase monotonously throughout the motion from extension to flexion. In most cases this expectation was met. In the upper part of the neck the rotation increased in significant steps from one position to the next. This observation is explained by the fact that these results represent the absolute rotation. The large rotation in the upper levels is due to the cumulative rotation of the lower levels.

Note that the rotation of C5, C6 and C7 is less in the neutral position than in the half extended position. In C6 and C7 the rotation in half flexion was also less than in half extension. This unexpected smaller rotation in the neutral positions of C5–C7 is possibly due to the sequence of motion in vertebrae. In section 2.3.3 the sequence of motion for flexion and extension is explained. It was emphasized that the direction of motion of the spinal region as a whole, does not necessarily determine the direction of rotation of the individual vertebrae. This is especially true for C6 and C7, where flexion is initiated and terminated. In the mid ranges of flexion, slight extension occurs at C6/C7 and in some individuals in C5/C6 [12]. This may be the reason for the lower rotation in the neutral and half flexed positions of C5-C7. The orientation of C7 also remained more or less the same throughout the motion, as seen in the DVF extracts in Figure 4-4. This minimal change in orientation is in agreement with the small ranges of rotation in observed in C7.

Overall the rotation of C2 is smaller than that of C3 and C4. With the cumulative rotation of the lower levels, the rotation of C2 should actually be higher than the rotation of C3 and C4. This smaller lower rotation is due to the landmark that was chosen to calculate the rotation of C2. Unlike the other vertebrae, C2 does not have a definite anterior aspect and therefore the superior part of the dens was chosen. The dens is positioned more medially than the other landmarks and therefore the angle of rotation is smaller. Although the position of the landmark for C2 definitely played a role, this smaller rotation is also in agreement with the results of the intervertebral rotation. C2 has a smaller ROM than the mid-cervical vertebrae. According to literature, Oc-C2 also exhibits some extension during the last stages of flexion [12].

The rotation for C1 was determined as described in section 3.5.1, but is not presented in Figure 4-1 since it has a different angle configuration (see Figure 3-13). The results of C1 are summarized in Table 4-1.

Table 4-1 - Absolute Rotation of C1

	Males		Females		All	
	ave	stdev	ave	stdev	ave	stdev
FE	108.44	6.48	100.94	11.15	104.87	9.58
HE	134.25	13.65	142.96	18.27	138.40	16.23
N	161.87	7.87	169.24	16.11	165.38	12.73
HF	205.67	14.25	214.27	16.19	209.76	15.45
FF	245.57	6.19	246.51	10.34	246.02	8.22

There was no significant difference between males and females in the magnitude and direction of the absolute rotation, but in this sample, females had a larger ROM. The ROM difference between gender groups is presented in Figure 4-2.

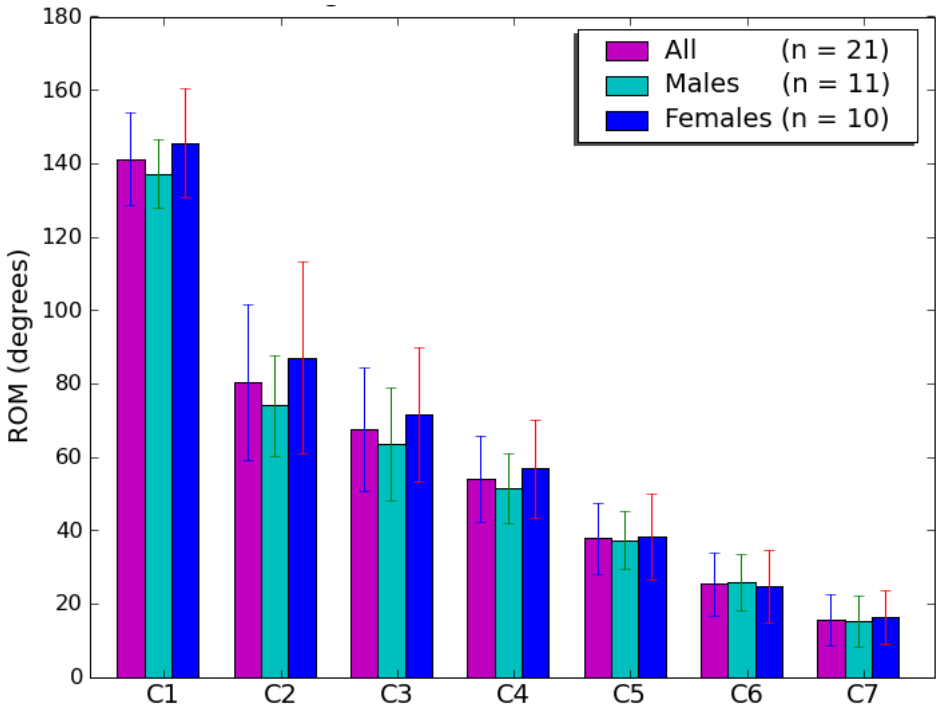

Figure 4-2 - Average ROM for each vertebral level

An Analysis of Variance (ANOVA) was done to determine if the mean difference in female ROM and male ROM is statistically significant. An ANOVA is the appropriate test, since the ROM was found to be normally distributing from the results of the Shopiro-Wilk analysis. It is clear that the mean varies between vertebral levels; therefore the analysis was done for each vertebral level.

Under the null hypothesis (that there is no mean difference between the absolute ROM of males and females in this sample), the variance estimated based on within-group variability should be about the same as the overall variance, and corresponding p-values of the ANOVA is presented in Table 4-2.

Table 4-2 – Testing for gender dependency in absolute ROM

V- level	Shopiro-Wilk	ANOVA p-value	Reject / Not Reject H_0
C1	0.989	0.1295	Not Reject Ho
C2	0.030	0.426*	Not Reject Ho
C3	0.226	0.2905	Not Reject Ho
C4	0.649	0.2917	Not Reject Ho
C5	0.970	0.8272	Not Reject Ho
C6	0.278	0.77637	Not Reject Ho
C7	0.344	0.66415	Not Reject Ho

***** This specific p-value is obtained from the Mann-Whitney U test. This test was used in the case of C2, where the ROM data was not distributed normally, according to the values obtained by the Shopiro-Wilk analysis.

From these results it was found that at a 5% significance level, the hypothesis of no mean difference between males and females could not be rejected. Therefore, in this sample the absolute ROM is not gender dependent.

The complete results consisting of the observations for each individual as well as the aggregated data over male, female and all subjects, is included in Appendix B and C.

4.2 Intervertebral rotation

From the absolute rotation angles, the Anterior Intervertebral Angles (AVA) were determined to analyse intervertebral rotation. Figure 4-3 presents the AVA for the lower cervical vertebrae.

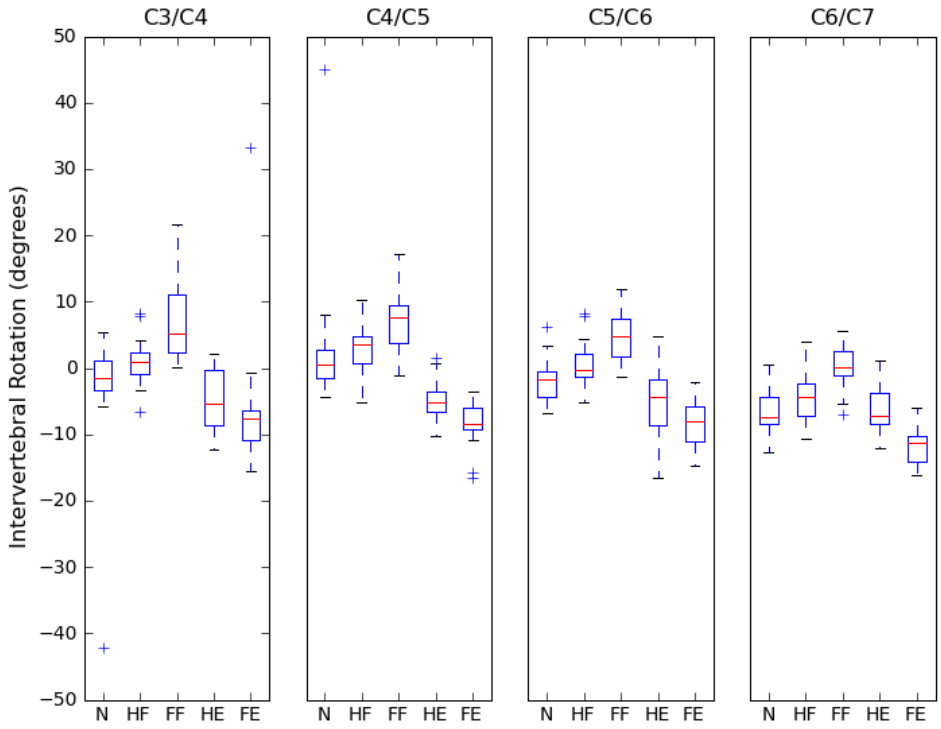

Figure 4-3 – Rotation in a motion segment for all subjects (n = 21)

In Figure 4-3 the positive angles, as seen in the half flexed and full flexed positions, indicate that the superior vertebrae of the motion segment rotated more, in terms of the angle configuration used, than the inferior vertebrae. Likewise, the negative angles imply that the superior angle is rotated less than the inferior angle. A notable variation in intervertebral angle was introduced by the fact that some subjects exhibited angles of converse symbol to the rest. An example of this is in motion segment C3/C4 in neutral, 15 of the subjects had a positive intervertebral angle and 6 had a negative

intervertebral angle. Therefore the box and whisker plot was used to present the data. It shows the median (Quartile 2), the median of the bottom half (Quartile 1) and the median of the top half of the data (Quartile 3). Outliers are also identified and indicated. The interquartile range is the range of the box and is where the mid half of the data points lie. This gives a good indication to the tendencies in the data without being influenced by outliers as much as an average would have been.

The pattern which the data follows is similar throughout the different vertebrae. In C6 and C7 the positive angles tend to be smaller and the negative angles tend to be larger. The 105 observations in different positions in the motion segment C6/C7, only 17 observations had positive intervertebral angles. Figure 4-1 shows that the difference in the increase in full flexion from C7 to C6 and C6 to C5 is smaller than the difference in decrease in full extension for the same vertebrae. The ROM is smaller in C6 and C7 than in the mid-cervical vertebrae (see Figure 4-5). The smaller ROM could explain the lower positive angles, but the extracts from the DVF in Figure 4-4, illustrate this observation in C6 and C7 the best. Note that the angle configuration is different in these images. The flexion and extension is swapped around and therefore the rotation angle increase anti-clockwise. The image on the far left is full extension and the image on the far right is full flexion. The motion segment C6/C7 can be seen in these images. Note that the orientation of C7 remains more or less the same throughout the motion. This was not the case in the other vertebrae. The motion in motion segment C7/T1 was restricted by only making movements in the neck. Therefore C7's absolute rotation was minimal. Due to C6 being much more rotated posteriorly than C7 in the extended position, difference in angle in extension was more negative than in the other motion segments. In flexion C6 was rotated more anteriorly than C7, but not significantly. Therefore the angle in flexion was of small positive value and often even negative.

Figure 4-4 – Extension to flexion in motion segment C6/C7

The ROM was determined from the extreme values of intervertebral rotation and is presented in Figure 4-5 and Figure 4-6.

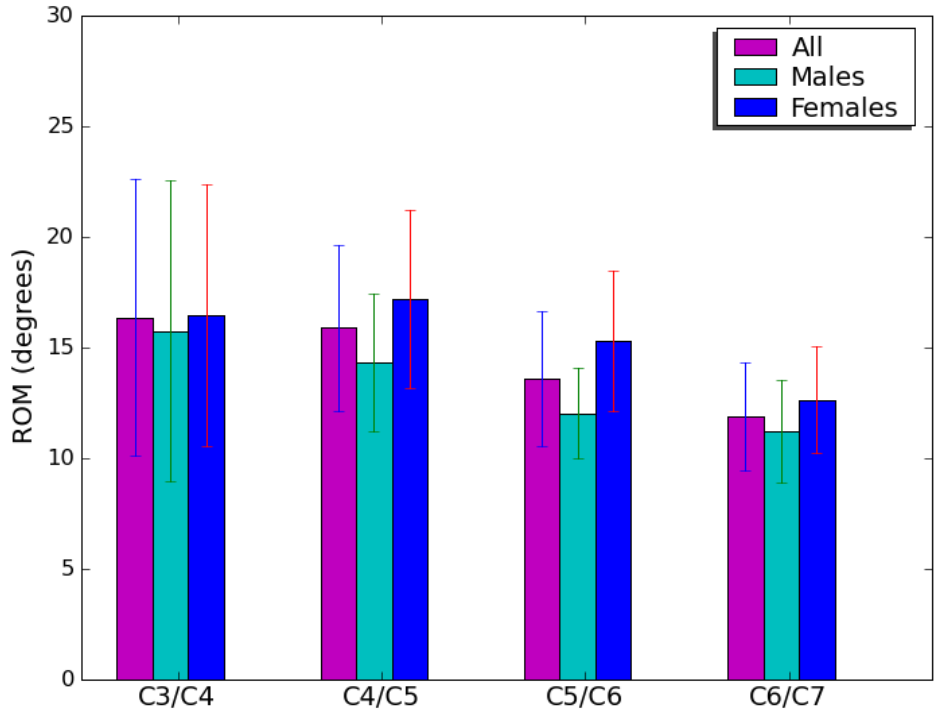

Figure 4-5 – Intervertebral ROM

The intervertebral angle for the motion segment C1-2/C3 was calculated as described in section 3.5.1.

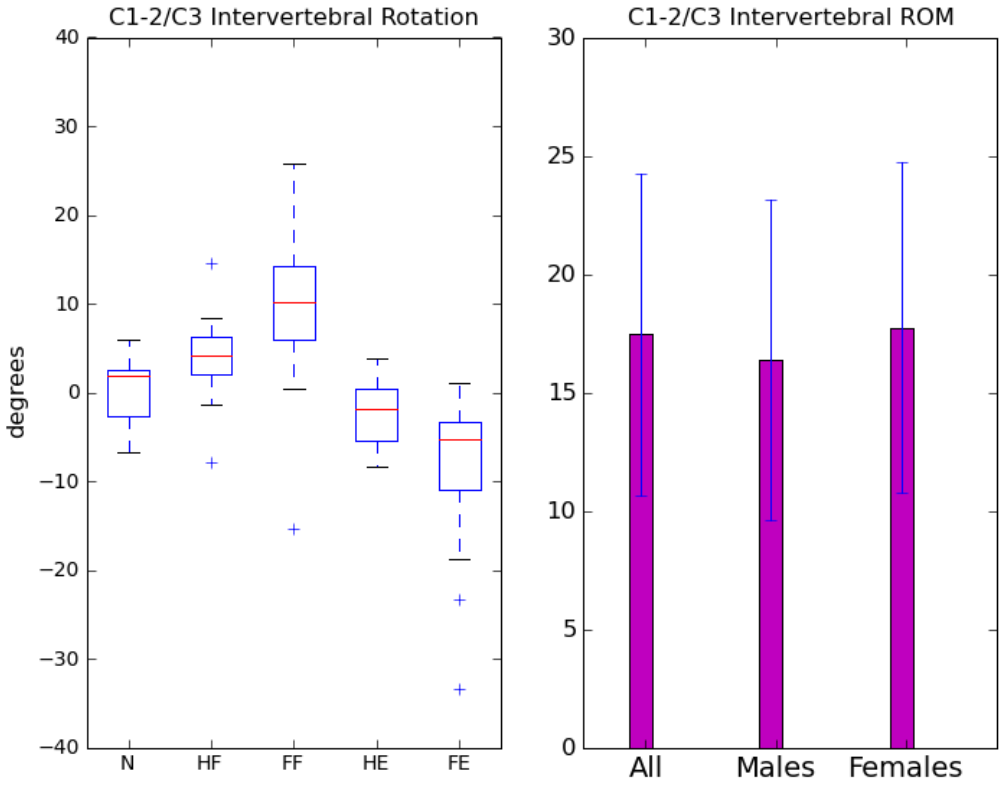

Figure 4-6 – Rotation and ROM in motion segment C1-2/C3

In Table 4-3 to Table 4-4 the results of the intervertebral ROM are compared to other ROM studies done with asymptomatic volunteers. The results of the other studies were overall higher than the results of the current study, except in C3/C4 where some of the results were lower.

Table 4-3 – Comparing results of intervertebral ROM

	Current Study		Reitman et al. 2004 [77]		Wu et al. 2007 [76]		Piché et al. 2006 [29]		Dvorak et al [103]	Holmes et al [104]
	Radiographs		DVF		DVF		Radiographs		Radiographs	Radiograph
	Ave (stdev)	n	Ave (range)	n	Ave (stdev)	n	Ave (stdev)	n	Ave (stdev)	Ave (stdev)
C1/C2	17.46 (6.79)	20	-	-	-	-	11.6 (5.3)	30	19	-
C2/C3			9.88 (2.57-7.18)	140	13.5 (4.8)	56	10.5 (4.7)	30	17	7.7
C3/C4	16.34 (6.26)	20	15.17 (8.88-21.47)	140	17.3 (7.4)	56	15.6 (5.7)	30	24	13.5
C4/C5	15.87 (3.75)	20	16.87 (9.52-24.23)	140	22.6 (7.9)	56	16.1 (6.2)	30	18	17.9
C5/C6	13.63 (3.14)	20	15.78 (7.47-24.90)	140	19.0 (6.6)	56	15.0 (7.3)	30	21	15.6
C6/C7	11.90 (2.47)	20	13.54 (3.18-23.9)	140	17.9 (9.1)	56	14.1 (4.4)	15	-	12.5

In Table 4-4 the males and females are compared separately to another study done with flexion and extension radiographs.

Table 4-4 – Comparing results of intervertebral ROM, females

	Males				Females			
Study	Current Study		Frobin et al. [79]		Current Study		Frobin et al. [79]	
	Ave (stdev)	n	Ave (stdev)	n	Ave (stdev)	n	Ave (stdev)	n
C1/C2	16.35 (6.76)	10	11.6 (4.57)	36	17.74 (6.97)	10	10.9 (4.78)	61
C2/C3			7.8 (3.09)	34			8.4 (3.43)	57
C3/C4	15.73 (6.78)	11	11.6 (3.57)	34	17.10 (5.87)	9	15.2 (4.72)	92
C4/C5	14.29 (3.11)	11	14.4 (4.55)	33	17.80 (3.70)	9	17.0 (5.46)	95
C5/C6	12.01 (2.04)	11	12.2 (5.19)	27	15.29 (3.17)	9	17.9 (6.60)	92
C6/C7	11.17 (2.32)	11	9.8 (5.73)	10	12.61 (2.42)	9	11.4 (6.82)	23

According to the current study and the study by Frobin et al. the females exhibited a generally larger ROM. The difference in males and females is investigated statistically. From Table 4-5 it can be seen that the hypothesis of no mean difference between males and females could not be rejected.

Table 4-5 – Result for intervertebral ROM and gender

V- level	Shopiro-Wilk	ANOVA p-value	Mann-Whitney p-value	Reject / Not Reject H0
C12/C3	0.00221		0.917690	Not Reject Ho
C3/C4	0.62063	0.783916		Not Reject Ho
C4/C5	0.03960		0.426167	Not Reject Ho
C5/C6	0.16724	0.311158		Not Reject Ho
C6/C7	0.02154		0.197116	Not Reject Ho

Cervical ROM

The ROM of the cervical spine was determined as explained in section 3.5.1. and is presented in Table 4-6.

Table 4-6 – Cervical ROM

ROM of the lower cervical spine		
	Males	Females
1	60.73	82.13
2	66.03	86.24
3	65.37	68.69
4	68.69	58.04
5	67.80	78.34
6	60.55	94.00
7	47.42	80.65
8	79.73	105.07
9	58.01	73.63
10	79.30	68.90
11	58.25	-
ave	64.72	79.57
stdev	9.41	13.51
All	71.79	(78.54)

These results are much lower when compared to other cervical ROM studies done with asymptomatic volunteers. Cervical ROM studies were mostly done with external motion capturing systems. The sensors were typically placed on C7 and the head and the angle of rotation between these sensors were calculated. Therefore the ROM in these comparative studies is higher than the ROM in the current study where the angle is only measured between C1 and C7. Cervical ROM of motion measured with

the Zebris Ultrasonic device was in the range of 130°, while with the goniometric CA6000 it was in the range of 120° [37].

As mentioned in section 3.2.2 ROM is influenced by variables such as age, disc degeneration, motivation, pain, time of day posture weight, muscle activity and athletic activity. The only variable that was observed during the study and that were not constant across the sample is weight. The correlation between weight and cervical ROM was determined with the Pearson's correlation coefficient. The results showed that there was no correlation between ROM and weight ($r = 0.2083$; $p = 0.0820$), but that neck girth and ROM had a strong negative correlation ($r = -0.4332$; p 0.0498).

Cervical ROM is normally distributed (Shopiro-Wilk $p = 0.566$) and therefore an ANOVA was done to investigate the influence of gender on cervical ROM. With a p value of 0.008, the null hypothesis stating that there are no mean differences between the cervical ROM of males and females in this sample was rejected at the level of significance of 5%.

Cervical ROM is therefore influenced by girth and gender. No other anthropometric variables play a significant role.

4.3 Surface marker motion

This section answers the four questions posed in section 3.5.2. Firstly it is necessary to have an understanding of what this surface marker data looks like. In Figure 4-7 the data for the surface markers and centre points of the vertebrae is plotted for an individual in different positions. In this figure a landmark on the head, the external occipital protuberance, was made the (0,0) point on each scan in a different position. In Figure 4-7 the motion path of each surface marker can be seen as it is rotated around the external occipital protuberance.

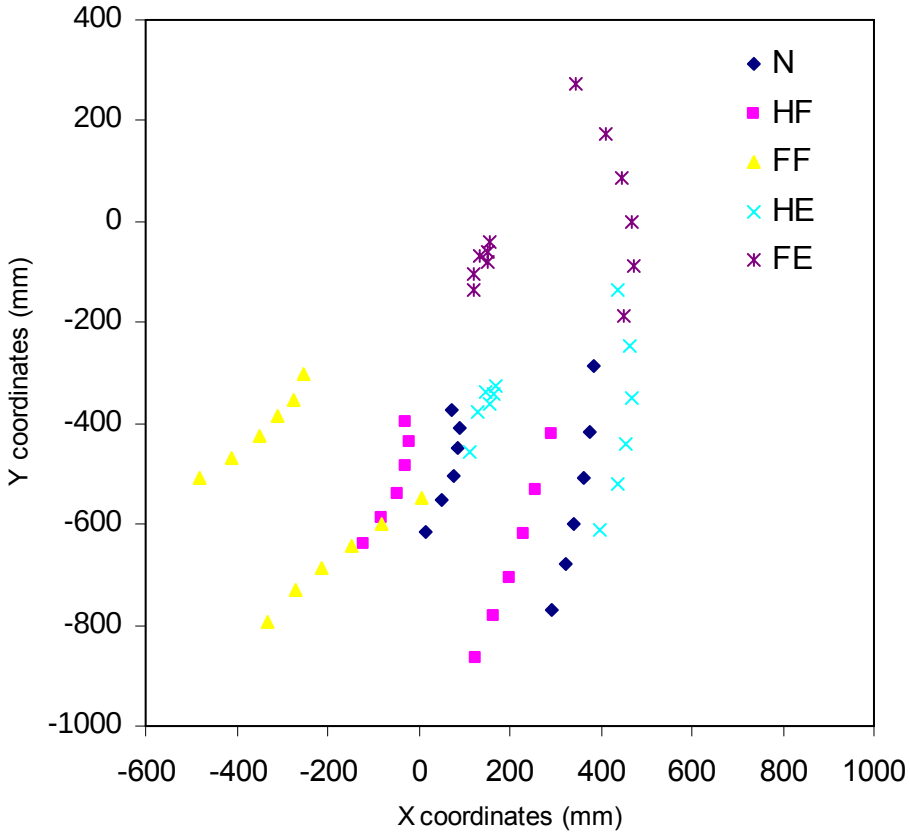

Figure 4-7 – Surface marker and vertebral centre in different positions

Figure 4-7 also shows the distance between the surface marker and the vertebrae and how it differed throughout positions. One can also see the surface markers stretching out during flexion and bulging together during extension. The motion paths for each individual vertebral level is now investigated and compared over all subjects.

4.3.1 Distance between surface marker and vertebra

The distance between the surface marker and the vertebra was calculated as explained in Figure 3-17, for each person, position and vertebral level. The ideal would be that R remains the same throughout all the motion, as if the ball bearing was attached to the vertebra with a rod of length R. As seen in Figure 4-8, this is not the case and R changes throughout the different positions with respect to the initial position of surface marker placement. This is however not a death sentence for vertebral prediction from skin surface markers, since R seems to change consistently with the difference between skin curvature and cervical spine curvature. The relationship between the two curvatures and R is investigated in this section.

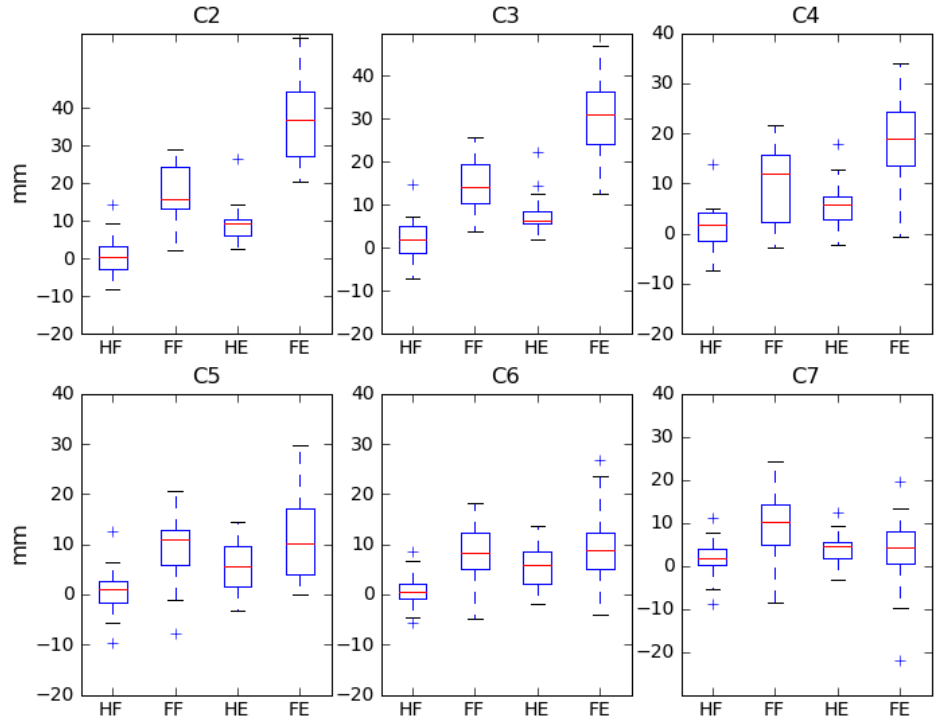

Figure 4-8 – Difference in R compared to neutral position; all subjects (n = 21)

The distance between the surface markers and the centres of the vertebrae aggregated over the different subjects is presented in Figure 4-9.

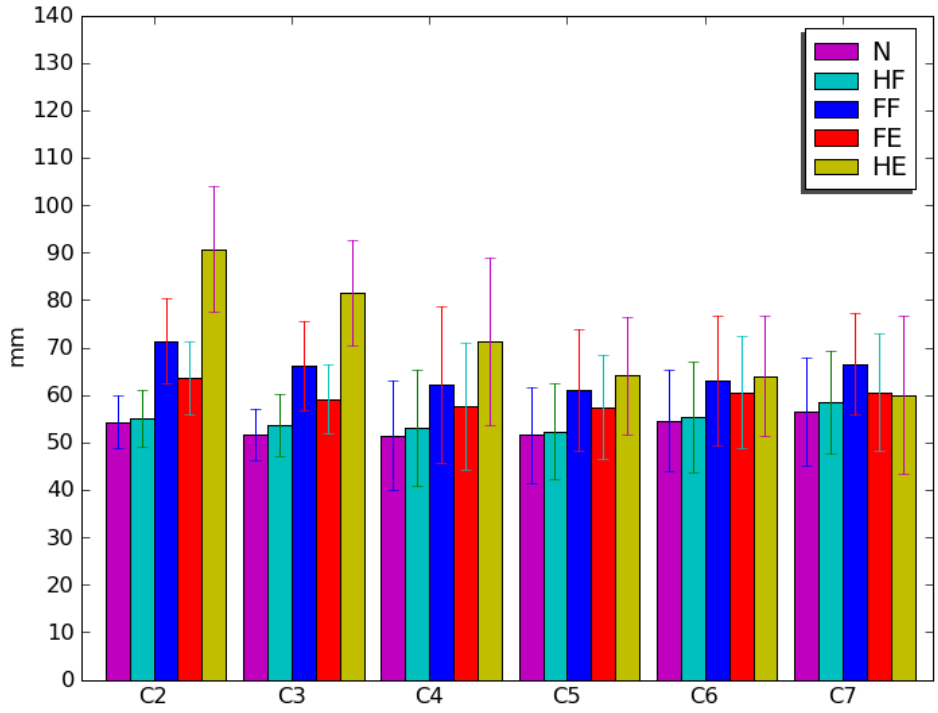

Figure 4-9 – Distance between surface marker and vertebra for all subjects (n = 21)

In the neutral position the spine has the natural lordotic curvature as seen in Figure 4-10. This lordotic curvature varies among individuals and therefore also the differences in R between the different vertebral levels in the neutral position. The different colour lines in Figure 4-10, represent the spinal curves of all the individuals in this position. In Figure 4-10 the curvature of the ball bearings can also be seen. This curvature excludes the top ball bearing which is the ball bearing for the occipital protuberance. This surface marker follow a similar curvature, but with a slightly stronger convexity than that of the vertebral curvature. This stronger convexity in the surface marker curvature explains the results of R. R is largest in C2 and C7, where the surface markers are furthest away from the vertebrae. The collective R therefore takes on a concave[a] form across the vertebral levels. This concave curve of R can clearly be seen in Figure 4-11, where the Rs of each position are grouped together. Keep in mind that R includes the 2mm radius of the ball bearing.

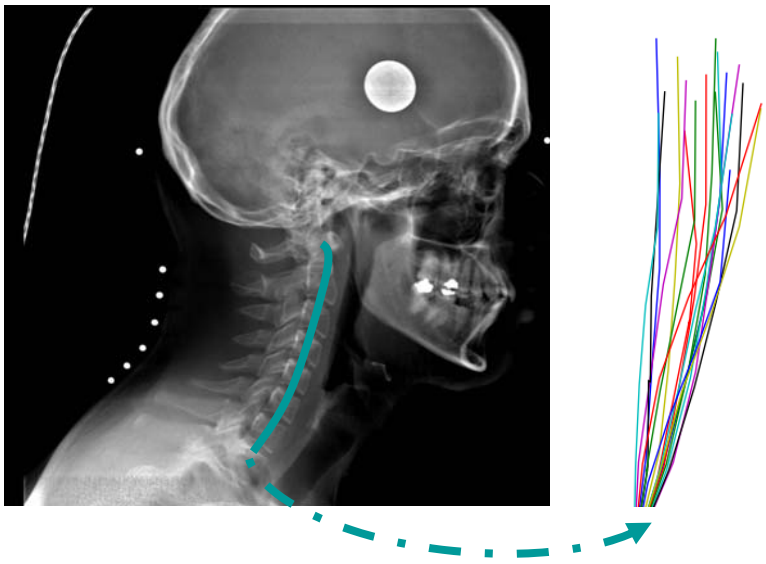

Figure 4-10 – Scan in the neutral position

[a] Curved inwards

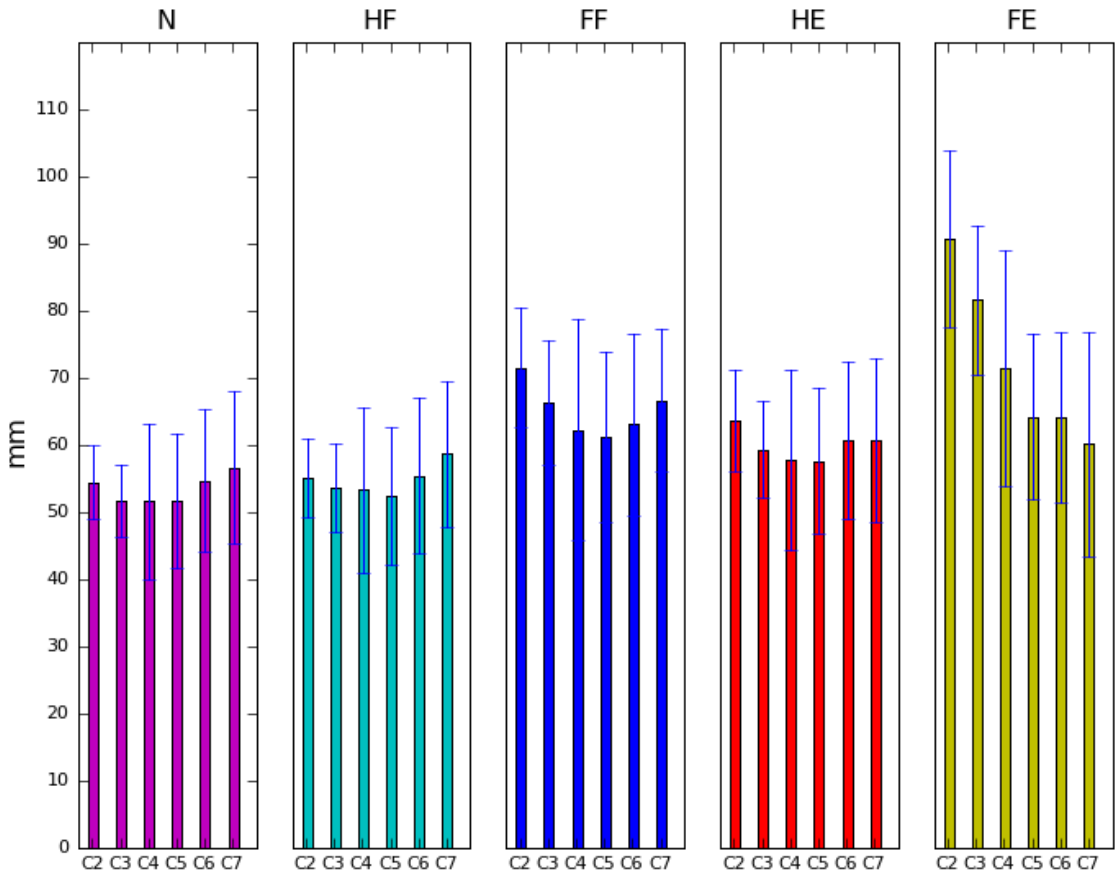

Figure 4-11 – R curvatures in different positions

In half flexion, as shown in Figure 4-12, the cervical spine has no curvature, but tends to a straight line. On the skin surface curvature only a remnant of the lordotic curvature remained. With both the vertebral and skin surface curvature tending towards a straight line, R is almost constant across vertebral levels. Due to the way the skin stretch during flexion, the surface markers shifted up and caused R to be a little larger than in the neutral position. The upward shift of the ball bearing at the C6/C7 is significant and therefore R is also the highest at this vertebral level. Apart from the increase in R (this is clearest in Figure 4-9), R-half flexion is very similar to R-neutral (see Figure 4-11). This similarity implies that the surface markers still represented the vertebrae as they had in the position it was placed in.

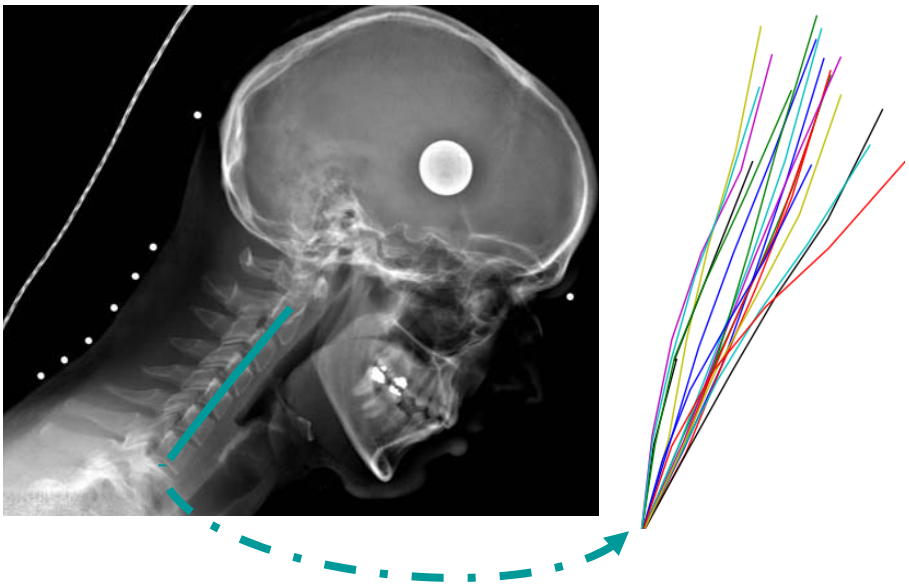

Figure 4-12 – Scan in the half flexed position

During full flexion (Figure 4-13), R differs more across vertebral level than in neutral and half flexion. From Figure 4-11 it is evident that R takes on the same curvature that the cervical spine exhibits in this position. While the skin surface remains a straight line, with the surface markers just stretching further apart from each other, the kyphotic curvature of the spine then results in the concave curvature of R across the vertebral levels. The vertebral curvature in full flexion differs due to ROM in a subject. The ROM explains the bigger standard deviation in this position.

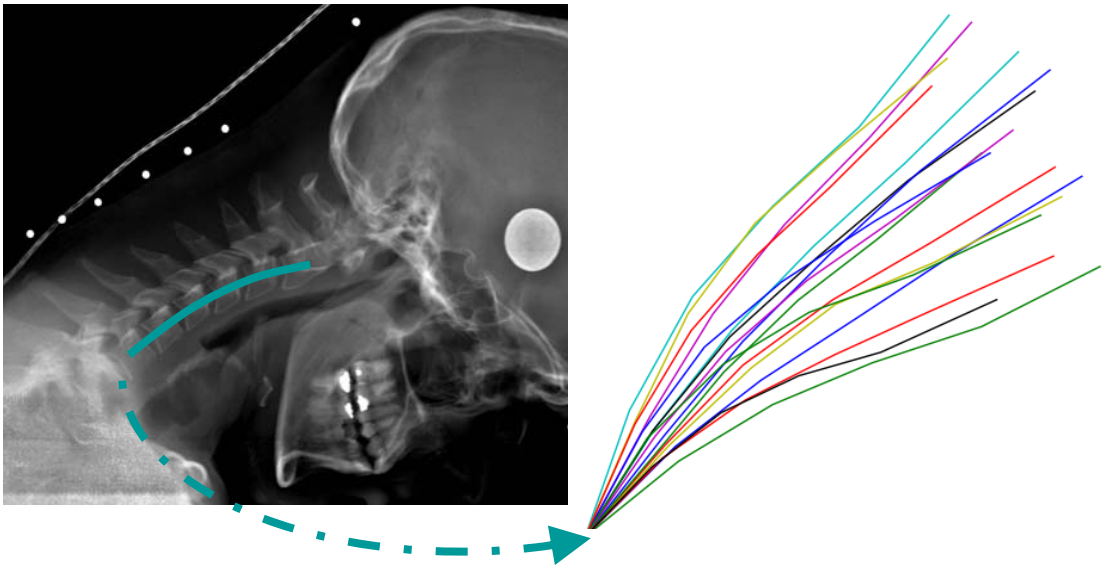

Figure 4-13 – Scan in the full flexed position

In half extension the natural cervical lordosis is accentuated in the spine and in the skin surface. From Figure 4-9 and Figure 4-11 it is evident that R follows a similar concave curvature as in the other positions. The skin fold however causes some surface markers to deviate from the curve, which also cause bigger standard deviations in the mid-cervical vertebrae as observed in Figure 4-9 and Figure 4-11. The skin fold is situated at different vertebral levels for different individuals. If the skin folds were always at C3-C4 as is the case in the specific scan of Figure 4-14, R of C3-C4 should have been larger. Compared to the other R curvatures, the mid-cervical vertebrae are all slightly larger. This is explained by the skin fold that forces the surface markers further away from the vertebrae, hence increasing R. It should also be noted that C6 exhibits different behaviour than in the other positions. From the specific scan it is not clear why this is the case, but a possibly reason could be the fact that at this level the skin surface could not curve as much outward as the spine did due to a lack of space. Therefore C6 was curved further outward than the corresponding surface marker.

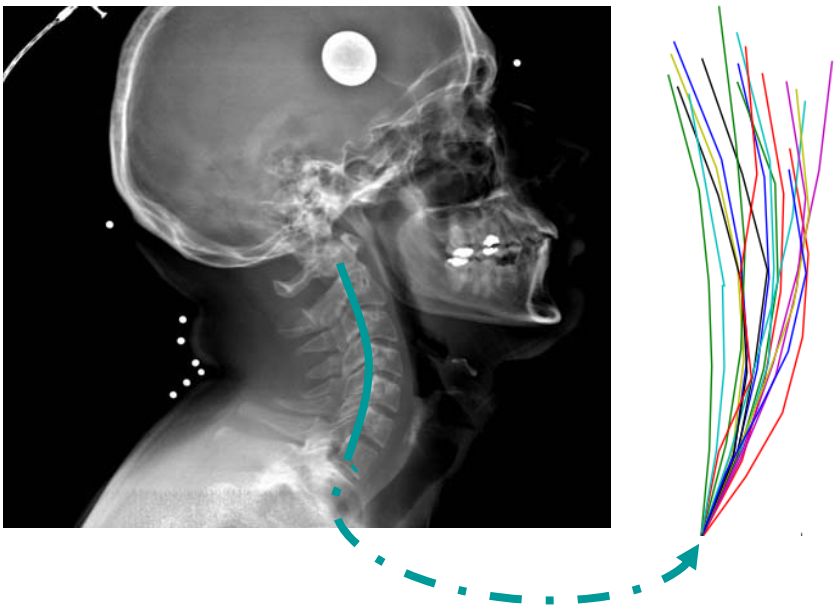

Figure 4-14 – Scan in the half flexed position

From simply looking at the scan in full extension, Figure 4-15, it does not seem like the surface markers could possibly be representing the vertebrae. The curves of the vertebrae are all similar, with the ROM influencing the degree of concavity. The skin profile however can not follow the extreme concavities of the spine since space is limited. The surface markers get either folded in between the skin or pushed outward due to the skin fold. The skin folds therefore influence the amount of surface marker deviation from the curvature of the vertebrae. In full extension the R curvature is not a kyphotic curve, but rather a stepwise increase from C7 upwards. Once again the skin folds differently for each

individual, but the curve of R could be explained by the fact that which ever way the skin folds, the C6 and C7 surface markers remain closest to the vertebrae and the rest of the surface markers are moved further away from the vertebrae due to the skin and soft tissue.

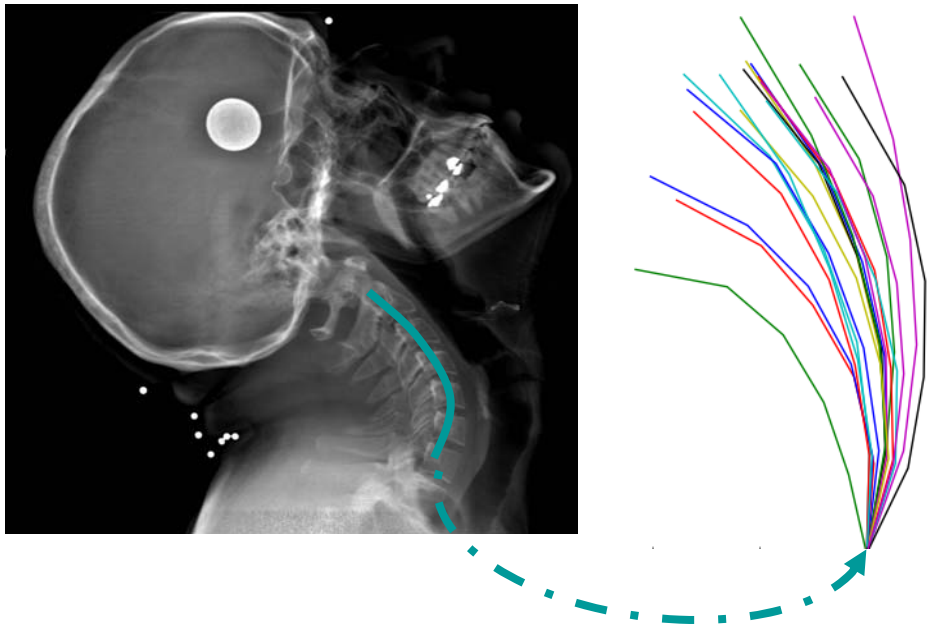

Figure 4-15 – Scan in the full flexed position

As summarised in Figure 4-11, the curvatures of R all follow a concave curve with the exception of full extension. In this section R was explained by the difference in curvature of the cervical spine and the neck's skin surface. With the concave curvature, the largest R is at C2 and C6-C7. The mid-cervical vertebrae were therefore closest to the vertebrae. This is counter intuitive: during the palpation process these vertebrae were most difficult to identify with palpation. It must however be kept in mind that the palpation dealt with the spinous processes and with R, the vertebral centre is of importance. By focusing on the difference in curvature between the vertebrae and the surface markers, this R curvature is clarified. In flexion the skin curvature is a straight line, while the vertebrae form a kyphotic curve. Therefore the mid vertebrae are closest to the surface markers. In neutral and extension, the vertebrae and skin surface follows a lordotic curve, but the skin curvature has a stronger convexity, once again causing the mid vertebrae to be closer to the surface markers.

Full extension is the only position where the concave curvature is not followed. The increase in R can be explained by the difference in the two curvatures, but the amount by which it increases from C2 to C7 would be difficult to predict for an individual, due to the skin folding at different places for different individuals.

4.3.2 Marker–vertebral rotation

Due to the skin that stretches and folds during motion, the ball bearing positions on the curvature and the distances between the surface markers change. It was clear from the scans, that in flexion the surface markers shifted up and rotated with respect to the vertebrae. Therefore R alone does not provide adequate information to predict the vertebrae and an angle parameter is also necessary to account for rotation. The vertebral rotation cannot be used as this angle parameter, since the surface marker deviated from the rotation of the vertebrae as seen in Figure 4-16. In this figure the difference in β in neutral and the position examined, was subtracted from the vertebral rotation from the neutral to the position investigated. Therefore the negative values in the flexed positions indicate that the surface marker rotated more than the vertebrae.

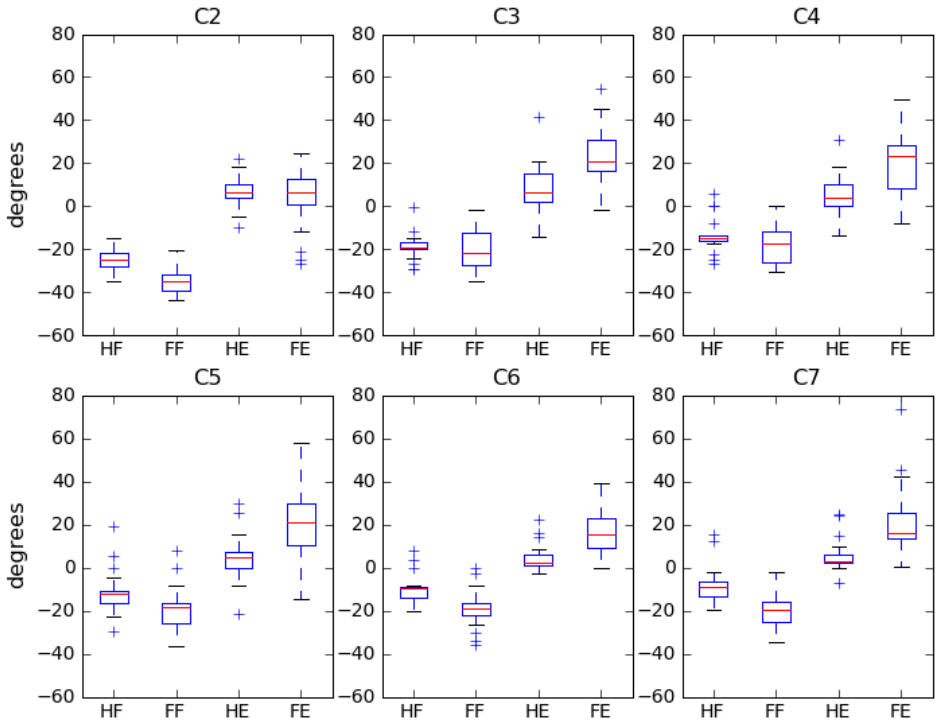

Figure 4-16 – Difference in vertebral rotation and surface marker rotation; all subjects (n = 21)

The difference in angle was overall smaller in the lower vertebral levels. In extension the surface markers rotated less. The deviation and range was also more in C3 to C6, where the skin fold caused arbitrary ball bearing motion.

The angle β gives more information on the position of the surface marker with respect to the vertebra.

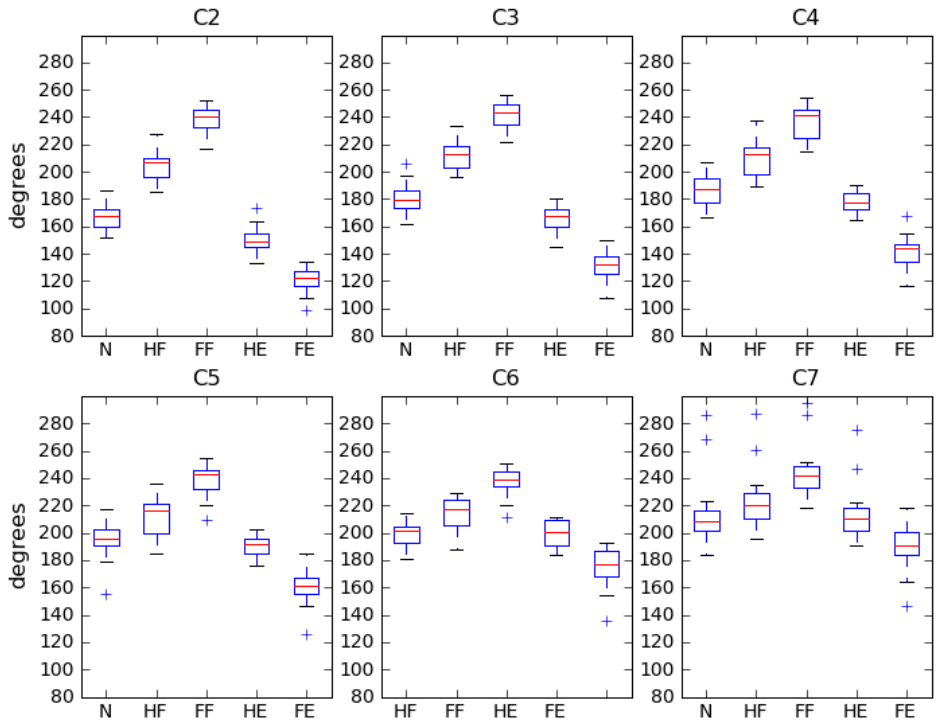

Figure 4-17 – β for each position and vertebral level; all subjects (n = 21)

With the distance and the angle between the surface marker and the vertebrae known, the vertebrae can be predicted form the surface marker position.

4.3.3 Discussion on vertebrae prediction

In section 4.3, the surface marker motion has been investigated by means of parameter R and β. Therefore, to be able to predict the vertebrae from the surface markers the parameters and curvature need to meet the following requirements.

1. Was the skin surface curvature consistent in the specific position or at least in a sub group of that position?
2. Was the deviation in R and β small enough for prediction or could the deviation be explained and controlled?

If the answer is yes to these questions, it can be concluded that the vertebrae can be predicted from the skin surface markers in the position and vertebral level. The questions posed are discussed to draw conclusions regarding vertebral prediction.

4.3.3.1 Skin surface marker curvature patterns

If the curvature of the surface markers is consistent across individuals it would be possible to predict the vertebrae from the surface markers by using R and β. The different curvatures are scaled for comparison and presented in the figures of this section.

Neutral

In the neutral position, as seen in Figure 4-19, the same curvature is followed and regression curve was fit (black line). The variation is acceptable, since it correlates with the variation in the spine curvature.

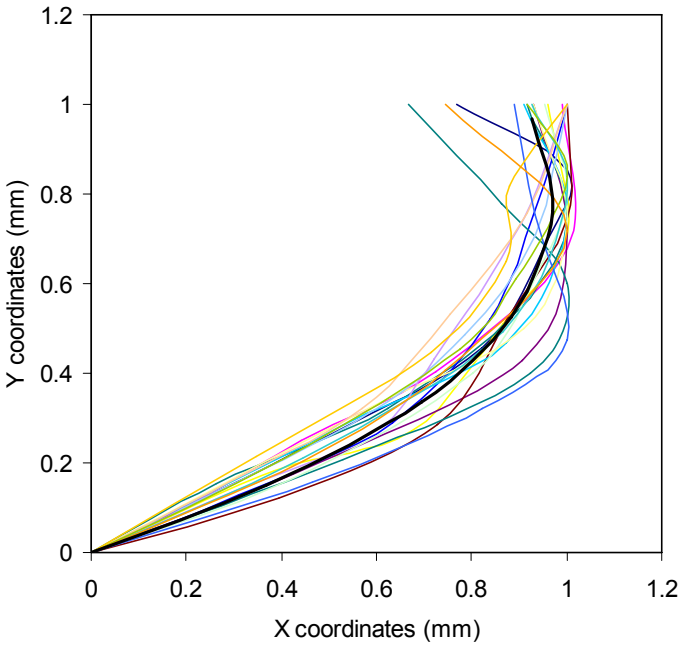

Figure 4-18 – Skin surface curvature in neutral, all subjects

In this study, the neutral position was determined by the radiologist. Variation in the neutral position could be controlled by improving the protocol for determining the neutral position.

Flexion

In flexion the skin surface curvature tended toward a straight line. In half flexion, Figure 4-20, the skin surface follow a slight lordotic curve, but tends toward a straight line, which is achieved during full flexion. In flexion the average trend (black line) was more closely followed, with individuals with a smaller ROM only having a remnant of the lordotic curve. The individuals with a larger ROM exhibits the same curvature, the curve (if not scaled) would just be longer.

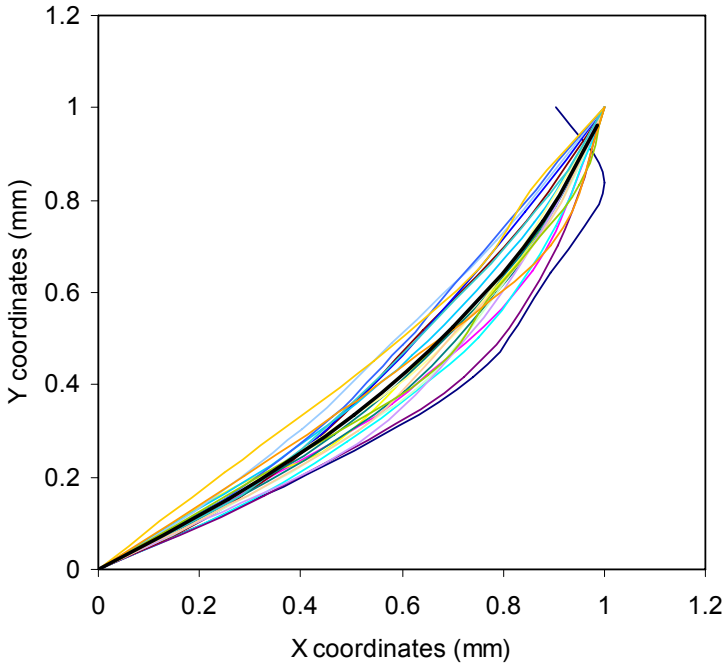

Figure 4-19 – Skin surface curvature in half flexion, all subjects

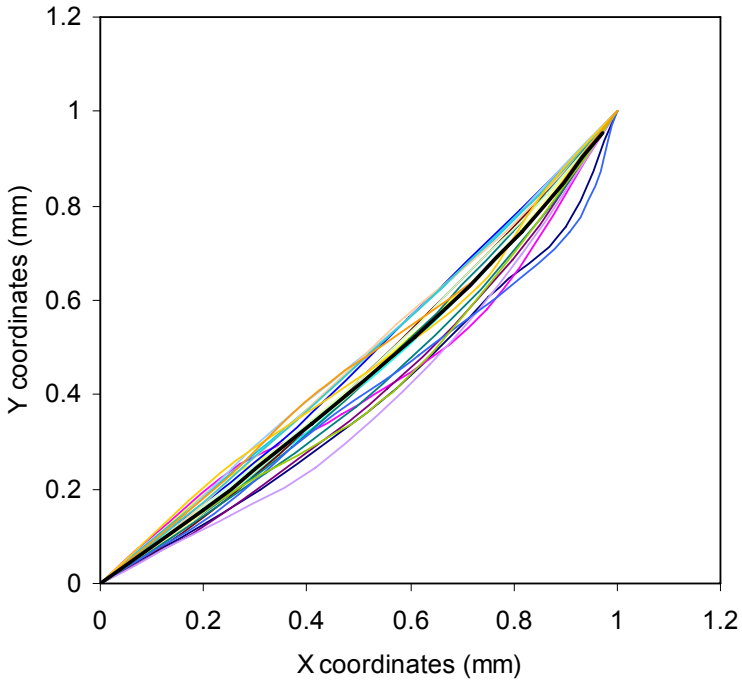

Figure 4-20 – Skin surface curvature in full flexion, all subjects

The consistency of the curvature is good in both flexed positions. Therefore in the flexed positions the parameters R and β could definitely be used to predict the vertebrae from the surface markers.

Extension

The average skin curvatures of the extended positions are not clear. Great variation occurs. In cases of a big skin fold, the surface markers were all in one line, folded between the skin folds as seen in Figure 4-21.

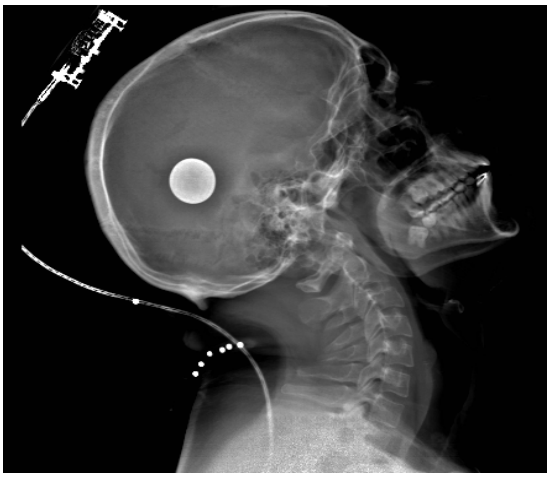

Figure 4-21 – Full extension in individual with large skin fold

Firstly the half extension is presented. The males and females are presented separately, since a difference was observed between the two gender groups.

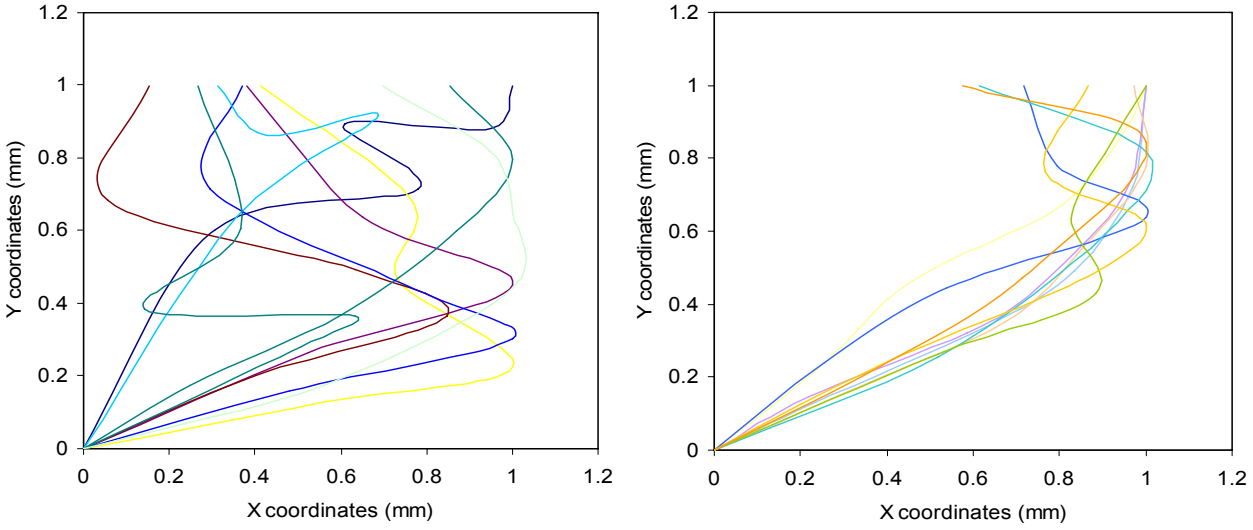

Figure 4-22 – Skin surface curvature in half extension, males and females respectively

In half extension the skin curvature differ between males and females. It can be concluded from Figure 4-22 that in this sample the females and males exhibited a skin fold in half extension. The difference is

that the females mostly had a fold at C3-C4 vertebral level, while the males exhibited a skin fold at the levels from C4 to C6. The skin fold at the lower levels was bigger and the lower surface markers were typically folded up in line between the skin fold. The upper surface markers typically bulged out. In the females the lower surface markers followed the curvature of the corresponding vertebrae, while the top vertebrae deviated from the curve, resulting in a larger R, as explained in section 4.3.1.

In full extension these graphs look even more like modern art, therefore they were grouped. Gender, ROM and skin fold were categorized into two groups and skin curvature was then plotted for each group. Grouping according to gender did not make a difference to the chaos. The graphs for skin fold and ROM are presented in Figure 4-23 and Figure 4-24 respectively.

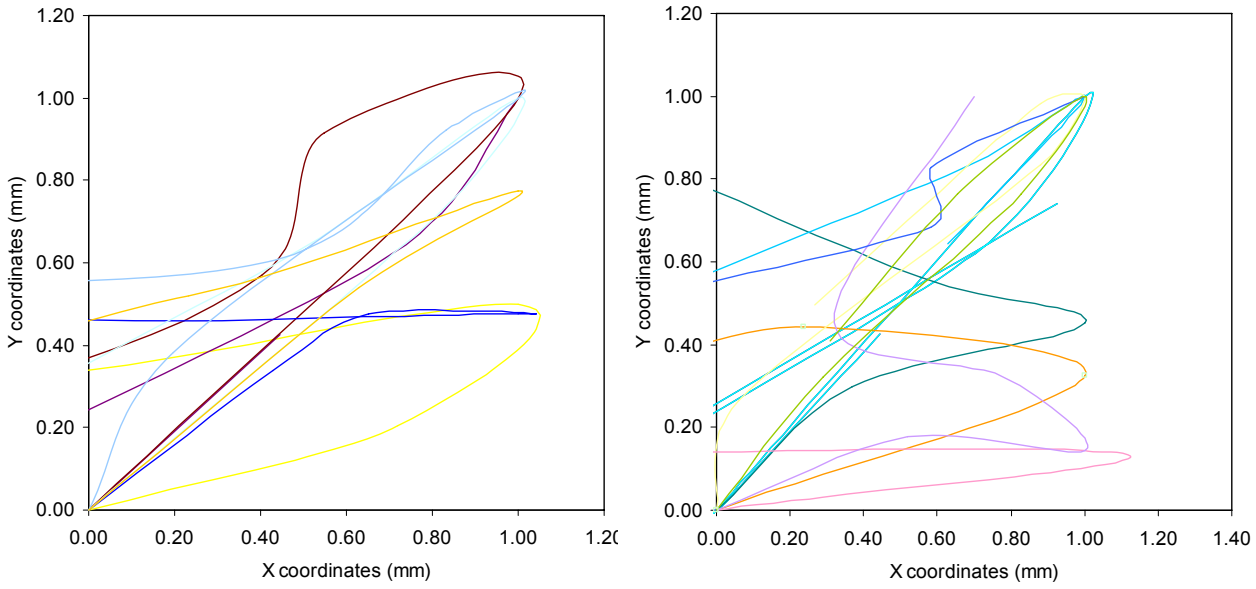

Figure 4-23 – Skin surface curvature in full extension, large (left) and small (right) skin fold subjects

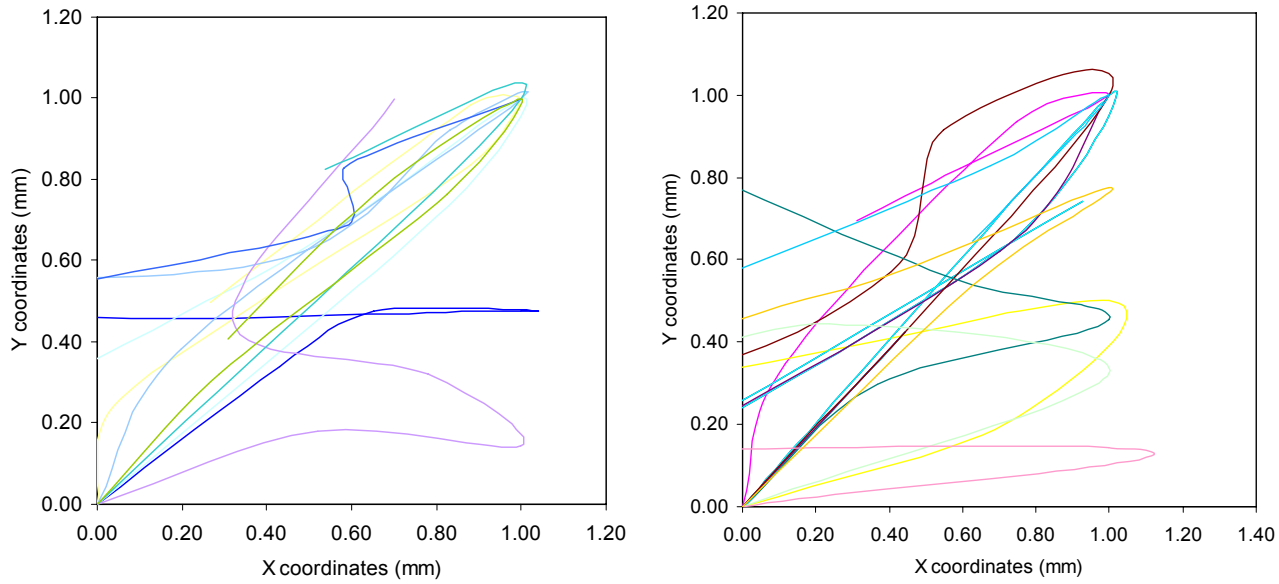

Figure 4-24 – Skin surface curvature in full extension, large (left) and small (right) ROM subjects

After partitioning the curvatures into groups of small and large skin fold and ROM, there still seems to be no pattern in the skin curvature during full extension.

The question of skin curvature consistency was answered by the graphs in this section. The skin curvature was consistent in neutral half flexion and full flexion. The variation was due to ROM being different across individuals, which also affects the curvature of the vertebrae. In the extended positions there were much more variation. In half extension, the variation could be reduced by grouping the curves according to gender. In full extension, the curves were grouped according to different parameters, but no pattern could be determined. This section is summarised in Table 4-7.

Table 4-7 – Surface marker curvature observed

Position	Curvature consistency
N	Strong Consistency
HF	Strong Consistency
FF	Strong Consistency
HE	Poor Consistency
FE	No consistency

4.3.3.2 Variance in R and β explained

The averages and standard deviations for R and β is presented in Table 4-8.

Table 4-8 – Standard deviations for R and β

stdev	N		HF		FF		HE		FE	
	R	β	R	β	R	β	R	β	R	β
C2	5.50	9.65	5.91	11.98	8.92	8.91	7.61	8.91	13.18	9.09
C3	5.44	11.09	6.59	11.04	9.35	8.94	7.22	8.94	11.05	10.68
C4	5.98	11.85	6.28	12.74	10.04	11.67	6.22	11.67	6.73	10.60
C5	7.38	12.95	7.34	12.93	9.12	11.46	7.09	11.46	7.57	12.82
C6	7.51	10.04	8.77	11.29	9.89	10.56	7.73	10.56	8.23	14.21
C7	11.32	23.96	10.84	20.26	10.60	18.24	12.29	18.24	16.68	16.88

For R, the standard deviation ranged between 5.44 and 16.68 mm. In β there is a range from 8.91° to 23.96°. When the averages of R and β is used to predict the vertebrae, this prediction will on average be out with 8.4 mm in the x direction and 1.9 mm in the y direction. The vertebra which has the biggest body is on average 20 mm in breadth and 10 cm in height. Therefore one can typically be out with about 50% of the actually breadth of the vertebrae and 20% of the actual height. Therefore it is necessary to look at ways of decreasing this variation.

To improve this prediction, the causes of variation in R and β need to be known, to make more intelligent predictions from the parameters R and β.

R and β was correlated with all the anthropometric variables to see which influence these parameters. All analyses were done at a significance level of 5%. Firstly, all data was tested for normality as this determines the type of analyses done. The Shopiro-Wilk[a] test for normality was done on all the data. The majority of data were normally distributed. In the cases where the hypothesis of normally distributed data was rejected, nonparametric[b] analysis was done.

All the anthropometric variables measured in section 3.3.3 were investigated for correlation with R and β. The relationship between gender and R and β was observed with ANOVA. The ANOVA was chosen, since it is a good test to compare categorical variables with. The null hypothesis of the ANOVA is that there is no mean difference between the groups investigated. In the case of non-normal data a nonparametric method, the Mann-Whitney U test was followed. This analysis assesses whether two samples of observations come from the same distribution. The null hypothesis is that the two samples are drawn from a single population.

---

[a] Generally accepted as the most reliable test for non-normality for small to medium sized samples.

[b] Nonparametric methods are often referred to as distribution free methods as they do not rely on assumptions that the data are from a given distribution

The relationship between R and β, and the continuous variables were tested with correlations coefficients. In the case of normal data Pearson's correlation coefficient was used. Pearson's correlation reflects the degree of linear relationship between two variables. In the exceptions where the data was not normally distributed, Pearson's correlation coefficient could be misleading. Spearman's rank correlation coefficient is a more accurate analysis in such cases, since it assesses how well an arbitrary monotonic function could describe the relationship between two variables, without making assumptions about their distribution. Both Pearson's and Spearman's correlation coefficients, range from positive one (+1) to negative one (-1). Positive one indicates a perfect positive correlation, while negative one indicates a perfect negative correlation. A correlation of 0 means there is no linear relationship between the two variables.

Variance in R

The results from testing for gender dependency in R are presented in Table 4-9.

Table 4-9 – ANOVA for R with gender

	N	HF	FF	HE	FE
	p-value	p-value	p-value	p-value	p-value
C2	0.0004	0.0422	0.0111	0.0036+	0.0111
C3	0.0005	0.0208	0.0120	0.0015	0.0741
C4	0.0009	0.0029	0.0406	0.0226	0.5299
C5	0.0015	0.0001	0.0022	0.01854+	0.4804
C6	0.0000	0.0000	0.0009	0.0005+	0.4459
C7	0.0131	0.0010	0.0026	0.0222	0.0513+

+ Mann-Whitney

These p-values of below 0.05 showed that the null hypothesis assuming no mean difference between males and females could be rejected. Therefore from these results, it is clear that R is gender dependant in all positions, except full extension. The correlations of R with the other anthropometric variables are presented in Table 4-10 - Table 4-14, from neutral to full extension.

Table 4-10 – Correlation for R with anthropometric variables in neutral

	Length		Weight		Girth		% Stretch		Skin fold		CROM	
	r	p-value	r	p-value	r	p-value	r	p-value	r*	p-value	r	p-value
C2	0.5897	0.0049	0.6999	0.0004	0.7810	0.0000	0.4594	0.0362	0.37	0.10	-0.4147	0.0616
C3	0.5505	0.0097	0.7375	0.0001	0.8627	0.0000	0.5025	0.0203	0.53	0.01	-0.3108	0.1702
C4	0.5156	0.0239	0.6592	0.0021	0.8351	0.0000	0.5081	0.0263	0.40	0.09	-0.4372	0.0613
C5	0.3818	0.0967	0.5787	0.0075	0.7133	0.0004	0.6626	0.0015	0.33	0.16	-0.3789	0.0995
C6	0.5418	0.0136	0.7430	0.0002	0.8646	0.0000	0.6622	0.0015	0.49	0.03	-0.4632	0.0397
C7	0.5984	0.0042	0.6146	0.0030	0.0564	0.0078	0.6791	0.0007	0.27	0.23	-0.0741	0.7495

* Spearman's coefficient

The anthropometric variables correlated well with R in the neutral position. Length, weight, girth and stretch played a definite and overall significant role for explaining the variation in R. All the significant correlations were positive correlations, implying that an increase in, for example neck girth, would result in a linear increase in R. Of all the variables girth correlated the strongest with R.

Table 4-11 – Correlation for R with anthropometric variables in half flexion

	Length		Weight		Girth		% Stretch		Skin fold		CROM	
	r	p-value	r	p-value	r	p-value	r	p-value	r*	p-value	r	p-value
C2	0.5020	0.0204	0.6342	0.0020	0.6981	0.0004	0.1230	0.5954	0.54	0.01	-0.1732	0.4527
C3	0.5323	0.0130	0.6368	0.0019	0.7319	0.0002	0.1890	0.4119	0.57	0.01	-0.1198	0.6050
C4	0.6910	0.0011	0.7251	0.0040	0.8395	0.0001	0.3113	0.1945	0.54	0.02	-0.3347	0.1614
C5	0.6640	0.0014	0.7951	0.0003	0.8945	0.0000	0.5112	0.0212	0.54	0.01	-0.4227	0.0633
C6	0.6361	0.0026	0.8205	0.0000	0.9118	0.0000	0.6009	0.0051	0.64	0.01	-0.4724	0.0354
C7	0.6472	0.0015	0.7372	0.0001	0.7124	0.0003	0.7252	0.0020	0.32	0.16	-0.2141	0.3515

* Spearman's coefficient

Similar results to that of R in the neutral position are observed in half flexion, with girth still the strongest factor. The only difference is that in half flexion, skin fold plays a more significant role than stretch. This is counterintuitive, since it was initially thought that stretch would be an indication of how much the surface markers move upward during flexion due to the stretch of the skin. Does full flexion confirm this counter intuitive result concerning stretch?

Table 4-12 – Correlation for R with anthropometric variables in full flexion

	Length		Weight		Girth		% Stretch		Skin fold		CROM	
	r	p-value	r	p-value	r	p-value	r	p-value	r*	p-value	r	p-value
C2	0.5423	0.0111	0.6787	0.0007	0.7741	0.0000	0.2775	0.2233	0.49	0.03	-0.0675	0.7711
C3	0.5218	0.0153	0.6404	0.0018	0.7658	0.0001	0.2553	0.2641	0.43	0.05	-0.0866	0.7090
C4	0.4720	0.0413	0.6567	0.0023	0.7534	0.0002	0.2558	0.2905	0.52	0.02	-0.0554	0.8217
C5	0.5170	0.0195	0.6738	0.0011	0.8138	0.0000	0.3882	0.0908	0.50	0.03	-0.1802	0.4470
C6	0.4853	0.0301	0.7096	0.0005	0.8634	0.0000	0.4671	0.0378	0.50	0.03	-0.2009	0.3958
C7	0.5369	0.0121	0.6699	0.0009	0.7381	0.0001	0.5721	0.0067	0.28	0.22	-0.0378	0.8707

Pearson; * Spearman

In full flexion stretch exhibits the same results. Stretch only correlates with the lower vertebral levels. The other results also coincide with the result of neutral and half flexion. The results of cervical ROM are generally lower than expected. It was thought that in the extreme positions ROM would play a significant role in determining variation in R. Even in the extreme position of extension ROM does not feature as a source of variation in R. This may be an indication that the difference in vertebral curvatures due to ROM, was consistent with the difference in surface marker curvatures, having therefore no effect on R. It could also be that there is a relation between ROM and R, but that it is not linear.

Table 4-13 – Correlation for R with anthropometric variables in half extension

	Length		Weight		Girth		% Stretch		Skin fold		CROM	
	r	p-value	r	p-value	r	p-value	r	p-value	r*	p-value	r	p-value
C2*	0.66	0.00	0.64	0.00	0.67	0.00	0.31	0.18	0.34	0.13	-0.46	0.03
C3	0.5157	0.0167	0.6851	0.0006	0.7552	0.0001	0.3499	0.1200	0.49	0.03	-0.1140	0.6227
C4	0.4026	0.0874	0.5810	0.0091	0.6386	0.0033	0.4055	0.0850	0.21	0.40	-0.0790	0.7480
C5*	0.38	0.09	0.57	0.01	0.58	0.01	0.38	0.10	0.37	0.11	-0.20	0.40
C6*	0.55	0.01	0.60	0.01	0.73	0.00	0.42	0.07	0.38	0.09	-0.31	0.19
C7	0.5116	0.0178	0.5820	0.0056	0.5472	0.0103	0.6140	0.0031	0.33	0.15	0.0122	0.9582

Pearson; * Spearman

In half extension the overall correlation decreased due to the arbitrary surface marker motion caused by the skin folds. Although the skin folds definitely influenced the motion of the surface marker, there was no correlation between skin fold and R. This was also different than expected. It was expected that the magnitude of the skin fold would give an indication of the motion of the surface marker in extension. Girth and weight still remained consistently correlated with R across all vertebral levels.

Table 4-14 – Correlation for R with anthropometric variables in full extension

	Length		Weight		Girth		% Stretch		Skin fold		CROM	
	r	p-value	r	p-value	r	p-value	r	p-value	r*	p-value	r	p-value
C2	0.4919	0.0235	0.4381	0.0470	0.5340	0.0126	0.3647	0.1040	0.25	0.27	-0.1177	0.6115
C3	0.5337	0.0127	0.4760	0.292	0.4956	0.0223	0.2890	0.2038	0.27	0.23	0.0790	0.7336
C4	0.4501	0.0532	0.2392	0.3239	0.1950	0.4237	0.0953	0.6980	0.14	0.58	0.0773	0.7530
C5	0.1412	0.5526	0.0880	0.7121	0.1896	0.4234	0.2468	0.2943	-0.27	0.24	0.2281	0.3333
C6	-0.1130	0.6353	0.1365	0.5661	0.2516	0.2846	0.3827	0.0958	0.01	0.97	0.3029	0.1942
C7*	0.35	0.12	0.44	0.05	0.35	0.11	0.61	0.00	0.1897	0.64	0.23	0.32

Pearson; * Spearman

In full extension the overall correlation of anthropometric variables with R was poor. No anthropometric variables correlate with R in this position.

In general the correlation between anthropometric variables and R was good, especially for variables such as girth, weight and also to a lesser extent length. These variables could definitely aid in the predicting of the vertebrae from the surface markers.

A best fit general regression was done to see in which position and vertebrae which variable or what combination of variables would contribute to predict R most accurately. The results are presented in Table 4-15. These best fit analysis is evaluated with the coefficient R^2, which is the proportion of variability in a data set that is accounted for by a statistical model.

Table 4-15 – Best fit regression for R from anthropometric variables

	Gender	Length	Mass	Girth	Stretch	Skin Fold	CROM	R^2
N C2				0.78				0.59
N C3				0.86				0.73
N C4		-0.32		1.08				0.71
N C5		-0.47		0.83	0.47			0.67
N C6		-0.44		0.92	0.39		-0.20	0.86
N C7			0.36		0.49			0.50
HF C2	0.58			1.20				0.53
HF C3	1.22			2.20		-0.63		0.62
HF C4				0.84				0.69
HF C5				0.89				0.79
HF C6		-0.25		0.91	0.24		-0.16	0.87
HF C7		0.29			0.52	0.36		0.71
FF C2				0.92			0.33	0.65
FF C3				0.90			0.30	0.62
FF C4				0.91			0.35	0.62
FF C5	-1.07	0.47	-1.28			1.28	0.41	0.76
FF C6			-0.93	1.39	0.22	0.43	0.21	0.85
FF C7	-0.79	0.54	-1.22		0.35	1.17	0.51	0.76
HE C2				0.59				0.32
HE C3				0.87			0.26	0.58
HE C4				0.64				0.37
HE C5		-0.59		1.07				0.49
HE C6	-0.47	-0.71		0.88				0.66
HE C7					0.56	0.34		0.43
FE C2	-0.54							0.26
FE C3		0.67					0.35	0.32
FE C4	1.70	0.87		1.59		-1.01		0.44
FE C5	1.67			2.53		-1.35		0.22
FE C6		-0.66	-0.70	1.32	0.50		0.46	0.52
FE C7					0.62		0.43	0.39

After the correlation results, it came as no surprise that neck girth played a prominent role in predicting R. As discussed previously it was unexpected that CROM did not correlate strongly with R in the extreme positions. CROM did however feature in the regression model and is taken into account along with girth, to predict vertebrae in full flexion.

These predictions are good. In neutral in the different levels up to 86% of the variation could be explained by the regression. In half flexion this value ranged between 53% and 79%. In full flexion the regression for R was very good and between 62% and 86% of variation could be accounted for throughout the vertebral levels. In extension the regression was still statistically significant, but on average less than 50% of variation could be accounted for by the regression model.

Variance in β

The correlation between anthropometric variables and β was much poorer than in R. Only few cases had a p-value of less than 0.05 and are presented in Table 4-18 and Table 4-17.

Table 4-16 – Correlation for β with anthropometric variables in neutral and flexed positions

	Variable	r / F	p-value
N C6	CROM	-0.4875	0.0292
N C7	CROM	-0.6047*	0.0037
N C7	Gender	-	0.0101+
N C6	Gender	16.2839°	0.0008
N C6	Girth	0.6566	0.0017
N C7	Girth	0.52819*	0.0139
N C6	Length	0.5772	0.0077
HF C7	CROM	-0.6495*	0.0225
HF C6	Gender	10.9055°	0.0040
HF C7	Gender	-	0.0101+
HF C6	Girth	0.6468	0.0021
HF C7	Girth	0.5430*	0.01387

Pearson ; * Spearman; + Mann-Whitney

CROM, gender and girth were the variables that correlated the best with β. No variable had a consistent strong correlation with β, except for CROM in full extension. Note that the strong correlations mainly occurred in the lower cervical vertebrae.

Table 4-17 – Correlation for β with anthropometric variables in the extended positions

	Variable	r	p-value
HE C6	CROM	-0.4754*	0.0342
HE C7	CROM	-0.4846	0.0260
HE C6	Gender	-	0.0029+
HE C7	Gender	-	0.0080+
HE C6	Girth	0.4716*	0.0358
HE C7	Girth	0.4800	0.0276
FE C6	Gender	-	0.0232+
FE C5	Girth	0.4966	0.0259
FE C6	Girth	0.5047*	0.0232
FE C7	Girth	0.4436	0.0440
FE C2	Mass	0.4754	0.2940
FE C5	Mass	0.4629	0.0398
FE C5	Skin Fold	0.4978	0.0255
FE C2	CROM	-0.5443	0.0107
FE C3	CROM	-0.5167	0.0165
FE C4	CROM	-0.5598	0.0127
FE C5	CROM	-0.6071	0.0045
FE C6	CROM	-0.6160*	0.0038
FE C7	CROM	-0.7481	0.0001

Pearson ; * Spearman; + Mann-Whitney

With the poor correlations the regression was also poorer. Only the regression models for those cases that were statistically significant are presented in Table 4-18. CROM, gender girth and length were found to be important for predicting β. The extreme positions were basically the only positions that yielded significant results. In full flexion girth and CROM contribute to predict β. Although only 30% of the variance can be accounted for, the results are similar across four of the vertebral levels in this position. In full extension CROM and skin fold were important variables to predict β. CROM was significant in all the vertebral levels and the combination of skin fold and CROM also yielded good R^2's, explaining on average 45% of the variance in β.

Table 4-18 – Best fit regression analysis for β from anthropometric variables

	Gender	Length	Mass	Girth	Stretch	Skin Fold	CROM	R^2
N C5		0.72			-0.48			0.34
N C6	-0.91				-0.36			0.50
N C7							-0.45	0.16
HF C6				0.65				0.39
FF C2				0.46			0.60	0.26
FF C3				0.51			0.66	0.34
FF C4				0.58			0.62	0.32
FF C6			-0.85	1.44			0.44	0.37
HE C5	-0.99	-0.81						0.27
HE C6	-1.40	-0.90						0.65
HE C7	-0.98	-0.89						0.26
FE C2	0.50		0.64				-0.64	0.41
FE C3							-0.52	0.23
FE C4						0.34	-0.52	0.35
FE C5						0.42	-0.55	0.49
FE C6						0.28	-0.70	0.58
FE C7							-0.75	0.54

It was clear that the use of the parameters R and β to predict the vertebrae with, could be improved by determining which anthropometric variables causes variation in R and β. Strong correlations were found between R and the anthropometrical variables. Some variables had a significant, but not as strong, correlation with β in the extreme positions. These results are collectively reviewed in Table 4-19, to answer and conclude question three.

In neutral and the flexed positions, the good correlation results of R outweighed the lack of correlation in β. Therefore it can be concluded that in neutral and flexion the prediction of vertebrae from skin surface marker can be successful. In half extension the prediction can not be done with the same amount of confidence than with the flexed positions. In full extension, the correlation of CROM

in β was not enough to outweigh all other factors pointing towards the fact that vertebral prediction would be less accurate in this position. This section is thus concluded in Table 4-20.

Table 4-19 – Concluding Question 3

Position	R	β
Neutral	Correlation: Gender, length, girth, weight and stretch Strong regression: Girth, length and stretch	No consistent causes of variation
Half Flexion	Correlation: Gender, length, girth, weight and skin fold Strong regression: Girth	No consistent causes of variation
Full Flexion	Correlation: Gender, length, girth, weight and skin fold Strong regression: Girth and CROM	No correlation found Regression: Girth and CROM
Half Extension	Correlation: Gender, girth, weight Regression: Girth	No consistent correlation Regression: Gender and length
Full Extension	Poor correlation Regression: various variables No consistent cause of variation	Correlation: CROM Regression: Skin fold and CROM

4.3.3.3 Summary of discussion on vertebrae prediction

The relationship between the surface marker motion and the vertebrae was described by R and β. For vertebral prediction the deviation in R and β was significant and the correlation between anthropometrical variables and these parameters were investigated to explain the variation. R could also be explained by the difference in vertebral and skin surface curvature. Therefore the skin surface curvature was investigated for consistency. These factors were investigated in the form of two questions:

1. Was the skin surface curvature consistent in the specific position or at least in a sub group of that position?
2. Was the deviation in R and β small enough for prediction or could the deviation be explained and controlled?

Theses questions were answered and is summarized in stated in Table 4-20.

Table 4-20 – Concluding discussion on vertebrae prediction

Position	Q1	Q2
Neutral		
Half Flexion		
Full Flexion		
Half Extension		
Full Extension		
 strong yes	 yes	 possibly	 no

Therefore it is concluded that skin surface markers could be used to represent the motion of the vertebrae, by predicting the vertebral position from the skin surface with parameters R and β in neutral and in flexion. In half extension, the vertebrae can not be predicted with the same amount of confidence as in flexion. The variance in β could not be accounted for and the regression fits were not as strong as in the flexed positions. The problem of the inconsistent skin curvature would also result in less accurate prediction. Overall, even though the prediction would not be as accurate as in flexion, half extension would receive a green light for vertebral prediction from skin surface markers. The red lights however start flickering for full extension. Curvature consistency and correlations for R was poor. With the big standard deviations for R, the controlled β would not be enough to accurately predict the vertebrae. Other alternatives methods should be investigated for motion capturing from skin surface for full extension. This could include placing the markers at different landmarks in the neck, not necessarily in the posterior parts of the neck.

5 Conclusions

In this thesis motion capturing in the cervical spine was investigated. At first the anatomy and kinematics of the cervical spine were studied. Thereafter ways of capturing cervical motion were investigated. Different external motion capturing systems and internal imaging technologies were researched and their advantages and disadvantages for use in the cervical spine were reported on. The advantages and disadvantages of the different motion capturing technologies were presented in Figure 2-22 and Figure 2-25. In summary, external motion capturing systems posed many practical advantages, but lacked the ability to capture motion accurately at intervertebral level. Concern that skin and soft tissue conceal the true vertebral motion also arose. Although internal imaging technologies did not have the practical advantages of low cost, safety, simplicity, portability and easily producing three dimensional position and orientation; it had the potential to provide valuable information of motion at intervertebral level.

The above mentioned investigation yielded the critical question for external motion capturing systems: "Can one use these systems in the spine with confidence that they reflect vertebral motion?" The answer pointed to using internal imaging technologies. With internal imaging technologies the critical question was: "Is there not a simpler way to capture motion?" and here the answer pointed towards external motion capturing systems. The conflict caused by this circular argument was the germination of the problem for the empirical study.

The fundamental question of whether surface markers can represent the motion of the vertebrae was attempted by observing the motion of surface markers and vertebrae on the same medium and instance. 21 asymptomatic subjects received low dosage X-rays in five different positions, while small radio opaque markers were placed on the neck representing each vertebral level.

The data from the surface markers and vertebrae were obtained and processed. Results included vertebral kinematics for simulation purposes as well as the relationship between surface markers and vertebrae. These results are discussed in summary.

Data for simulation purposes

Absolute rotation and intervertebral rotation were determined for the cervical spine. The results compared well to previous rotation studies. From the extreme values of rotation absolute ROM and intervertebral ROM could be determined. These results will be used in continuous studies in this field to serve as input for human simulation models. The data of individuals could be used in the model,

along with their anthropometric variables, or the average data could be used. This study only reported on the age group between 20 – 30 years.

Surface markers for spinal motion capturing

Initially this question was approached by determining to what extent the surface marker failed to follow the motion of the vertebrae. This parameter was determined from the assumption that a surface marker would follow the vertebrae perfectly if it rotated and translated in exactly the same manner. The assumption that the vertebrae were perfectly represented in the neutral position was also made, and the absolute distance with which the surface marker misrepresented the vertebrae, ε, was obtained by comparing the neutral position to other positions. ε was highest in the full extension, followed by full flexion, half flexion and then half extension. The distance between the surface marker and the vertebra, R, was also determined along with β, the absolute angle between the vertebra and surface marker. The first observation from the values of R was that the difference in curvature of the surface marker and that of the vertebrae explains R across the vertebral levels. This observation took the focus of measuring each vertebral level in units of misrepresentation, but rather focusing at the complete curvature formed by the different vertebral levels. From the notion that the curvatures for the surface markers and the vertebrae are different, the argumentation for answering the question proposed in the study is continued. With different curvatures, different motion patterns can be expected and the essence is not in reporting how different they were, but finding the cause of the variation and whether this variation drive could be applied to predict vertebral motion from surface marker motion.

In order to predict the vertebrae from the surface markers using parameters R and β the following requirements need to be met.

- Consistent skin curvatures across individuals in a specific position.
- Controlled variation in R and β.

The curvatures were consistent in neutral half flexion and full flexion. In half extension the skin curvatures were consistent across male and female, but in full extension no curvature pattern was observed.

Strong correlations between R and anthropometrical variables were observed. The variable that correlated the strongest overall was neck girth. Strong regression fits were determined which in the neutral and flexed positions accounted on average for 70% of the variation. Full extension was once again the exception and poor correlations along with poor regression fits were observed. With β the

results were different in the sense that the correlations were overall poor and mostly not even statistically significant. Surprisingly, full extension exhibited a strong negative correlation with ROM.

In Table 4-20, it was concluded that in neutral, half flexion and full flexion it is possible to predict the vertebral position from surface marker by using parameters R and β and anthropometrical variables as indicated in Table 4-15 and Table 4-18 to reduce the variation and improve the accuracy of predictions. It was also concluded that prediction in half extension is possible, but would be less accurate. The ability to predict vertebrae from surface markers in the extended position was strongly doubted and alternative methods should be investigated for external motion capturing in this position.

Further work

This study only dealt with the concept of using surface markers and its viability. The study recognized variables that would play a role in different positions and vertebral levels, but did not develop a validated model to predict the vertebrae positions and rotations. Further work would include developing the model and refining the impact that anthropometric variables have on the parameters that are used for vertebral prediction. Further work would also include parameters to more points on the vertebrae.

Work is already done in the research group and should be continued on image recognition. A source of error in the data processing was the subjective manner in which the vertebral corners were identified.

Further work could also be done on improving surface marker placement techniques.

6 References

[1] Watkins J. Structure and Function of the Musculoskeletal System. Human Kinetics; 1999.

[2] *URL: http://www.indyspinemd.com/Normal/index.asp [Cited 2008 Nov 18]

[3] Bertagnoli R, Kumar S. Indications for full prosthetic disc arthroplasty: a correlation of clinical outcome against a variety of indications. Eur Spine J 2002;11(Suppl. 2):S131-S136.

[4] Maniadakis N, Gray A. The economic burden of back pain in the UK. Pain. 2000;84:95–103.

[5] van Tulder MW, Koes BW, Bouter LM. A cost-of-illness study of back pain in The Netherlands. Pain 1995;62:233–240.

[6] *In Project Briefs: Back Pain Patient Outcomes Assessment Team (BOAT). In MEDTEP Update, Vol. 1 Issue 1, Agency for Health Care Policy and Research, Rockville, MD, Summer 1994.

[7] *European Markets for Spinal Motion-Preserving Devices, May 2006, Report #A307 [Cited 2008 Jan 24]. Available from: URL: http://www.medtechinsight.com/ReportA307.html

[8] Singh K, Vaccaro A, Albert T. Assessing the potential impact of total disc arthroplasty on surgeon practice patterns in North America. Spine J 2004;4:195S–201S.

[9] Cunningham BW. Basic scientific considerations in total disc arthroplasty. Spine J 2004;4:219S–230S.

[10] *N. De Beer, PhD Proposal, 2007. University of Stellenbosch.

[11] Humphreys SC, Hodges SD, Lumpkin KJ, Eck JC, Wurster R, Hagen J, Farmer D. Assessing lumbar sagittal motion using videography in an in vivo pilot study. Int J Ind Ergon 2007;37:653–656.

[12] Grant R. Physical therapy of the cervical and thoracic spine. 3rd ed. Churchille Livingstone.

[13] Zhang X, Xiong J. Model-guided derivation of lumbar vertebral kinematics in vivo reveals the difference between external marker-defined and internal segmental rotations. J Biomech 2003;36:9–17

[14] URL: http://www.ispub.com/xml/journals/ijn/vol4n1/cervical-fig1.jpg [Cited 2008 March 4]

[15] Trew M, Everett. Human movement: An introductory text, T. 3rd ed. Churchille Livingstone;1997.

[16] Henry Gray's Anatomy of the Human Body. Images obtained from Wikipedia. URL: http://www.wikipedia.org

[17] Netter FH. Atlas of Human Anatomy. 3rd ed. Teterboro (New Jersey): Icon Learning Systems; 2003. Plate 15 – 18.

[18] Bogduk N, Twomey LT. Clinical Anatomy of the Lumbar Spine. 2nd ed. Churchill Livingstone.

[19] Porterfield JA, DeRosa C. Mechanical neck pain: Perspectives in functional anatomy. W.B.Saunders Company; 1995.

[20] *University of Maryland Medical Centre, Spine Program Available from: URL: http://www.umm.edu/spinecenter/education/anatomy_and_function_of_the_spine.htm [Cited March 27]

[21] *Website Spineuniverse URL: http://www.spineuniverse.com/displayarticle.php/article2816.html [Cited 2008 March 21]

* Websites, unpublished articles and expert opinions

[22] *URL: http://www.oispine.com/subject.php?pn=spinal-anatomy-018 [Cited 2008 Nov 19]

[23] Dvorak J, Panjabi MM, Novotny JE, Antinnes JA, (1991) In vivo Flexion/Extension of the normal cervical spine. J Orthop Res 9:828-834

[24] Cagnie B, Cools A, De Loose V, Cambier D, Danneels L. Reliabiilty and normative database of the zebris cervical range-of–motion system in healthy control with preliminary validation in a group of patients with neck pain. J Manipulative and Physiol Ther 2007;30(6):450 – 455.

[25] Assink N, Bergman GJD, Knoester B, Winters JC, Dijkstra PU. Assessment of the cervical range of motion over time, differences between results of the Flock of Birds and the EDI-320: A comparison between an electromagnetic tracking system and an electronic inclinometer. Man Ther 2008;13(5):450-455.

[26] Brendan McCane, J. Haxby Abbott, Tamara King. On calculating the finite centre of rotation for rigid planar motion. Med Eng Phys 2005;27(1):75-79.

[27] Gatton ML, Pearcy MJ. Kinematics and movements sequencing during flexion of the lumbar spine. Clin Biomech 1999;14:376-383.

[28] Ma HT, Yang Z, Griffith JF, Leung PC, Lee RYW. A new method for determining lumbar spine motion using Bayesian belief network. Med Biol Eng Comput 2008;46:333–340.

[29] Piché M, Benoît P, Lambert J, Barrette V, Grondin E, Martel J, Paré A, Cardin A. Development of a computerized Intervertebral motion analysis of the Cervical Spine for clinical application. J Manipulative and Physiol Ther 2006;30(1).

[30] Castro WHM, Sautmann A, Schilgen M, Sautmann M. Noninvasive three-dimensional analysis of cervical spine motion in normal subjects in relation to age and sex: an experimental examination. Spine 2000; 25(4):443-449.

[31] Feipel V, Rondelet B, Le Pallec JP, Rooze M. Normal global motion of the cervical spine: an electrogoniometric study. Clin Biomech 1999; 14:462-470.

[32] Mannion AF, Klein GN, Dvorak J, Lanz C. Range of global motion of the cervical spine: intraindividual reliability and the influence of measurement device. Euro Spine J 2000; 2(9):379–385.

[33] Troke M, Moore AP, Maillardet FJ, Cheek E. A normative database of lumbar spine ranges of motion. Man Ther 2005;10:198–206.

[34] Mannion A, Troke M. A comparison of two motion analysis devices used in the measurement of lumbar spinal mobility. Clin Biomech 1999; 14:612-619.

[35] Malmstrom EM, Karlberg M, Melander A, Magnusson M. Zebris versus Myrin: a comparative study between a three-dimensional ultrasound movement analysis and an inclinometer/compass method: intradevice reliability, concurrent validity, intertester comparison, intratester reliability, and intraindividual variability. Spine 2003; 28(21):E433–40.

[36] Lee RYW, Laprade J & Fung EHK A real-time gyroscopic system for three-dimensional measurement of lumbar spine motion. Med Eng Phys 2003; 25(10):817-824.

[37] Goodvin C, Park EJ, Huang K, Susaki K Development of a real-time three-dimensional spinal motion measurement system for clinical practice. Med Bio Eng Comput 2006;44(12):1061-1075.

[38] Plamondon A, Delisle A, Larue C, Brouillette D, McFadden D, Desjardins P, Larivière C. Evaluation of a hybrid system for three-dimensional measurement of trunk posture in motion. Appl. Ergonomics 2007; 38:697-712.

[39] Boonstra MC, van der Slikke RMA, Keijsers NLW, van Lummel RC, de Waal Malefijt MC, Verdonschot N, The accuracy of measuring the kinematics of rising from a chair with accelerometers and gyroscopes.

[40] Jasiewicz JM, Treleaven J, Condie P, Gwendolen J, Wireless orientation sensors: Their suitability to measure head movement for neck pain assessment. Man Ther 2007;12:380-385.

[41] Zhou H, Hu H, Tao Y. Inertial measurement of upperlimb motion. Med Bio Eng Comput 2006;44:479-487.

[42] Henmi S, Yonenobu K, Masatomi T. A biomechanical study of the activities of daily living using neck and upper limbs with an optical three dimensional motion analysis system. Mod Rheumatol 2006;16:289-293.

[43] Negrini S, Negrini A, Atanasio S, Santambrogio GC. Three-dimensional easy morphological (3-DEMO) classification of scoliosis, part I. Scoliosis 2006; 1:20.

[44] Cerveri P, Pedotti A, Ferrigno G. Non-invasive approach towards the in vivo estimation of 3D inter-vertebral movements: methods and preliminary results. Med Eng Phys 2004;26:841–853.

[45] van Herp G, Rowe P, Salter P, Paul JP. Three-dimensional lumbar spinal kinematics: a study of range of movements in 100 healthy subjects aged 20 to 60+ years. Rheumatology 2000; 39:1337-1340.

[46] Amiri M, Jull G, Bullock-Saxton J. Measuring range of active cervical rotation in a position of full head flexion using the 3D Fastrak measurement system: an intra-tester reliability study. Man Ther 2003;8(3):176–179.

[47] Bull AMJ, McGregor AH. Measuring spinal motion in rowers: the use of an electromagnetic device. Clin Biomech 2000;15:772-776.

[48] Demaille-Wlodyka S, Chiquet C, Lavaste JF, Skalli W, Revel M, Poiraudeau S. Cervical range of motion and cephalic kinesthesis: ultrasonographic analysis by age and sex. Spine J 2007;32(8):E254–E261.

[49] Vogt L, Segith C, Banzer W. Movement behaviour in patients with chronic neck pain. Physiotherapy Res Int 2007; 12(4):206–212.

[50] Dvir Z, Prushansky T, Reproducibility and instrument validity of a new ultrasonography-based system for measuring cervical spine kinematics. Clin Biomech 2000;15(9):658-664.

[51] Vogt L, Banzer W. Measurement of lumbar spine kinematics in incline treadmill walking. Gait and Posture 1999; 9:18–23.

[52] Simcox S, Parker S, Davis, GM, Smith RW, Middleton JW, Performance of orientation sensors for use with a functional electrical stimulation mobiliy system. J Biomech 2005;38:1185 – 1190.

[53] *With permission from T Cloete, MScIng student in Biomedical Engineering, 2007- 2008. University of Stellenbosch.

[54] Gracovetsky S, Newman N, Pawlowsky M, Lanzo V, Davey B, Robinson L. A database for estimating normal spinal motion derived from noninvasive measurement. Spine 1995 20:1036–1046.

[55] Hassan EA, Jenkyn TR, Dunning CE. Direct comparison of kinematic data collected using an electromagnetic tracking system versus a digital optical system. J Biomech 2007;40:930–935.

[56] Pearcy MJ, Hindle RJ. Axial rotation of lumbar intervertebral joints in forward flexion. Proc Inst Mech Eng [H] 1991; 205: 205–209

[57] *URL: http://www.cortechsolutions.com/Fastrak.htm [Cited 2008 Nov 19]

[58] *Dan Ratta. Inside Sales Representative Polhemus USA. E-mail: danr@polhemus.com

[59] Lee RYW, Wong TKT. Relationship between the movements of the lumbar spine and hip. Human Movement Science 2002; 21(4):481-494.

[60] Shum GLK, Crosbie J, Lee RYW. Effect of low back pain on the kinematics and joint coordination of the lumbar spine and hip during sit-to-stand and stand-to-sit. Spine 2005; 30(17):1998-2004.

[61] Shum GLK, Crosbie J and Lee RYW (2007). Three dimensional kinetics of the lumbar spine and hips in low back pain patients during sit-to-stand and stand-to-sit. Spine 32(7):E211-219.

[62] Shum GLK, Crosbie J and Lee RYW (2005). Symptomatic and asymptomatic movement coordination of the lumbar spine and hip during an everyday activity. Spine 30(23):E697-720**.**

[63] * Website of Zebris Medical GmbH. Spinal Analysis Systems. URL: http://www.zebris.de [Cited 2008 Feb 29]

[64] Li RC, Jasiewicz JM, Middleton J, Condie P, Barriskill A, Hebnes H, et al. The development, validity, and reliability of a manual muscle testing device with integrated limb position sensors. Archives of Physical Medicine and Rehabilitation 2006; 87:411–7.

[65] Luinge HJ, Veltink PH, Baten CTM. Estimating orientation with gyroscopes and accelerometers. Technol Health Care 1999; 7:455–9

[66] Williamson R, Andrews BJ. Detecting absolute human knee angle and angular velocity using accelerometers and rate gyroscopes. Med Biol Eng Comput 2001; 39(3):294–302.

[67] Mayagoitia RE, Nene AV, Veltink PH. Accelerometer and rate gyroscope measurement of kinematics: an inexpensive alternative to optical motion analysis systems. J Biomech 2002;35(4):537– 42.

[68] *URL: http://www.animazoo.com/Gypsy6.aspx [Cited 2008 Nov 19]

[69] *Website of Xsens, Inertial sensing technologies. URL: http://www.xsens.com/en/products/human_motion/mtx.php [Cited 12 June 2008]

[70] Fujii R, Sakaura H, Mukai Y, Hosono N, Ishii T, Iwasaki M, Yoshikawa H, Sugamoto K. Kinematics of the lumbar spine in trunk rotation: in vivo three-dimensional analysis using magnetic resonance imaging. Euro Spine J.

[71] Lee RYW. Kinematics of rotational mobilisation of the lumbar spine. Clin Biomech 2001;16(6):481-488.

[72] Nattrass CL, Nitschke JE, Disler PB, Chou MJ, Ooi KT. Lumbar spine range of motion as a measure of physical and functional impairment: an investigation of validity. Clin Rehab 1999; 13:211–218

[73] *Extracted from the website RadiologyInfo, Safety URL: http://www.radiologyinfo.org/en/safety/index.cfm [Cited 13 June 2008]

[74] Frobin W, Leivseth G, Biggemann M, Brinckmann P, Saggital plane segmental motion of the cervical spine. A new precision measurement protocol and normal motion data of healthy adults. Clin Biomech 2002;17:21-31.

[75] Schuler TC, Subach BR, Branch CL, Foley KT, Burkus JK, Segmental Lumbar Lordosis: Manual versus Computer-Assisted Measureent Using seven Different techniques. J Spinal Disord Tech, 2004; 17:372-379.

[76] Wu SK, Lan HHC, Kuo LC, Tsai SW, Chen CL, Su FC. Feasibility of a video-based motion analysis system in measuring the segmental movements between upper and lower cervical spine. Gait & Posture 2007; 26:161-166.

[77] Reitman CA, Mauro KM, Nguyen L, Ziegler JM, Hipp JA. Intervertebral Motion Between Flexion and Extension in Asymptomatic Individuals. Spine 2004; 29(24): 2832–2843.

[78] Wu SK, Kuo LC, Lan HHC, Tsai SW, Chen CL, Su FC. The quantitative measurements of the intervertebral angulation and translation during cervical flexion and extension. Euro Spine J 2007;16:1435–1444.

[79] Zheng Y, Nixon MS, Allen R, Lumbar spine visualisation based on kinematic analysis from videofluoroscopic imaging. Med Eng Phys 2003;25:171–179.

[80] Cooper R, Cardan C, Allen R. Computer visualisation of the moving human lumbar spine. Compute Biol and Med 2001;31:451–469.

[81] Bifulco P, Sansone M, Cesarelli M, Allen R, Bracale M. Estimation of out-of-plane vertebra rotations on radiographic projections using CT data: a simulation study. Med Eng Phys 2002;24:295–300.

[82] Ackerman SJ, Steinberg EP, Bryan N, BenDebba M. Trends in Diagnostic Imaging for Low Back Pain:Has MR Imaging Been a Substitute or Add-on? Radiology 1997; 203:533-538

[83] Ishii T, Mukai Y, Hosono N, Sakaura H, Nakajima Y, Sato Y, Sugamoto K, Yoshikawa H. Kinematics of the Upper Cervical Spine in Rotation In Vivo Three-Dimensional Analysis. Spine 2004: 29(7): E139–E144.

[84] Ishii T, Mukai Y, Hosono N, Sakaura H, Fujii R, Nakajima Y, Tamura S, Iwasaki M, Yoshikawa H, Sugamoto K. Kinematics of the Cervical Spine in Lateral Bending In Vivo Three-Dimensional Analysis. Spine 2006: 31(2): 155–160.

[85] Bryant JT, Reid JG, Smith BL., Stevenson JM. Method for determining vertebral body positions in the sagittal plane using skin markers. Spine 1989 14: 258–265.

[86] Lee YH, Chiou WK, Chen WJ, Lee MY, Lin YH. Predictive model of intersegmental mobility of lumbar spine in the sagittal plane from skin markers. Clin Biomech 1995;10(8):413-420.

[87] Chiou WK, Lee YH, Chen WJ, Lee MY, Lin YH. A non-invasive protocol for the determination of lumbar spine mobility. Clin Biomech 1996;11(8):474-480.

[88] Campbell-Kyureghyan N, Jorgensen M, Burr D, Marras W. The prediction of lumbar spine geometry: method development and validation. Clin Biomech 2005;20:455–464.

[89] Mörl F. Three-dimensional relation of skin markers to lumbar vertebrae of healthy subjects in different postures measured by open MRI. Euro Spine J 2006;15:742-751.

[90] Vergara M, Pageb A, Sanchoa JL. Analysis of lumbar flexion in sitting posture: Location of lumbar vertebrae with relation to easily identifiable skin marks. Int J Ind Erg 2006;36:937–942.

[91] Ryu JH, Miyati N, Kouchi M, Mochimaru M, Lee KH. Analysis of skinmovement with respect to flexional bone motion using MR images of a hand. J Biomech 2006;39:844-852.

[92] *Website of Lodox URL: http://www.lodox.com [Cited 17 June 2008]

[93] Irving BJ, Maree GJ, Hering ER, Douglas TS. Radiation dose from a linear slit scanning X-ray machine with full body imaging capabilities. Radiat Prot Dosimetry 2008 Apr 16.

[94] Ionizing radiation safety standards for the general public. Position statement of the Health Physics Society. Adopted: September 1992 Revised: June 2003.

[95] Dolan P. MA Adams. Recent advances in lumbar spinal mechanics and their significance for modeling Clin Biomech 2001;16(1):S8 – S16.

[96] Vogt L, Segieth C, Banzer W. Movement behaviour in patients with chronic neck pain. Physiotherapy Res Int 2007;12(4):206–212.

[97] Wilke HJ, Neef P, Hinz B, Seidel H, Claes L. Intradiscal pressure together with anthropometric data – a data set for the validation of models. Clin Biomech 2001;16(1):S111–S126.

[98] Mannion AF, Klein GN, Dvorak J, Lanz C. Range of global motion of the cervical spine: intraindividual reliability and the influence of measurement device. Euro Spine J 2000 June 2; 9:379–385.

[99] International Standards for Anthropometric Assessment. The international Society for the Advancement of Kinanthroprometry, 2001.

[100] Frobin W, Leivseth G, Biggemann M, Brinckman P. Vertebral height, posterioranterior displacement and dens-atlas gap in the cervical spine: precision measurement protocol and normal data. Clin Biomech 2002;17:423-431.

[101] *Medcyclopedia. URL: http://www.medcyclopaedia.com [Cited 2008 March 11]

[102] Huang RC, Tropiano P, Marnay T, Girardi FP, Lim MR, Cammisa FP. Range of motion and adjacent level lumbar degeneration after lumbar total disc replacement. Spine J 2006;6:242-247.

[103] Dvorak J, Froehlich D, Penning L, Baumgartner H, Panjabi MM. Functional radiographic diagnosis of the cervical spine:flexion/extension. Spine 1988;13:748-55.

[104] Holmes A, Wang C, Han ZH, Dang GT. The range and nature of flexion-extension motion in the cervical spine. Spine 1994;19:2505-10.

Appendix A - Absolute Rotation

		C2					C3					C4				
		FE	HE	N	HF	FF	FE	HE	N	HF	FF	FE	HE	N	HF	FF
Males	1	138.19	156.92	175.27	183.37	216.28	157.39	174.36	182.77	190.62	224.68	167.74	183.33	188.41	193.26	224.51
	2	138.10	150.87	166.95	183.92	220.86	163.94	174.21	186.25	193.31	244.92	170.34	182.45	187.71	192.90	233.87
	3	148.86	169.91	178.44	188.26	214.93	162.46	177.50	184.63	195.10	226.35	165.07	176.63	182.55	191.19	212.73
	4	138.76	162.68	173.35	184.89	214.12	157.03	175.57	183.39	191.49	225.12	170.94	185.84	187.76	198.05	224.90
	5	120.80	159.88	171.31	182.69	206.39	149.60	172.11	180.49	193.10	215.65	162.76	182.48	183.79	196.40	213.23
	6	137.21	157.90	169.66	181.36	208.53	164.19	178.75	187.22	201.04	247.55	164.84	178.57	186.04	193.25	225.92
	7	158.54	178.12	179.01	191.93	205.66	204.36	186.88	187.51	198.45	212.30	171.16	184.78	182.52	190.31	200.77
	8	130.98	155.86	174.20	189.95	218.01	158.18	171.10	186.74	201.85	229.61	163.99	176.06	186.82	199.97	220.08
	9	139.61	153.68	172.81	179.64	202.22	156.05	166.34	179.43	188.35	210.58	167.01	174.99	182.31	189.18	209.26
	10	116.25	152.94	171.70	185.32	211.58	154.25	168.29	178.48	192.58	214.87	158.53	172.81	179.49	192.32	213.55
	11	146.36	168.44	174.86	185.20	209.46	161.27	176.77	183.17	189.98	219.21	168.42	180.48	185.07	192.01	215.97
Females	1	92.92	155.21	161.50	178.79	202.80	135.56	174.99	178.66	194.40	219.88	143.14	187.37	184.35	193.43	213.20
	2	136.19	176.26	176.90	195.12	220.96	154.52	186.00	189.35	205.23	232.76	165.56	185.48	184.06	201.11	227.49
	3	129.37	160.52	169.67	181.38	198.56	157.60	180.64	185.86	196.03	213.31	165.10	188.95	186.09	194.00	211.66
	4	135.38	176.57	180.19	187.62	199.44	153.88	185.54	184.77	196.23	209.46	163.24	190.89	188.33	193.44	204.44
	5	142.87	165.01	177.57	182.79	208.64	167.41	183.90	190.50	196.93	221.44	176.17	192.42	193.88	200.06	218.87
	6	101.85	153.80	172.80	187.15	208.88	142.56	171.53	180.66	193.41	217.55	153.05	171.93	175.39	191.00	205.24
	7	126.15	159.08	170.85	188.41	212.66	151.45	173.05	183.86	195.63	224.75	167.00	177.92	184.50	194.92	219.07
	8	76.09	160.90	173.80	188.39	219.66	134.67	183.98	191.50	199.54	246.26	147.20	194.13	194.13	198.82	231.63
	9	140.50	168.08	183.63	201.30	218.33	160.42	179.50	194.50	213.81	236.08	167.22	184.95	193.15	211.38	231.65
	10	144.09	159.02	172.81	184.42	205.23	164.95	177.93	182.09	192.46	217.54	172.33	177.96	224.24	190.15	209.85

		C5					C6					C7				
		FE	HE	N	HF	FF	FE	HE	N	HF	FF	FE	HE	N	HF	FF
Males	1	174.78	190.87	192.86	197.21	223.00	180.67	191.37	189.68	195.03	213.88	191.43	200.78	199.52	202.25	214.52
	2	177.99	186.10	186.95	191.57	224.26	183.73	193.79	187.51	192.51	222.57	191.19	199.06	188.94	194.75	216.91
	3	175.92	182.44	187.01	195.01	208.87	187.03	190.13	192.98	198.66	210.26	194.88	195.25	196.17	200.66	206.37
	4	176.65	190.45	185.04	192.98	213.41	182.81	192.62	185.92	193.19	205.50	197.18	204.52	198.68	203.64	212.48
	5	167.21	183.42	185.29	189.99	203.84	178.33	193.64	190.35	192.71	203.55	188.73	200.87	201.11	197.00	201.59
	6	170.92	182.08	187.46	192.52	215.04	181.09	193.48	194.13	197.61	214.47	195.64	202.83	199.98	208.21	214.57
	7	181.24	191.59	186.89	195.50	201.86	186.23	192.02	187.89	191.23	196.89	197.75	200.14	199.13	199.52	199.69
	8	172.50	181.74	189.32	196.34	212.38	180.55	190.99	191.28	197.57	209.14	191.22	199.52	196.69	202.44	209.03
	9	171.75	182.35	182.88	185.38	200.67	182.84	191.05	186.89	189.05	200.08	193.42	199.29	193.59	195.92	202.00
	10	167.86	179.43	179.44	189.67	207.31	176.64	189.89	180.54	188.25	202.51	189.44	200.22	187.95	192.01	201.23
	11	177.19	184.75	188.61	193.18	213.29	181.71	187.06	191.36	193.76	206.70	193.28	194.45	198.78	201.41	207.18
Females	1	159.69	197.58	183.40	192.92	212.18	174.40	205.25	188.00	195.56	207.72	190.58	211.77	195.83	204.55	210.49
	2	173.60	184.80	183.55	196.33	218.58	185.51	190.54	187.96	196.75	213.33	201.41	198.91	196.38	201.11	214.14
	3	174.71	194.90	178.12	189.13	202.53	181.83	199.25	184.88	181.30	194.56	193.53	202.66	184.88	184.30	191.97
	4	172.56	192.36	186.53	189.05	202.33	182.29	194.39	188.21	187.01	200.95	193.50	196.63	192.50	189.37	197.42
	5	184.82	197.53	192.75	197.28	214.01	193.98	196.27	191.27	197.65	207.89	208.09	198.58	197.79	202.98	207.75
	6	162.05	177.91	176.71	187.86	198.15	176.44	194.55	179.41	184.04	194.85	186.39	198.26	188.81	185.45	196.00
	7	170.75	176.29	181.38	185.78	205.87	172.80	178.01	180.67	181.34	194.08	187.19	190.03	188.53	188.37	199.39
	8	162.97	200.72	190.69	193.78	222.13	166.34	195.85	187.32	191.90	214.65	176.69	194.78	186.82	190.07	210.52
	9	170.76	189.28	187.26	201.02	214.57	177.13	187.72	181.13	192.70	204.04	186.58	190.91	188.51	195.46	202.44
	10	180.70	180.78	179.24	186.56	202.95	188.44	184.42	180.73	185.12	198.33	194.44	188.80	180.59	181.16	193.43

Appendix B - Intervertebral Rotation

		C2/C3					C3/C4					C4/C5					C5/C6					C6/C7				
		FE	HE	N	HF	FF	FE	HE	N	HF	FF	FE	HE	N	HF	FF	FE	HE	N	HF	FF	FE	HE	N	HF	FF
Males	1	2.42	4.20	13.21	0.46	-3.31	-5.65	-2.64	0.18	-8.98	-10.36	-4.45	-3.95	1.51	-7.53	-7.04	3.18	2.18	9.12	-0.50	-5.89	-9.84	-7.22	-0.64	-9.41	-10.76
	2	-4.01	3.91	2.49	-5.97	-8.27	-1.46	0.41	11.05	-8.24	-6.41	0.76	1.33	9.61	-3.65	-7.65	-0.57	-0.93	1.69	-7.69	-5.74	-1.43	-2.24	5.65	-5.26	-7.46
	3	5.87	6.87	14.11	3.29	1.13	2.09	3.91	13.63	0.88	-2.61	-4.47	-3.82	3.85	-5.81	-10.85	-5.97	-3.65	-1.39	-7.69	-11.11	-3.18	-2.01	3.89	-5.12	-7.85
	4	-2.75	3.31	8.89	-3.09	-7.02	-4.37	-6.56	0.22	-10.26	-13.91	2.72	5.07	11.49	-4.61	-5.71	-0.88	-0.21	7.91	-2.17	-6.16	-12.76	-10.46	-6.98	-11.90	-14.37
	5	2.39	1.93	10.22	-0.27	-4.39	-3.31	-3.29	2.42	-10.37	-13.16	-1.50	6.41	9.40	-0.95	-4.45	-5.06	-2.72	0.29	-10.22	-11.12	-10.77	-4.29	1.95	-7.24	-10.41
	6	-6.82	-7.93	-15.31	-7.53	-11.43	1.19	7.78	21.63	0.18	-0.65	-1.42	0.73	10.87	-3.50	-6.08	-6.67	-5.09	0.58	-11.40	-10.17	-5.84	-10.60	-0.10	-9.36	-14.55
	7	1.94	6.81	7.94	2.42	-33.47	4.99	8.14	11.53	2.11	33.19	-4.37	-5.18	-1.09	-6.82	-10.08	-1.00	4.27	4.98	-0.43	-4.99	-11.25	-8.30	-2.80	-8.12	-11.52
	8	-0.82	2.32	19.48	-1.89	-6.63	-0.09	1.87	9.53	-4.95	-5.81	-2.50	3.64	7.70	-5.68	-8.51	-1.96	-1.24	3.24	-9.25	-8.05	-5.41	-4.87	0.12	-8.53	-10.67
	9	2.49	5.57	9.23	-0.63	-2.82	-2.88	-0.83	1.32	-8.66	-10.97	-0.58	3.80	8.59	-7.36	-4.74	-4.01	-3.67	0.59	-8.69	-11.09	-6.70	-6.87	-1.92	-8.24	-10.58
	10	5.79	14.61	25.69	-1.70	-4.79	-1.01	0.26	1.32	-4.52	-4.28	0.05	2.65	6.24	-6.62	-9.33	-1.10	1.42	4.80	-10.46	-8.78	-7.41	-3.76	1.28	-10.34	-12.80
	11	2.34	5.79	14.52	0.59	0.31	-1.91	-2.03	3.24	-3.71	-7.16	-3.54	-1.17	2.69	-4.27	-8.77	-2.75	-0.58	6.59	-2.31	-4.52	-7.42	-7.66	-0.48	-7.39	-11.57
Females	1	-2.70	1.06	5.46	-4.19	-12.26	-5.69	0.97	6.68	-12.38	-7.58	0.95	0.51	1.02	-10.21	-16.55	-4.60	-2.65	4.46	-7.67	-14.71	-7.83	-8.99	-2.77	-6.51	-16.18
	2	3.10	8.34	21.66	3.85	0.92	5.29	4.12	5.27	0.51	-11.03	0.51	4.79	8.91	0.68	-8.05	-4.41	-0.43	5.25	-5.74	-11.91	-8.42	-4.36	-0.81	-8.37	-15.90
	3	-3.86	-1.33	0.40	-6.55	-11.02	-0.23	2.03	1.65	-8.32	-7.49	7.97	4.87	9.13	-5.95	-9.61	-6.76	7.83	7.97	-4.35	-7.12	0.00	-3.00	2.60	-3.41	-11.70
	4	5.30	3.89	5.99	0.76	-0.38	-3.56	2.79	5.02	-5.36	-9.37	1.81	4.40	2.11	-1.47	-9.31	-1.68	2.03	1.38	-2.02	-9.73	-4.29	-2.36	3.53	-2.24	-11.21
	5	0.52	2.04	17.04	-5.49	-6.91	-3.38	-3.14	2.58	-8.52	-8.77	1.14	2.78	4.86	-5.11	-8.65	1.48	-0.36	6.12	1.26	-9.15	-6.53	-5.34	0.14	-2.31	-14.12
	6	3.07	5.42	9.86	-5.14	-18.75	5.26	2.42	12.31	-0.40	-10.50	-1.31	3.14	7.09	-5.97	-8.99	-2.71	3.82	3.30	-16.64	-14.39	-9.40	-1.41	-1.15	-3.72	-9.95
	7	-0.52	6.30	14.29	-1.86	-5.26	-0.64	0.71	5.67	-4.87	-15.56	3.12	9.15	13.20	1.62	-3.74	0.71	4.44	11.79	-1.72	-2.05	-7.86	-7.04	-5.31	-12.02	-14.40
	8	-6.71	1.46	3.91	-8.35	-23.41	-2.63	0.72	14.63	-10.16	-12.53	3.43	5.03	9.50	-6.59	-15.77	3.38	1.89	7.49	4.87	-3.37	0.49	1.83	4.13	1.07	-10.35
	9	1.03	7.41	10.43	-0.78	-3.40	1.35	2.43	4.43	-5.45	-6.80	5.89	10.37	17.08	-4.33	-3.54	6.13	8.31	10.53	1.56	-6.37	-7.38	-2.76	1.60	-3.19	-9.45
	10	2.16	5.35	10.80	-5.51	-4.50	-42.15	2.31	7.69	-0.03	-7.38	45.00	3.59	6.90	-2.82	-8.37	-1.49	1.44	4.62	-3.64	-7.75	0.14	3.96	4.90	-4.38	-6.00

Appendix C - *R*

	R	Full Extension						Half Extension						Neutral					
		C2	C3	C4	C5	C6	C7	C2	C3	C4	C5	C6	C7	C2	C3	C4	C5	C6	C7
Males	1	91.08	71.99	67.13	64.65	67.85	65.43	68.22	60.20	60.52	59.32	67.50	65.62	62.11	53.97	54.09	54.96	59.01	64.01
	2	90.75	79.56	67.05	71.77	83.29	86.18	70.17	71.79	75.22	81.38	85.24	89.07	65.25	65.47	67.78	70.67	74.03	79.90
	3	99.07	88.74	74.02	60.92	60.81	64.91	69.14	61.52	58.98	56.57	61.85	69.38	61.06	55.91	54.96	56.60	63.69	68.84
	4	88.98	86.13	74.75	62.45	62.10	63.07	61.86	59.76	57.62	58.12	63.44	67.09	55.74	51.81	50.08	52.35	57.14	62.55
	5	116.05	89.46	71.09		64.12	65.97	68.33	63.04	55.82		63.67	68.37	57.16	54.55	53.08		58.51	62.82
	6	109.46	89.40	72.42	61.74	57.20	12.63	67.26	64.40	56.63	56.12	62.15	36.35	58.45	58.31	58.93	58.66	61.36	34.60
	7	83.32	70.74	61.93	54.46	57.58	59.11	61.62	54.67	53.15	54.51	57.79	61.33	52.17	48.06	48.34	51.05	55.53	59.50
	8	100.84	102.79	85.38	82.13	80.42	80.74	61.06	64.86	63.85	61.70	68.50	73.10	56.23	58.68	57.67	58.41	62.69	67.51
	9	107.02	83.35	69.63	68.00		65.73	86.79	70.17	60.41	63.50		67.13	60.07	55.59	55.61	56.88		60.87
	10	90.97	90.23	72.21	61.16	63.81	69.89	68.32	72.78	66.39	61.62	67.50	72.17	55.53	50.42	48.42	48.83	53.80	59.70
	11	93.50	89.03	78.12	65.50	57.45	62.66	62.48	55.78	55.06	54.74	56.51	59.51	53.08	52.80	55.24	55.40	58.30	62.85
Females	12	89.17	69.74	63.11	62.48	73.13	68.09	57.27	55.44	56.99	61.72	60.79	59.35	52.11	49.37	48.71	58.51	53.12	54.73
	13	91.14	73.54	58.65	52.55	62.00	61.41	53.08	50.96	50.11	51.01	55.07	57.62	50.50	48.87	48.05	49.42	53.12	55.95
	14	85.94	81.36	83.79	73.54	60.06	58.52	69.12	62.37	60.97	61.15	59.73	59.20	58.71	52.85	49.75	46.67	49.32	57.17
	15	73.44	76.72	69.17	63.85	65.59	17.60	51.38	48.26	49.46	51.82	57.11	29.91	47.24	44.80	45.49	46.19	51.66	27.30
	16	72.26	72.35	73.64	63.43	60.20	55.67	58.63	55.87	54.90	52.99	54.81	55.49	50.55	48.15	47.01	46.38	50.28	52.63
	17	68.06	70.43	69.52	71.99	70.85	61.90	56.33	52.63	51.17	55.50	58.04	58.22	45.03	45.82	45.16	42.28	47.29	52.66
	18	102.78	95.66	975.39	63.46	54.41	59.81	63.55	53.98	969.86	49.14	52.37	56.57	52.94	48.72		52.25	49.26	54.32
	19	95.08	87.29	75.26	70.38	70.49	67.54	58.72	58.93	56.53	51.49	51.19	52.97	49.38	46.30	43.72	42.21	43.67	47.90
	20	90.59	88.38	67.80	52.05	53.36	57.22	62.04	59.42	51.57	56.37	55.84	57.97	52.47	50.44	45.87	44.19	47.38	52.79
	21	65.53	54.50		54.32	55.58	56.04	59.34	46.08		50.13	52.78	56.35	44.93	41.78		40.45	43.17	47.94

	R	Half Flexion						Full Flexion					
		C2	C3	C4	C5	C6	C7	C2	C3	C4	C5	C6	C7
Males	1	61.26	57.62	59.21	61.40	65.73	71.57	75.54	68.87	68.56	67.06	67.42	72.61
	2	59.68	58.48	60.47	64.92	70.65	79.73	88.12	83.67	83.61	85.97	88.61	94.30
	3	59.69	56.56	58.36	61.33	69.96	75.39	78.22	69.95	66.90	67.46	76.16	80.49
	4	54.70	54.85	54.39	55.86	60.26	66.37	74.89	68.95	64.11	62.17	64.81	71.69
	5	55.66	53.34	51.99		59.24	65.34	68.14	61.41	56.79		61.67	68.85
	6	61.83	63.54	62.43	61.40	64.62	42.31	87.37	82.82	75.74	71.77	72.03	58.81
	7	53.52	50.36	49.75	50.42	55.15	61.52	66.49	61.57	45.54	58.79	62.37	70.59
	8	64.35	65.87	61.85	59.42	63.28	69.73	81.71	78.58	72.48	69.48	72.86	78.67
	9	52.06	51.97	51.36	53.21		61.58	65.79	63.23	57.95	56.66		65.19
	10	52.77	52.35	51.94	52.09	55.67	61.41	70.20	65.42	63.50	62.58	66.26	72.61
	11	56.88	58.17	60.20	58.11	59.37	62.82	78.31	75.34	72.20	66.28	63.27	65.66
Females	12	48.04	46.92	46.06	48.72	52.27	55.61	58.89	53.33	49.88	50.59	52.99	56.61
	13	59.81	55.51	52.38	51.56	53.74	58.57	74.99	68.37	64.37	62.41	61.41	66.23
	14	53.66	51.77	46.73	45.12	44.91	48.27	61.01	58.29	50.28	45.69	44.54	48.51
	15	48.22	45.38	43.95	44.75	49.80	38.46	58.85	55.46	53.41	53.88	58.92	51.43
	16	52.86	50.76	48.71	46.95	50.74	54.45	66.34	58.66	54.08	50.07	49.65	53.77
	17	48.26	47.82	43.79	40.18	41.77	47.37	64.48	57.38	51.98	55.22	60.17	68.97
	18	48.15	46.82		47.36	44.78	50.98	66.40	61.26		58.04	54.40	59.14
	19	51.92	51.60	47.20	44.68	45.90	49.71	73.71	70.56	62.40	59.82	61.91	66.03
	20	66.97	65.36	59.68	56.73	56.00	60.33	80.26	76.15	67.60	64.88	65.75	68.81
	21	45.34	40.06		41.51	43.35	48.06	59.48	51.26		53.23	53.66	58.27

Appendix D - β

B		Full Extension						Half Extension						Neutral					
		C2	C3	C4	C5	C6	C7	C2	C3	C4	C5	C6	C7	C2	C3	C4	C5	C6	C7
Males	1	116.23	133.60	148.40	162.91	177.31	190.32	137.55	158.09	182.23	198.15	210.89	214.02	160.15	181.67	196.01	204.81	211.25	216.33
	2	134.51	149.33	167.64	184.58	190.13	200.18	147.67	170.21	187.67	199.16	207.25	215.93	170.36	178.52	182.34	191.61	201.43	211.80
	3	126.49	132.46	145.14	166.81	186.76	205.43	147.68	160.07	172.60	185.99	205.20	219.42	166.67	177.17	189.23	197.64	213.88	223.15
	4	124.45	133.50	146.27	167.27	190.31	211.28	155.27	172.33	185.52	198.21	208.91	219.52	161.13	178.49	187.03	195.37	204.11	215.84
	5	111.02	118.54	133.49		165.62	181.15	145.00	158.65	175.28		210.43	218.00	162.61	173.70	177.91		204.54	211.17
	6	116.66	126.87	141.08	164.39	188.62	218.44	147.78	162.86	176.59	195.33	209.89	246.87	173.81	186.60	195.67	202.24	212.84	267.96
	7	130.74	145.32	154.67	173.54	193.02	207.09	161.72	175.54	189.99	199.91	209.76	221.76	172.31	183.19	194.59	201.99	211.67	223.35
	8	130.44	138.10	145.29	160.28	173.70	183.72	158.00	171.46	179.03	194.17	205.89	215.13	186.05	197.22	199.87	201.68	207.22	214.86
	9	117.21	128.15	143.67	156.99		186.94	132.81	145.41	164.92	180.91		206.04	155.78	167.68	169.71	179.33		203.30
	10	123.99	130.20	144.56	167.43	185.20	194.63	149.27	160.38	170.77	190.98	207.86	213.57	158.42	172.40	182.70	190.99	197.27	201.92
	11	126.64	134.74	142.45	161.15	178.02	190.56	148.92	165.60	178.43	186.71	188.22	196.61	177.75	192.67	201.54	202.88	201.18	206.29
Females	12	108.51	120.59	133.10	146.23	154.25	163.67	150.97	171.14	182.60	191.28	196.37	202.51	152.24	162.13	166.28	155.39	181.49	189.76
	13	122.84	131.95	149.30	171.19	181.32	193.82	173.57	180.95	184.55	192.21	194.65	204.87	184.18	186.49	187.04	191.57	192.87	203.67
	14	126.87	140.89	146.81	154.87	172.49	190.27	149.87	167.90	175.59	184.28	191.07	201.51	156.52	168.99	167.16	192.95	198.83	208.71
	15	122.67	135.67	147.00	160.21	180.16	213.29	163.86	179.50	188.19	202.40	209.69	275.34	171.55	184.13	185.81	196.09	204.85	285.78
	16	130.50	150.15	154.95	164.02	177.24	188.74	154.87	168.87	175.59	180.13	184.41	193.24	171.60	179.22	180.94	180.07	182.58	192.09
	17	107.38	123.18	134.60	147.29	158.79	171.44	136.98	155.80	172.80	187.51	200.42	209.94	166.33	206.49	206.82	191.63	201.06	210.50
	18	113.39	121.67		148.39	167.85	182.37	133.77	148.26		181.89	183.42	190.48	160.10	174.88		216.91	191.29	194.60
	19	99.24	108.13	116.15	126.05	135.66	145.99	158.97	175.16	185.77	192.63	200.40	204.15	170.24	189.05	190.77	197.81	195.98	198.22
	20	120.28	125.48	136.68	157.86	175.86	185.07	150.41	163.71	177.39	192.70	193.39	197.76	184.28	196.00	202.74	204.34	201.04	201.22
	21	127.57	145.40		178.73	187.91	196.80	139.68	178.21		176.29	183.85	190.51	167.54	167.88		179.57	180.56	183.31

	B	Half Flexion						Full Flexion					
		C2	C3	C4	C5	C6	C7	C2	C3	C4	C5	C6	C7
Males	1	185.21	204.31	214.20	221.10	225.60	229.32	229.65	237.58	243.57	247.31	247.09	247.24
	2	202.48	204.57	203.21	210.39	218.84	227.43	245.06	243.12	240.35	241.64	245.00	249.06
	3	195.36	202.79	212.64	218.04	229.28	235.15	237.79	239.55	242.26	243.01	250.39	251.48
	4	196.52	208.61	213.14	216.02	221.17	229.54	243.25	246.00	245.36	243.19	243.07	248.31
	5	192.34	198.23	198.38		216.09	220.55	230.11	229.99	225.44		234.86	236.15
	6	210.09	216.26	218.13	218.96	224.50	260.68	248.93	250.55	249.87	248.34	249.10	285.94
	7	208.93	212.76	216.55	218.36	223.81	232.13	233.36	234.50	222.77	235.50	238.07	243.81
	8	224.82	229.32	227.01	222.22	224.19	228.80	250.48	252.12	249.05	242.79	242.28	243.98
	9	189.59	195.80	191.29	192.81		212.13	228.63	230.93	224.72	222.01		233.10
	10	206.64	216.00	220.19	221.35	220.81	220.75	238.61	243.69	245.81	245.43	243.74	241.67
	11	210.24	218.78	222.66	218.98	212.01	213.24	246.37	250.73	249.97	244.42	233.00	227.78
Females	12	197.03	197.81	192.55	194.26	198.84	204.81	232.96	230.44	222.94	220.38	220.06	223.04
	13	224.23	222.25	217.42	216.04	212.39	219.29	251.86	249.31	245.25	242.91	237.55	241.21
	14	186.14	196.22	189.72	184.48	187.34	196.02	217.29	222.19	215.10	209.66	211.48	217.73
	15	209.33	212.79	213.26	214.80	217.57	286.68	229.68	232.01	232.20	232.29	234.21	294.51
	16	201.99	204.74	203.28	199.68	199.38	206.96	241.76	239.29	234.58	228.03	221.12	224.98
	17	212.71	219.99	216.45	197.49	202.16	209.05	237.67	245.27	241.93	245.06	246.67	248.34
	18	207.27	215.78		225.76	211.87	210.03	241.38	244.80		249.78	238.51	235.83
	19	213.08	223.91	222.24	223.50	217.64	215.44	250.34	255.86	254.26	254.83	250.09	247.39
	20	227.29	233.95	237.59	235.89	228.87	226.13	244.72	249.45	251.87	249.96	244.13	240.58
	21	207.08	202.35		208.91	205.05	203.32	240.74	235.33		238.38	233.89	230.51